

Instituto Politécnico Nacional

Centro de Investigación en Computación

Long term analysis of the spatial and temporal dynamics
of an ecological model based on cellular automata

A thesis submitted in fulfillment of the requirements for the degree of
Doctor of Philosophy in Computer Science

Mario Martínez Molina

Advisors:

Dr. Marco Antonio Moreno Armendáriz

Dr. Juan Carlos Seck Tuoh Mora

December 9, 2014



INSTITUTO POLITÉCNICO NACIONAL SECRETARÍA DE INVESTIGACIÓN Y POSGRADO

ACTA DE REVISIÓN DE TESIS

En la Ciudad de México, D. F. siendo las 12:00 horas del día 21 del mes de noviembre de 2014 se reunieron los miembros de la Comisión Revisora de la Tesis, designada por el Colegio de Profesores de Estudios de Posgrado e Investigación del:

Centro de Investigación en Computación

para examinar la tesis titulada:

"Long term analysis of the spatial and temporal dynamics of an ecological model based on cellular automata"

Presentada por el alumno:

MARTÍNEZ
Apellido paterno

MOLINA
Apellido materno

MARIO
Nombre(s)

Con registro:

A	1	1	0	8	2	3
---	---	---	---	---	---	---

aspirante de: **DOCTORADO EN CIENCIAS DE LA COMPUTACIÓN**

Después de intercambiar opiniones los miembros de la Comisión manifestaron **APROBAR LA TESIS**, en virtud de que satisface los requisitos señalados por las disposiciones reglamentarias vigentes.

LA COMISIÓN REVISORA Directores de Tesis

Dr. Marco Antonio Moreno Armendáriz

Dr. Juan Carlos Seck Tuoh Mora

Dr. Sergio Suárez Guerra

Dr. René Luna García

Dra. Nareli Cruz Cortés

Dr. Víctor Hugo Ponce Ponce

PRESIDENTE DEL COLEGIO DE PROFESORES

Dr. Luis Alfonso Villa Vargas

INSTITUTO POLITÉCNICO NACIONAL
CENTRO DE INVESTIGACION
EN COMPUTACION
DIRECCION




INSTITUTO POLITÉCNICO NACIONAL
SECRETARÍA DE INVESTIGACIÓN Y POSGRADO

CARTA CESIÓN DE DERECHOS

En la Ciudad de México el día 5 del mes de diciembre del año 2014, el (la) que suscribe Martínez Molina Mario alumno (a) del Programa de Doctorado en Ciencias de la Computación con número de registro A110823, adscrito al Centro de Investigación en Computación, manifiesta que es autor intelectual del presente trabajo de Tesis bajo la dirección del Dr. Marco Antonio Moreno Armendáriz y del Dr. Juan Carlos Seck Tuoh Mora y cede los derechos del trabajo intitulado Long term analysis of the spatial and temporal dynamics of an ecological model based on celular autómata, al Instituto Politécnico Nacional para su difusión, con fines académicos y de investigación.

Los usuarios de la información no deben reproducir el contenido textual, gráficas o datos del trabajo sin el permiso expreso del autor y/o director del trabajo. Este puede ser obtenido escribiendo a la siguiente dirección mariomartinezmolina@live.com. Si el permiso se otorga, el usuario deberá dar el agradecimiento correspondiente y citar la fuente del mismo.



Mario Martínez Molina

Nombre y firma

Resumen

La dinámica espacial y temporal de un modelo presa-predador basado en autómatas celulares, donde el movimiento de predadores es modelado a través de un algoritmo de optimización por cumulo de partículas, es analizada.

Simulaciones de la versión global del modelo, muestran que solo es posible observar la dependencia de la densidad cuando el factor social de los predadores es lo suficientemente bajo para permitir la dispersión de individuos a través de la lattice, o cuando la magnitud de las oscilaciones alrededor de la mejor posición hallada por el enjambre son lo suficientemente grandes para permitir un rápido movimiento de partículas dentro del autómata celular.

Un análisis cualitativo de la implementación local revela que las interacciones sociales entre predadores provocan la formación de clusters, y que al incrementar la movilidad de los mismos, el modelo exhibe comportamiento oscilatorio.

Abstract

The spatial and temporal dynamics of a prey-predator model based on cellular automata, where the movement of predators is modeled through a Particle Swarm Optimization algorithm, is analysed.

Simulations of the global version of the model show that density dependence is only present when the social factor of predators is low enough to allow the dispersal of individuals across the lattice of the model, or when the magnitude of the oscillations around the best position found by the swarm are large enough to allow a fast coordinated movement of particles across the cellular automaton.

A qualitative analysis of the local implementation reveals that the social interactions among predators provoke the formation of clusters, and that by increasing the mobility of predators the model exhibits oscillatory behavior.

Acknowledgements

Contents

1. Introduction	1
1.1. Motivation	1
1.2. Objectives	1
1.2.1. Particular objectives	2
1.3. Lattice models in ecology	2
1.4. Organization of this thesis	8
1.5. Publications	9
2. Background	10
2.1. Non Linear Dynamics in Ecosystems	10
2.2. Cellular Automata	13
2.2.1. Elementary cellular automata	14
2.2.2. Spatial dynamics of elementary cellular automata	15
2.3. Mean field theory for elementary cellular automata	18
2.4. Probabilistic Cellular Automata (PCA)	21
2.5. Particle Swarm Optimization	22
3. State of the art	27
3.1. Mean field theory approaches	27
3.1.1. A prey-predator system with pursuit and evasion	27
3.2. Time series analysis	29
3.2.1. Spectral density	30
3.2.2. Power-law scalings and patchiness	31
3.3. Finite size effects	32
4. Proposed model	35
4.1. Description	35
4.2. PSO as a migration algorithm	37
4.3. Global implementation	38
4.4. Local Implementation	38
5. Spatial and population dynamics	41
5.1. Analysis of the global implementation	41
5.1.1. Dynamics in the absence of movements	41
5.1.2. Social interactions, cognitive knowledge and density dependence	41
5.2. Analysis of the local implementation	46
5.2.1. Social dynamics	46
5.2.2. Predator mobility and density dependence	48

6. Mean field analysis	55
6.1. Mean field terms for the proposed model	55
6.1.1. Intraspecific competition	55
6.1.2. Prey reproduction	56
6.1.3. Death of Predators	57
6.1.4. Reproduction of predators	57
6.1.5. Predation	58
6.2. Mean field models for the long term dynamics	58
6.2.1. Predator dynamics	58
6.2.2. A model without migration	60
6.2.3. A mean field model for small neighborhoods	63
6.2.4. The migration stage	66
7. Conclusions	72

List of Figures

2.1.	Evolution of the logistic map for an increasing reproduction rate.	11
2.2.	Period-doubling bifurcation.	12
2.3.	Bifurcation diagram for the logistic equation.	13
2.4.	Evolution of rule 169.	15
2.5.	Symmetry classes for a ring of length 5.	16
2.6.	De Bruijn diagrams for rule 169.	17
2.7.	A shift of two cells to the right in one generation.	17
2.8.	A shift of two cells to the right in one generation according to rule 169.	18
2.9.	Shifts of three cells in two generations for rule 169.	19
2.10.	Mean field theory predictions.	20
2.11.	Experimental results for rule 169.	21
2.12.	A plot of the function defined in Equation 2.21.	23
2.13.	Change in position of the particles depicted in Figure 2.12.	26
3.1.	Von Neumann “predation neighborhood” and M_2^T “pursuit and evasion neighborhood” ($r = 2$).	28
3.2.	Fixed points and limit cycles of the pursuit and evasion model.	29
4.1.	A season of the model.	36
4.2.	Movement of predators in the global implementation. (a) Individuals move to the direction of the swarm’s best known position. (b) The swarm moves to the recently discovered “good” zone.	38
4.3.	Local implementation of the migration algorithm.	39
5.1.	Temporal dynamics under an increasing predator reproduction radius.	42
5.2.	Target patterns and spirals form when the rate of dispersal of both species is approximately equal (Lattice size = 512×512 cells).	43
5.3.	As $ V _{max}$ grows the size of the cluster increases, and density dependence becomes more evident (Lattice size = 64×64 cells.)	44
5.4.	Dispersion of predators in a simulation where $k_1 = 2.0$ and $k_2 = 0.0$ (Lattice size = 64×64 cells.)	45
5.5.	Population dynamics under a pure cognitive movement.	46
5.6.	As a result of a weak social factor ($k_2 = 0.05$) and a strong cognitive factor ($k_1 = 1.0$), the swarm disperses, but keeps moving towards P_g^t	47
5.7.	Density dependence is non existent as a consequence of the increase of the social factor ($k_1 = 1.0$ and $k_2 = 0.35$).	47
5.8.	Spatial dynamics due to the social interactions among predators. (a) Predators grouped together. (b) A cluster divides as a consequence of a finite $M_{r_1}^2$. The size of the clusters increases as a result of a fast movement to cells with a high fitness: (c) $k_2 = 1.0$, (d) $k_2 = 1.5$, (e) $k_2 = 2.0$, (f) $k_2 = 2.5$	49

5.9. Effects of an $\omega > 0$ on the movement patterns of predators: (a) Distribution before migration. (b) During the first stages of migration, a predator executes long range movements that will likely produce the fragmentation of a cluster. (c) The final stages of migration are characterized by small steps that favor exploitation and form new clusters. 50

5.10. Population dynamics of the local implementation under an increasing k_2 51

5.11. Transition to the oscillatory regime. 52

5.12. Invasion of preys by predators. 53

5.13. Population dynamics of the proposed model under the parameters of Table 4.1. The left inset shows a monotonic approach to a fixed point during the transient phase of the simulations, which corresponds to traveling wavefronts that appear during the invasion process. The right inset shows that oscillations have a very regular period and are out of phase. 54

6.1. This interpolation assumes proportionality between Ψ_t and the number of preys in the neighborhood M_c 56

6.2. A simple life cycle for preys and predators 58

6.3. Population dynamics of the reproduction of predators: mean field model and computer simulations. 59

6.4. Comparison of the population dynamics of the reproduction of predators: adjusted mean field model vs computer simulations. 60

6.5. Increasing the value of z produces a good agreement of results between the mean field equations and the CA model. 61

6.6. The life cycle of a model where there is no migration stage. 62

6.7. A comparison of the mean field model and a computer simulation for $\epsilon_Y = 1, y = 1, \epsilon_Z = 1, z = 1$ and $c = 1$ 63

6.8. Mean field model vs computer simulation: $\epsilon_Y = 1, y = 20, \epsilon_Z = 1, z = 20$ and $c = 20$. . 63

6.9. Phase plots of the mean field model vs computer simulations: $\epsilon_Y = 1, y = 20, z = 20$ and $c = 10$ 64

6.10. Phase plots of the mean field model vs computer simulations: $y = 20, \epsilon_Z = 1, z = 20$ and $c = 10$ 65

6.11. Functional form for the growth rate of preys. In (a) $\epsilon_Y = 1, 2, 3, y = 1$, and $\Psi_0 = 0.0001$; in (b) Equation 6.11 was plotted for $\epsilon_Y = 1, 2, 3$ using 100 values of Ψ_t linearly distributed in $[0, 1]$ 65

6.12. Comparison of the results obtained from the computer simulations and the results of the mean field model with adjusted parameters. 67

6.13. Measurements of the death probability of predators for parameters sets A and B 69

6.14. Simulations using set B compared to a mean field model that uses adjusted parameters via statistical regression. 70

6.15. Scaling behavior of the proposing model. Small lattices produce orbits to a noisy limit cycle; as the size of the lattice increases, the amplitude of the oscillations diminishes and the limit cycle destabilizes. For large lattices a new decrease of the amplitude is observed; however, the oscillations still have a regular period and their amplitude remains bounded, yet difficult to predict. 71

List of Tables

1.1. Game matrix for the “hawks and doves” game.	6
2.1. Transition table for rule 169.	15
2.2. Configurations for a ring of length 5.	16
2.3. Configurations in decimal notation.	16
2.4. Transition table for the probabilistic cellular automaton.	22
2.5. Status of the swarm after initialization.	24
4.1. A summary of the parameters of the model	40
5.1. Parameters used to produce target and spiral patterns.	43
5.2. Parameters used to investigate the behavior of the model under the effects of the PSO algorithm.	45
5.3. Parameters used to analyze the behavior of the proposed model under the effects of the local PSO algorithm.	48
5.4. Parameters used in computer simulations.	53
6.1. Adjusted parameters for the mean field model via statistical regression.	66
6.2. Parameters used to analyse the migration stage.	68
6.3. Parameters obtained through statistical regression for simulations using parameters sets A and B	69

Chapter 1

Introduction

1.1. Motivation

Since their creation in the decade of 1950 by John von Neumann and Stanislaw Marcim Ulam, a great effort has been devoted to the study of the long term dynamics of cellular automata. The experimental analysis made by Wolfram on elementary cellular automata [1], which ended with the classification that bears his name, sparked a great interest in the development of a sound mathematical foundation that could explain the behavior displayed by these dynamical systems. Wolfram himself was one of the first in pursuing this goal, in [2] he provided an statistical analysis of the evolution of elementary cellular automata. Other works have focused on phenomena such as chaos [3] [4] [5], periodic behavior in the long term time limit [6] [7], or complex dynamics [8], however, the vast majority of this works deal with transition functions of the deterministic type.

Probabilistic cellular automata can be regarded as generalizations of those that employ deterministic rules, one of the first studies of these systems was made by Domany and Kinzel [9], they studied the phase transitions of a probabilistic model by mapping its behavior to that of an Ising system, and proved that the resulting behavior was equivalent to a directed percolation process. The results obtained served as an starting point to other works that studied the phase transitions of the Domany-Kinzel model, or similar automata [10] [11] [12] [13]. More recent works have investigated the phase transitions of two-dimensional models [14], ergodicity [15] [16], or critical behavior [17].

Other results concerning the long-term dynamics of probabilistic cellular automata have been obtained in other research fields, here, probabilistic cellular automata are commonly used as a modeling tool. Of particular interest for this dissertation is the field of ecological modeling, where cellular automata are used due to their capability to model local the interactions among organisms explicitly, moreover, probabilistic transition rules are frequently used in order to take into account traits like the efficiency of a predator, or phenomena like the movement of individuals. Finally, long-term dynamics of theoretical ecosystems is of great interest to ecologists, who aim to build predictive models, or to gain a greater understanding of the processes that control an ecosystem.

When observed, the spatial dynamics of cellular automata might appear random, complex, or even ordered. Such patterns are commonly responsible of the statistical properties that define a model. Understanding the role that local interactions have in determining the long-term dynamics of a probabilistic cellular automaton is the main motivation of this dissertation.

1.2. Objectives

The main objective of this research is to describe the long term dynamics, spatial as well as temporal, of an ecological model based on cellular automata.

1.2.1. Particular objectives

- Development of a prey-predator model based on cellular automata, that serves as an experimental framework to study the global behavior of a lattice model.
- Design of a migration algorithm based on Particle Swarm Optimization (global and local) to model the movement of predators in a lattice model.
- Compare the global and local implementations of the migration algorithm through computer simulations, analysis of spatial patterns and statistical methods. Such comparison will serve to perform a qualitative analysis of the local interactions of the model and its effects on the long term dynamics of the model.
- Development of a mean-field model to predict the long-term mean densities of preys and predators at small and large spatial scales.

1.3. Lattice models in ecology

To mark an exact moment when models based on cellular automata attracted the attention of ecologists is a difficult task, so instead, we will start with an interesting article by D. A. Dewdney that appeared in the column "Computer Recreations" of the Scientific American magazine [18]. The article describes a model called Wa-Tor, short for 'water torus', since its only inhabited by sharks and fishes, and they live in a torus shaped lattice. The rules that govern this model are applied synchronously in discrete time steps, and are as follows:

- A fish moves randomly to one of its four adjacent neighbors, provided that the cell is not already occupied by a shark or a fish. If the four cells are already occupied, the fish does not move.
- A shark checks its four nearest neighbors, if some of them are occupied by fishes, it moves to one of them at random and then devours the fish. If there are no fishes among its neighbors, a shark moves just as a fish does, i.e., avoiding other sharks.

Reproduction is controlled by two parameters: *fbreed* and *sbreed* determine the number of time steps that a fish or shark respectively must exist before producing a single offspring. An additional parameter *starve* designates the number of time steps that a shark can survive without eating a fish. The spatial dynamics of the Wa-Tor model show that fishes moving in a region with no sharks, quickly reproduce to form a school, if such group is discovered by one or more sharks, they attack the school from the edges and promptly devour most of the group, isolated sharks die from starvation. Even though such patterns are at most an over-simplification of a natural process, they show that a model with an interesting spatial dynamics can be built parting from the explicit description of the interactions among the members of a theoretical population (later we will review some extension made to the Wa-Tor model in order to study scaling problems in ecology). A first step is then to define the evolution rules based on reasonable assumptions about the natural process that is to be studied, if such assumptions are "correct", it is expected that the results obtained from the model help to understand the behavior of the desired process, or even predict some of its statistical properties.

A phenomenon that is particularly useful to study the relationship between spatial patterns and the long-term dynamics of a lattice model is that of competition. Such phenomenon occurs as an interaction between individuals of the same (intraspecific competition), or different species (interspecific competition), that share a need for one or more resources [19]. Competition occurs because individuals aggregate at some level, for the intraspecific case, competition depends upon the proximity of neighbors within a group; for the interspecific case, competition commonly occurs at the boundaries between organisms of different species. In both cases, however, the spatial arrangement of individuals determines the level of competition that any individual experiences. Silvertown et al., (see [20]) used a cellular automaton to study interspecific competition among five species of grass, the automaton follows a replacement rule in order to model invasion of competitive strong species. The rule is as follows: at each time step species i in a cell is replaced randomly by a neighbouring species j with

probability p_{ij} weighted by the number of neighbors containing species j . Replacement probabilities p_{ij} were obtained taking as basis a field study on invasion rates in hexagonal plots of grass. Experiments were made to determine the importance of aggregation on the persistence of a competing species, the results show that if individuals of the five species of grass are placed randomly on the lattice, the least competing species are rapidly driven to extinction by the more invasive ones (those with a greater replacement probability). If initial conditions are changed so each species starts in an aggregated manner, the extinction of the least invasive species is delayed, such outcome is to be expected, since now competition only occurs at the boundaries between groups of different species. In the end, however, only the two strongest invaders persist in the long term.

Another study that focus on the coexistence of competing species appears in [21]. The authors analyse the relationship between the stability of an ecosystem and its complexity (a complex ecosystem contains a great diversity of species that interact between them), in particular, it is suggested that complex ecosystems are more stable than simple ones. The model employs a two-dimensional lattice, where each cell can be in one of 254 different states, each state identifies a different species. A replacement rule governs the evolution of the model as follows: an individual of species i moves to another cell, if the cell is occupied by an individual of species j , then with probability $p_m(i, j)$ the individual of species i occupies the target cell and the individual of species j is killed. The rule can operate in two modes:

- Global (mean-field) mode. Individuals move randomly to any cell of the lattice, thus eliminating any spatial structure of the model, hence the mean-field name.
- Local mode. Individuals move randomly to one of their four nearest neighbors, for this mode the lattice implements reflective boundaries.

Probabilities $p_m(i, j)$ are calculated using the “interaction coefficients” a_{ij} and a_{ji} , these quantities determines the effects that one species has on the other, which is an analogous treatment to the one found in other competition models, e.g., if $a_{ij} < 0$ and $a_{ji} > 0$ then species i has a negative effect on species j , however, species j has a positive effect on species i , these conditions corresponds to a prey-predator relationship, with species i being the predator. In a competing environment such as the one used by the authors, it is expected that only some of the species that exist initially survive in the long-term. The results show that in all instances where the evolution rule operates in local mode, individuals belonging to the same species aggregate into clusters, such mechanism allows inferior competitors to survive in zones where the density of strong competitors is low, which results in an ecosystem with a greater diversity of species than the observed in the simulations ran with the global mode of operation.

Lattice models whose evolution is determined by replacement rules that operate within a neighborhood will often exhibit aggregation of individuals into clusters. This process occurs when an individual is excluded by a neighbor belonging to a stronger competitor species, the space originally occupied by the excluded individual will be colonized either by the competitor or by its offspring, a sequence of such events will produce a cluster of the invading species. In a model where multiple species compete among each other, the long-term density of each one depends on the number of interactions with other species and on the probability with which replaces them. Other works that analyse the coexistence of multiple competing species, use probabilistic rules that depend on the local density of a species to determine the new state of a cell. In [22] the authors study species diversity using a lattice model where 10 species compete, the probability of colonization of a particular cell by any species is proportional to the density within the nearest neighbors of a cell, results from computer simulations are of similar nature to those observed in models that use replacement rules. There is aggregation of species into clusters, however, dominance of a species depends solely on the spatial distribution of its individuals, the authors note that despite that in the long-term dominance of a single species should be expected, it is possible for several species to coexist if some cells are made unsuitable for colonization. Additional results concerning spatial patterns and their effect on competition can be found in [23] and [24].

Besides competition, another mechanism that favours the formation of patterns in ecological lattice models is the dispersal of individuals through movement and reproduction [25] [26]. A good approach to model such phenomenon is to use transition rules that correspond to a diffusion process. In [27] Comins et al. study a host-parasitoid model on a rectangular grid of patches. Each generation a fraction

of hosts and parasitoids disperse towards the eight nearest neighboring patches, while the remainder individuals stay behind to reproduce; interactions between host and parasitoids occur according to the standard Nicholson-Bailey model of parasitism. The effects of the diffusion on the spatial dynamics of the model are evident in simulations of the "epidemic" type: there is a wavefront of hosts, traveling at constant speed, that invades unoccupied space; this event is followed by a front of parasitoids that consumes the original wave of hosts. Depending on the fraction of hosts that disperse each generation several spatial patterns might be observed: low rates of host dispersal lead to spatial chaos, intermediate rates results in spirals, and low rates of host dispersal combined with high rates of parasitoid dispersal produce "crystal" patterns. The authors note that despite the fact that the presence of any of these patterns leads to the coexistence of both species, there is a threshold for the size of the grid below which extinction is always observed.

A comparative study of the effects of diffusion processes in spatial models appears in [28], the authors analyse the behavior of four different spatial prey-predator models (reaction-diffusion equations, coupled map lattices, cellular automata and integrodifference equations) where prey suffer the invasion of predators. Simulations of one-dimensional versions of each model show the expected wave front of predators invading the prey-only state, leaving behind a coexistence state. The authors focus their attention on the spatial dynamics behind the initial wavefront of predators where three different phenomena are observed:

- Regular spatio-temporal oscillations. For this case, periodic travelling waves moving at a different speed than the original front are observed, such waves correspond to a family of solutions for the model based on reaction diffusion equations. A similar behavior is observed for the coupled map lattice and the integrodifference equations: there are periodic waves behind the invasion front, however, these move in the opposite direction. A plot in the prey-predator plane for the coupled map lattice shows that densities move irregularly around a limit cycle. In the cellular automaton periodic waves are also observed sometimes moving along the invasive front and sometimes moving in the opposite direction.
- Irregular spatio-temporal oscillations. For the reaction diffusion equations, certain parameters might force the travelling wave solution into irregular oscillations, the authors note that such pattern might be associated with spatial chaos. The same behavior is observed for the coupled map lattice and the integrodifference equations, irregularities expand from the focus of the invasion suggesting again that such dynamics are chaotic. No spatial irregularities are observed in the cellular automaton when biological relevant parameters are used.
- Irregular fluctuations. Here, there is a band of periodic waves immediately behind the invasive front, following this band there are irregular oscillations with no apparent pattern. This behavior corresponds to a transient due to an unstable periodic wave solution, an analogous behavior is observed in the coupled map lattice and the integrodifference equations model. This behavior was not observed in the cellular automaton model.

Similar patterns were obtained in [29] for a probabilistic cellular automaton. By carrying numerical simulations, the authors were able to obtain the critical exponents for the automaton, thus allowing the classification of the model into the directed percolation universality class.

Fu et al. [30] showed that for a lattice model where individuals engage in pairwise interactions, according to the rules of the prisoner's dilemma or the snowdrift game, it is possible for cooperators to expand and dominate a population, even though a "defection" yields the most benefit. Simulations using the prisoner's dilemma rules shows that for a low cost-benefit ratio, cooperators expand into a single cluster with a few strands of defectors, as individuals incurs in higher cost for lower benefits, defectors split the cluster of cooperators into smaller fragments, finally there is a critical point beyond any attempt of invasion by the cooperators fails. When the snowdrift rules are used, low cost-benefit ratios also lead to a single cluster of cooperators, however, defectors now form isolated "spots"; as the cost-benefit ratio increases, the cluster breaks down into filament-like structures containing a few cooperators.

Diffusion-like transition rules offer a simple and mathematically tractable way to describe the dispersal of individuals in a lattice model; however, there has been efforts to develop other strategies

that better mimic phenomena found in natural ecosystems. A lattice model that focuses on the survival strategies taken by preys and predators appears in [31], the model considers a *pursuit and evasion* neighborhood where predators move to catch preys, and preys move to escape from predators, and a *predation neighborhood* where predation takes place. The transition rules that govern this model are as follows:

1. A prey is captured and eaten with probability d_h by each predator in its predation neighborhood.
2. A prey produces an offspring with probability b_h at an empty neighbouring cell, providing that there are no predation in its neighborhood.
3. If predation is successful, a predator has probability b_p of producing an offspring at the cell previously occupied by the prey.
4. Independently of any other events, a predator has probability d_p of dying.
5. Preys flee from predators, and predators pursue preys. In order to catch a prey, predators move to one of their eight nearest neighbors following the direction of highest prey-density; similarly, to escape from predators, preys move in the opposite direction of highest predator density. An average of $m_h HN$ preys are selected to flee from predators, where m_h is a positive integer, H is the density of preys and N is the total number of cells in the lattice, similarly, a fraction $m_p PN$ of predators are selected to pursue preys, where m_p is a positive integer and P is the density of preys.

Simulations of this model show that as they move away from predators, preys form clusters which are promptly surrounded by predators. For $m_p = m_h = m$, there is a critical value $m = m_0$ below which predators become extinct and preys cover the whole lattice. Above this value, a non trivial fixed point where preys and predators coexist is obtained. Large values of m produce an inhomogeneous lattice where several patterns may be observed: there are growing clusters of preys with only a few predators, collapsing clusters of preys surrounded by predators and regions dominated by predators that quickly die due to starvation. More interesting is the temporal evolution of the model under these conditions, there is a long transient with oscillations of big amplitude and some noisy oscillations can be observed in the long term, however, such behavior is damped as the size of the lattice is increased, in the limit $N \rightarrow \infty$ an evolution to a fixed point should be expected. In [32], [33] and [34], the analysis of the model proposed by Boccarda et al. is extended: the study of the evolution of the system in terms of the birth and death rate of predators reveals an absorbing state and a stationary regime where both population coexist. Furthermore, it is stated that the oscillatory behavior of the populations of preys and predators is caused by a dynamic percolation process, i.e., alternating percolation and non-percolation events.

In [35] the authors analyse the effects that predator pursuit (PP) and prey evasion (PE) have on the spatial synchrony of a prey-predator model. PP indicates that predators move from locations of low prey density to those with a higher density of preys, also predators move away from zones with a high predator density; similarly, PE corresponds to preys moving from zones with a high predator density to location where predators are scarce, also preys move away from zones with a high prey density. The resulting spatial dynamics are chaotic and present aggregation of preys and predators, such behavior indicates that there is no spatial synchrony in the observed patterns. Simulations of the models without PP and PE show spatial waves which indicates the presence of spatial synchrony.

A model that studies the movement of predators and its role on the persistence of preys and predators appears in [36]. The authors employ a prey-predator model that includes pursuit and evasion processes based on a “range of vision”, i.e., when moving, a predator chooses the direction of highest concentration of preys, on the contrary, preys move in the direction with the lowest number of predators. Simulations where different ranges of vision are assigned at random to an official to an initial population predators (such ranges remain fixed and children inherit this trait from their parents) show that those predators having the highest range of vision are able to survive; on the other hand, preys having the smallest vision range survive the simulation.

The models presented so far are only an small example of the wide range of spatial patterns that may be observed in lattice models; however, a question remains: What role do local interactions and

spatial patterns play in determining the long-term dynamics of an stochastic lattice model? A good place to start is a series of formal results about a two-state stochastic lattice model known as the basic contact process. The model describes the life cycle of a plant through the following rules:

1. A plant (a cell in state one) dies (changes its state to zero) with probability γ ; otherwise survives (remains in state one) with probability $1 - \gamma$.
2. If a plant at a cell x survives, then there is probability $\beta(x, y)$ of sending a seed to the cell y .
3. If one or more seeds are sent to a cell y , or if plant at y survives, then y has state one at the next time step; otherwise the cell will be in state zero.

This model has been the subject of a great number of studies, and many of its properties are now well understood, for a summary of the most important results about the contact process see [37] and [38]. The following results are listed due to its relevance to this dissertation:

- There exist a critical value of γ called γ_c , above which the probability that the plant avoids extinction is zero. This follows from the fact that as the death probability increases, it is more difficult for the plant to survive.
- If the plant does not go extinct, the process converges exponentially fast to the equilibrium. Moreover when the value of γ is close to γ_c the rate of convergence is slow.
- The most important result about the contact process is the *complete convergence theorem* [39], which states that if the plant avoids extinction, then the process will converge to an stationary distribution which is the limit when the process starts with a configuration where all cells are in state one. In words, the theorem says that for an arbitrary initial configuration, if the plant survives for a long enough time, then in the limit it looks like as if the process has started from a configuration where all cells are in state one. An interesting consequence of the theorem is that the only stationary distributions for the model are: a) the limit starting from the all ones configuration, b) the trivial stationary distribution of the all zeroes configuration and c) a linear combination of both. The complete convergence theorem provides a complete landscape of the outcome of the interactions in the basic contact process; for some prey-predators models, besides the trivial all zeroes configuration that represents extinction, and a configuration where species coexist, it is also possible to obtain another stationary distribution where the lattice is completely covered by preys.
- In order to analyse the behavior of a lattice model, it is common to construct a set of equations that describe the change in density of all states in the model; such set is obtained by considering that there is no correlation between the states of the cells of the lattice. It is well known that such equations constitutes only a poor representation of the behavior of a lattice model; however if the dispersal range r is large, then the states of the cells are almost independent and the equations become more accurate. In general the prediction made by the mean field equations becomes exact in the limit $r \rightarrow \infty$. In [38] Durrett and Levin show such behavior for the density of empty cells observed in the lattice model, and the mean field equations that describe the change in density of such cells.

In a related work (see [40]), Durrett and Levin analyse the evolutionary game known as “hawks and doves”, the interaction between these two species are described by the following game matrix:

	H	D
H	a	b
D	c	d

Table 1.1: Game matrix for the “hawks and doves” game.

where:

- H denotes a hawk.
- D represents a dove.
- a , b , c and d are the interactions payoffs, e.g., a is the payoff to a hawks when interaction with other hawks, such quantity represents the density dependent growth rate of hawks.

The authors propose that the behavior of an stochastic spatial model could be determined from the properties of the corresponding “mean field” equations, i.e., the equations for the densities of states which results from pretending that the states of adjacent cells are independent. The following classification is given:

- Case I. If there is a globally attracting fixed point then there is a unique equilibrium that is the limit starting from any initial state in which both species have positive density.
- Case II. There exist two locally attracting fixed points in the equations, their long-term behavior depends on the initial conditions; meanwhile, for the corresponding spatial model, the stronger species always covers the entire lattice.
- Case III. Periodic orbits in the mean field equations. The long-term behavior of the corresponding lattice model depends on the scale of the lattice. At small scales, random oscillations of the densities of both populations can be observed; for medium length scales, the oscillations become smoother; finally for large scales, there is an oscillatory transient after which densities become almost constant.

Case I is observed in models where the fitness of one type of individual is enhanced by the presence of individuals of another kind, examples of such interactions can be found in [41] [42]. Case II corresponds to a classic competition scenario, if a strong competitor establishes itself in some region of the lattice, it will keep growing until the lattice is completely covered (see [22] [23] [43]).

Case III corresponds to oscillatory behavior, one of the most interesting phenomena that can be observed both in natural and theoretical prey-predator systems. The report on the number of pelts of the Canadian lynx and the snowshoe hare sold by the Hudson Bay-Company between 1835 and 1904 is one the most well known data sets in ecology, and is perhaps the best example of the consequences of prey-predator interactions. A plot of this data set shows oscillations that can be intuitively understood as follows: an increase of the population of lynxes causes an increase of the number of hares eaten, such reduction in the amount of food available for the lynxes provokes a new decrease of their population, which in turn allows a new increase in the number of hares. The mathematical study of such interactions goes back to the decade of 1920 with the work of Alfred Lotka, who proposed a model to explain oscillations observed in the number of fishes caught in the Adriatic sea, and the work of Vito Volterra who obtained a similar model using reacting chemical components that also showed oscillatory behavior.

A model that studies the grazing patterns of the snowshoe hare population and their relationship with the oscillatory behavior of the population appears in [44]. The model employs the following rules to mimic the life cycle of the hares:

1. Motion. Hares are able to move to a neighboring cell at each time step, however, there is a greater probability of motion in the direction where the density of vegetation is higher.
2. Vegetation growth. Vegetation grows at rate VI on every patch until a maximum density MV is reached
3. Nourishment. Hares eat the vegetation at their cell and transform a fraction of the ingested food into biomass of their own population, according to a given efficiency.
4. Breeding. In order to reproduce, one male and one female must be present at the same cell, additionally hares can't reproduce until sexual maturity has been reached. When breeding they produce between two and eight new individuals, each new individual is placed randomly at one of the nearest neighbors if such neighbor is empty, otherwise, the offspring dies.

5. Death. Hares can die in one of four ways: they can die immediately after birth if no empty neighbors is available for dispersal. There is a global death rate independent of any other event. An individual may die of malnutrition if it has not eaten a minimum amount of vegetation after a given number of time steps. Finally an individual dies of old age after reaching the maximum allowed age for its species.

Each rule takes into account several parameters that reflect the biological information available about the ecosystem, e.g., the vegetation increase rate, breeding period of the hares, number of offspring, etc. Simulations of the model, using lattices with sizes ranging from 30×30 cells to 90×90 cells, show a limit cycle with a period of 9 to 11 years, which correspond to the period observed in the Hudson Bay data set. If a global motion rule is used, i.e., if hares are allowed to move to any cell of the lattice, the limit cycle disappears. The spatial dynamics of the model show target patterns and spirals that are responsible for the cyclic behavior observed: when a pattern is expanding, the density of hares increases accordingly, the time required until a peak is reached introduces temporal lags which produce the cyclic behavior. More important that the cyclic behavior per se is the fact that the local cycles of different regions of the lattice are synchronized, i.e., if measures of the density of hares are taken in proper subsets of the lattice, it is found that the cycles observed in these subsets are approximately in phase, again such results agree with data collected in natural populations.

Models studying more complex food chains also report the presence of regular oscillations, Blasius et al. [45] proposed a model to study the population dynamics of the Canadian lynx and the snowshoe hare. The model consist of a system of differential equations that represent a three-level food chain with predators feeding on herbivores, and herbivores consuming vegetation. Besides showing a typical limit-cycle behavior, this food chain model shows that the populations of preys and predators oscillate with an almost constant frequency. However, the amplitude at each peak of the time series is highly unpredictable, both of these features are present in the hare-lynx population data. When simulated in a regular array of patches linked by migration, all patches became synchronized to the same frequency. Nevertheless, the amplitudes of the populations observed in each individual patch were only weakly correlated. On the contrary when diffusion was eliminated, the population of each patch behave independently with no phase synchronization.

1.4. Organization of this thesis

This document is organized as follows: in Chapter 2 we start with a brief analysis of the logistic equation, this will serve to familiarize the reader with some basic terms. Furthermore, the logistic equation will serve to present an example of a dynamical system, used to model an ecological phenomenon, with a wide range of dynamics. Also, it will serve to introduce the basic tools of analysis that will later be used to describe the long term behavior of a cellular automaton. Next, the formal definition of cellular automaton is given, followed by the analysis of the spatial and temporal dynamics of elementary cellular automata. The rest of the chapter is devoted to present the theory behind Particle Swarm Optimization a tool borrowed from the field of evolutionary computing that will serve to improve the proposed model.

Chapter 3 presents some methodologies used to study the long-term dynamics of lattice models. For completeness, we also present previous works where such methodologies have been successfully applied.

Chapter 4 describes in detail the proposed model. We put special emphasis in explaining the use of Particle Swarm Optimization to model the movement of predators in the lattice.

Our experiments and results are presented in Chapter 5. We perform a qualitative analysis of the spatial dynamics of the model, aimed to describe the relationship between the local interactions of individuals and the long term dynamics of the model.

In Chapter 6 we perform a mean-field analysis of the proposed model. Besides showing that for large neighborhoods the dynamics of the mean-field equations and the dynamics of the proposed model are closely related, we show that the functional form of quantities such as the death probabilities of preys and predators remain unchanged for a varying neighborhood size.

Finally the conclusions are given in Chapter 7

1.5. Publications

- Mario Martínez Molina, Marco A. Moreno Armendáriz, Nareli Cruz Cortés and Juan Carlos Seck Tuoh Mora. Modelling prey-predator dynamics via particle swarm optimization and cellular automata. In **Advances in Soft Computing**, volume 7905 of Lecture Notes in Computer Science, pages 189-200. Springer Berlin / Heidelberg. 2011
- Mario Martínez Molina, Marco A. Moreno Armendáriz, Nareli Cruz Cortés and Juan Carlos Seck Tuoh Mora. Prey-predator dynamics and swarm intelligence on a cellular automata model. **Applied and Computational Mathematics**, volume 11-2, pages 243-266. 2012. Journal Citations Report, impact factor: 0.55 (2011)
- Mario Martínez Molina, Marco A. Moreno Armendáriz and Juan Carlos Seck Tuoh Mora. On the spatial dynamics and oscillatory behavior in a prey-predator model based on cellular automata and local particle swarm optimization. **Journal of Theoretical Biology**. Journal Citations Report, impact factor: 2.351 (2012)

Chapter 2

Background

2.1. Non Linear Dynamics in Ecosystems

The increase in size of a population, where reproduction occurs within an specific time frame, i.e., the population increases in discrete time steps, can be described through the next first-order non-linear difference equation:

$$N_{t+1} = f(N_t) \tag{2.1}$$

where N_t is the size of the population at time t . In an ecological context, f must satisfy the following properties [46]:

1. $f(0) = 0$
2. $f(N_t)$ increases monotonically to the value K , which represents the carrying capacity of the ecosystem.
3. If $f(N_t) > K \Rightarrow f(N_t) \rightarrow -\infty$

A well known equation that fulfills these requirements is the logistic map:

$$N_{t+1} = N_t (a - bN_t) \tag{2.2}$$

where:

- b determines the level of intraspecific competence that is present in the population, when $b = 0$, there is no competence, and N_t grows exponentially.
- a is the net reproduction rate of the population.

Figure 2.1a shows a plot of the logistic map with $a = 2$ and $b = 0.5$, here it is possible to observe an evolution towards a simple fixed point. As the value of a increases, it is possible to observe a wide range of dynamics: for $a = 3.5$, a limit cycle with period two is observed (see Figure 2.1b). The period of this limit cycle is doubled for $a = 3.55$ (see Figure 2.1c). If the value of a keeps increasing, the limit cycles disappear, and the population oscillates in an seemingly unpredictable manner. However, each N_{t+1} in this “random” sequence is related to the population size at time t , thus a plot of N_{t+1} vs N_t (see Figure 2.1d) reveals a well defined relationship between N_t and N_{t+1} . Due to the quadratic term in Equation 2.2, such relationship takes the form of a parabola.

By calculating the orbit, and obtaining the fixed points of a dynamical system such as Equation 2.2, it is possible to describe the dynamics that govern its behavior [47, 46]. The fixed points of the logistic map can be obtained by noting that if $N_t = K$, then $N_{t+1} = N_t$, and Equation 2.2 can be rewritten as follows:

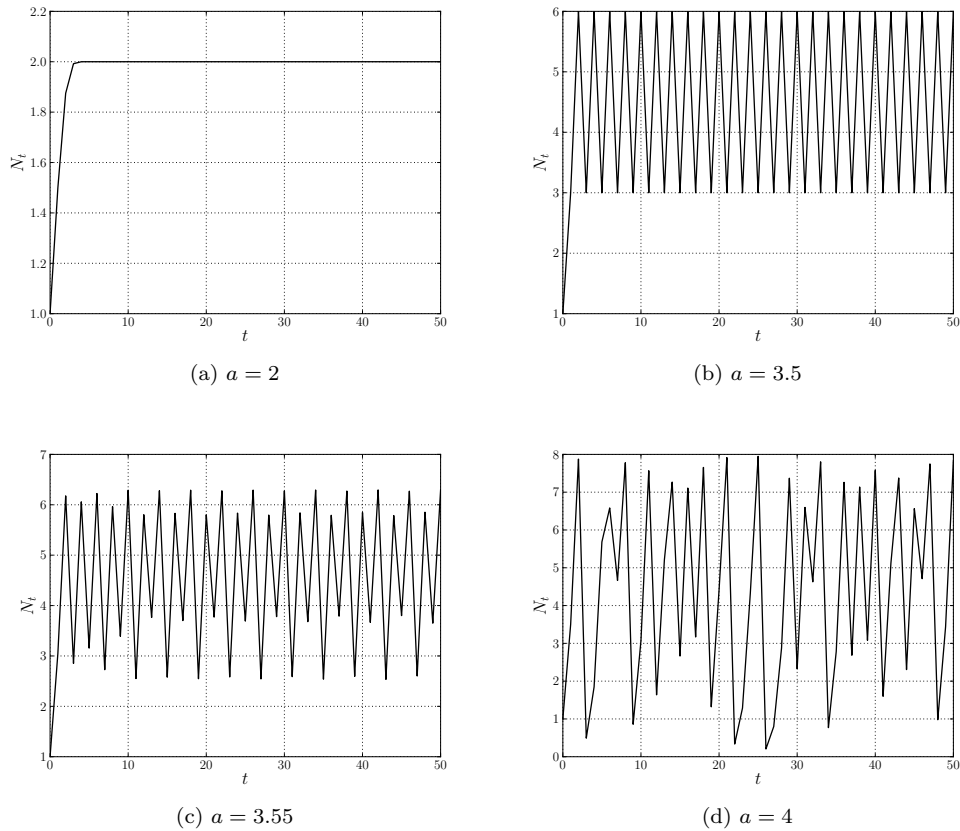


Figure 2.1: Evolution of the logistic map for an increasing reproduction rate.

$$N_t = N_t (a - bN_t) \quad (2.3)$$

By solving Equation 2.3 the next fixed points are obtained:

$$\begin{aligned} N_1^* &= 0 \\ N_2^* &= \frac{a-1}{b} \end{aligned}$$

N_1^* is a trivial fixed point, since any population devoid of individuals, will remain in that way for all time steps. If $a = 2$ and $b = 0.5$, then $N_t = 2$, which is consistent with Figure 2.1a. The fixed point N_2^* will be locally stable if and only if $|f'(N^*)| < 1$, since $f'(N_2^*) = 2 - a$, this fixed point will be locally stable in the interval $1 < a < 3$. Moreover, when $a \geq 1$, $f(N_t)$ does not have the desired properties of a model that describes the increase in size of a population.

When $a = 3$, $f'(N_2^*) = -1$, the graph of $f(N_t)$ is perpendicular to the line with slope 1 at the point where $N_{t+1} = N_t$. For $a > 3$, N_2^* becomes unstable ($|f'(N^*)| > 1$), forming a limit cycle of period 2, the fixed points of this limit cycle can be found by solving $f^2(N_t) = N_t$, where $f^2(N_t)$ denotes $f(f(N_t))$, thus we may proceed as follows:

$$\begin{aligned} f^2(N_t) &= N_t \\ [N_t(a - bN_t)] [a - b(N_t(a - bN_t))] &= N_t \end{aligned}$$

Expanding the factors:

$$(a^2 - 1)N_t + (-a^2b - ab)N_t^2 + 2ab^2N_t^3 - b^3N_t^4 = 0 \quad (2.4)$$

Since $f^2(N_1^*) = N_1^*$ and $f^2(N_2^*) = N_2^*$, these are two solutions to Equation 2.4, thus it is possible to divide such equation by the factor $(N_t - N_1^*)(N_t - N_2^*)$ to obtain:

$$b^2N_t^2 - b(a+1)N_t + a+1 \quad (2.5)$$

The roots of this polynomial define the cycles of period two for the logistic map:

$$q_1 = \frac{a+1 + \sqrt{a^2 - 2a - 3}}{2b} \quad (2.6)$$

$$q_2 = \frac{a+1 - \sqrt{a^2 - 2a - 3}}{2b} \quad (2.7)$$

Note that the limit cycle exists only in the interval $[-\infty, -1] \cup [3, \infty]$, furthermore the existence of the cycle depends on the level of competence present in the population ($b \neq 0$). Of course, the values of a lesser than -1 are not of interest for our analysis. When $a = 3.5$ and $b = 0.5$, the points that define the limit cycle are: $q_1 = 3$ and $q_2 = 6$, such result is consistent with Figure 2.1b.

Figure 2.2 shows the plot of $f^2(N_t)$ before and after the bifurcation, the fixed and periodic points may be found by locating the intersection of $f^2(N_t)$ with the identity function. If $a < 3$, then N_2^* is an attracting fixed point. For all $a \geq 3$, N_2^* becomes a repelling fixed point, the graph of $f^2(N_t)$ twists around this fixed point to produce a limit cycle with period two, having periodic points q_1 and q_2 .

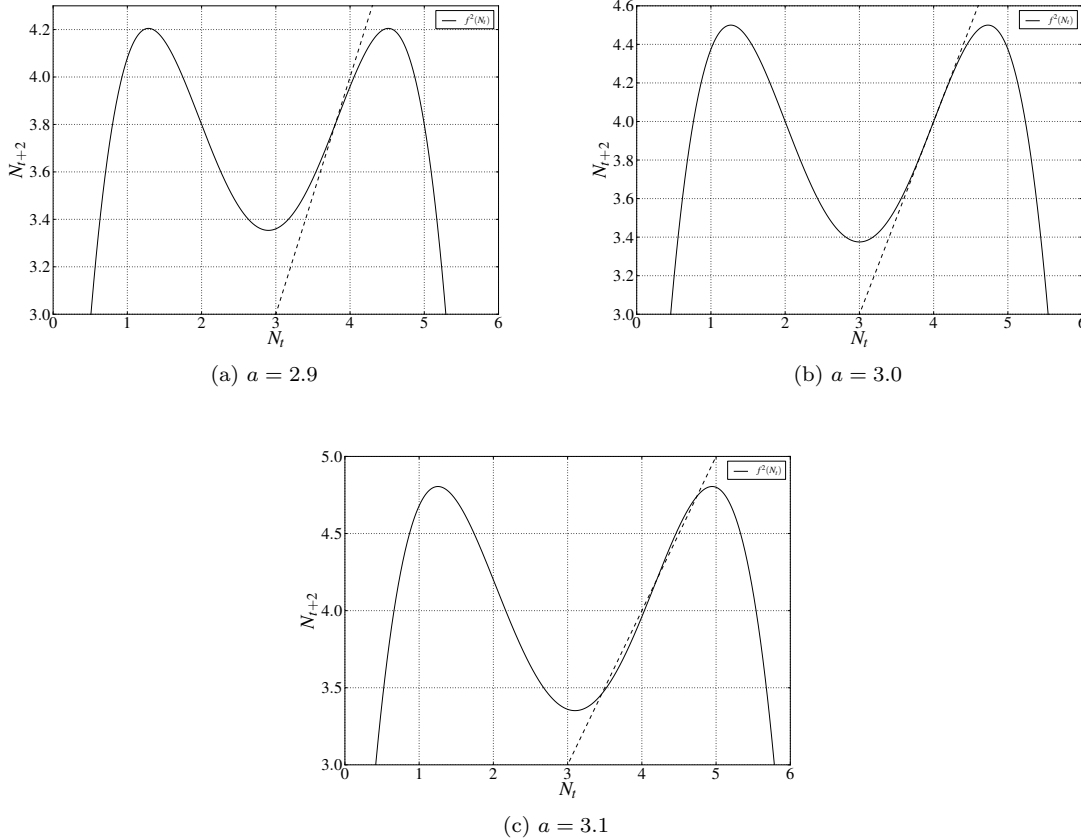


Figure 2.2: Period-doubling bifurcation.

Each point in the limit cycle might experience a new bifurcation, thus a limit cycle with period two becomes a limit cycle with period four. This behavior is illustrated by the bifurcation diagram of the logistic map (see Figure 2.3), this diagram captures the asymptotic behavior of Equation 2.2. As the values of a increases. Note that in the interval $1 < a < 3$ there is only a single fixed point for each a ; for $a > 3$, such fixed point bifurcates into a limit cycle of period two, this cycle then bifurcates into a limit cycle of period four. This sequence of bifurcations continues as the value of a keeps increasing, eventually a point is reached where the orbit is not attracted to any kind of limit cycle. This period doubling phenomenon is one of the best known routes to chaos [46].

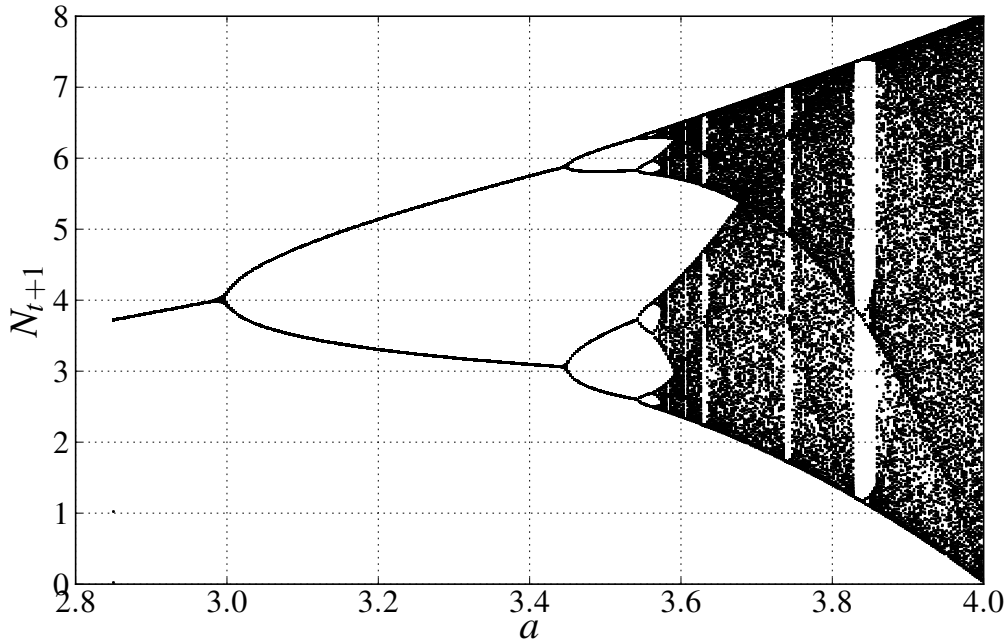


Figure 2.3: Bifurcation diagram for the logistic equation.

2.2. Cellular Automata

CA are dynamical systems discrete in time and space. They are adequate to model systems that can be described in terms of a massive collection of objects known as cells, which interact locally and synchronously. A cellular automaton is totally defined by the tuple $A = (d, Q, N, f)$, where:

- $d \in \mathbb{Z}^+$, is the dimension of the lattice $L \subseteq \mathbb{Z}^d$.
- Q is a finite set of states.
- N is a d -dimensional neighborhood vector:

$$N = (\vec{n}_1, \vec{n}_2, \dots, \vec{n}_m) \quad (2.8)$$

where each $\vec{n}_i \in \mathbb{Z}^d$ and $\vec{n}_i \neq \vec{n}_j$. Each \vec{n}_i specifies the relative locations of the neighbors of each cell [48], in particular, cell \vec{n} has coordinates $(0, 0, \dots, 0)$ and neighbors $\vec{n} + \vec{n}_i$ for $i = 1, 2, \dots, m$. In a two dimensional cellular automaton the Moore neighborhood is often used, it comprises the cell to evolve and its 8 nearest neighbors. It can be generalized as the d -dimensional M_r^d neighborhood [48] defined as:

$$M_r^d = \{n_i \in \mathbb{Z}^d \mid n_i = (n_{i_1}, \dots, n_{i_d}), n_{i_j} \leq r\} \quad (2.9)$$

- $f : Q^m \rightarrow Q$ is a local transition function that specifies the new state of a cell, taking into account the states of its neighbors.

A configuration of a d -dimensional cellular automaton is a function:

$$c : \mathbb{Z}^d \rightarrow Q \quad (2.10)$$

that assigns a state to each cell. The state of cell $\vec{n} \in \mathbb{Z}^d$ at time t is given by $c^t(\vec{n})$, the set of all configurations is $Q^{\mathbb{Z}^d}$. The local transition function provokes a global change in the configuration of the automata. Configuration c is changed into configuration c' , where for all $\vec{n} \in \mathbb{Z}^d$:

$$c'(\vec{n}) = f[c(\vec{n} + \vec{n}_1), c(\vec{n} + \vec{n}_2), \dots, c(\vec{n} + \vec{n}_m)] \quad (2.11)$$

The transformation $c \mapsto c'$ is the global transition function of the cellular automaton, defined as:

$$G : Q^{\mathbb{Z}^d} \rightarrow Q^{\mathbb{Z}^d} \quad (2.12)$$

The evolution in time of the cellular automaton is given by a sequence of iterations of function G , this sequence represents the orbit of a dynamical system starting from an initial configuration c :

$$orb(c) = c, G(c), G^2(c), \dots, G^t(c)$$

A configuration c is:

- A fixed point of G , if $G(c) = c$.
- Periodic, if $G^t(c) = c$, for some $t \in \mathbb{Z}$.
- Eventually fixed, if there is $n \in \mathbb{N}$ such that $G^{n+1}(c) = G^n(c)$, i.e., $G^n(c)$ is a fixed point for some n .
- Eventually periodic if there is $n \in \mathbb{N}$ and $t \in \mathbb{Z}^+$, such that $G^{n+t}(c) = G^n(c)$, i.e., $G^n(c)$ is periodic for some n .

2.2.1. Elementary cellular automata

This class of one-dimensional cellular automata were first studied by Wolfram [49], they can be defined by the tuple (d, Q, N, f) as follows:

- $d = 1$
- $Q = \{0, 1\}$
- $N = \{(-1), (0), (1)\}$
- $f : Q^3 \rightarrow Q$

Since $|Q| = 2$ and $|N| = 3$, there are 8 different configurations for a neighborhood, by assigning an element of Q to each configuration we construct a transition table for the cellular automaton, the last column of such table can be regarded as a binary digit, that when converted to decimal notation can be used to identify a CA rule. Table 2.1 shows the transition table for the rule 169, Figure 2.4 shows the corresponding evolution.

$c(\vec{n}-1)$	$c(\vec{n})$	$c(\vec{n}+1)$	$c(\vec{n})$
0	0	0	1
0	0	1	0
0	1	0	0
0	1	1	1
1	0	0	0
1	0	1	1
1	1	0	0
1	1	1	1

Table 2.1: Transition table for rule 169.

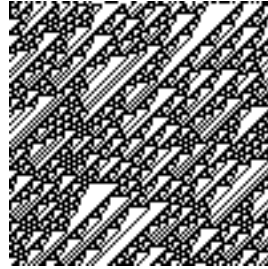


Figure 2.4: Evolution of rule 169.

2.2.2. Spatial dynamics of elementary cellular automata

In order to make easier the analysis of a cellular automaton, it is common to consider periodic boundaries, for one-dimensional automata, this means that the cells at the border of the lattice are connected, thus the lattice takes the form of a ring. The evolution of such rings depends greatly on their length, e.g., rings of length one, where a cell is its own left and right neighbor may evolve as follows:

- If the state of the ring is quiescent, then the configuration is a fixed point. For rule 169, “1” is a quiescent state since $f(1, 1, 1) = 1$, so the evolution of the ring is:

$$1 \mapsto 1$$

- The configuration is eventually fixed. The ring evolves towards a quiescent state, from which it cannot scape. A ring with the state “0”, evolving according to rule 169, fulfills these conditions.

$$0 \mapsto 1 \mapsto 1$$

- Periodic evolution: a state “0” evolves into state “1”, which evolves again into “0”. Rule 1 is a good example of this phenomenon:

$$0 \mapsto 1 \mapsto 0$$

As the length of the ring increases, its evolution may lead to configuration with longer periods, or multiple fixed points. Table 2.2 lists all of the 32 possible configurations for a ring of length 5. Several of such configurations show cyclic symmetry, e.g., 00001 \rightarrow 01100 and 00010 \rightarrow 11000. Table 2.3 shows these configurations in decimal notation, using this information it is possible to construct a diagram that shows the sequence of transitions for the ring (see Figure 2.5), the result of this construction is a collection of “trees rooted on cycles”, where each group of configurations belonging to a particular cycle represents a different symmetry class.

From Figure 2.5 we can conclude:

- Configuration 31 is a fixed point.
- Configuration 0 is eventually fixed since it evolves into configuration 31
- There are two cycles of period 5, the first is formed by configurations 26, 21, 11, 22 and 13, the second is formed by configurations 27, 23, 15, 30 and 29
- There is one cycle of period 15, formed by configurations 1, 12, 9, 16, 6, 20, 8, 2, 10, 4, 17, 5, 2, 24 and 18

c	$G(c)$	c	$G(c)$
00000	11111	10000	00110
00001	01100	10001	00101
00010	11000	10010	00001
00011	01010	10011	00011
00100	10001	10100	01000
00101	00010	10101	01011
00110	10100	10110	01101
00111	00110	10111	01111
01000	00011	11000	10010
01001	10000	11001	10001
01010	00100	11010	10101
01011	10110	11011	10111
01100	01001	11100	11000
01101	11010	11101	11011
01110	01100	11110	11101
01111	11110	11111	11111

Table 2.2: Configurations for a ring of length 5.

c	$G(c)$	c	$G(c)$
0	31	16	6
1	12	17	5
2	24	18	1
3	10	19	3
4	17	20	8
5	2	21	11
6	20	22	13
7	6	23	15
8	3	24	18
9	16	25	17
10	4	26	21
11	22	27	23
12	9	28	24
13	26	29	27
14	12	30	29
15	30	31	31

Table 2.3: Configurations in decimal notation.

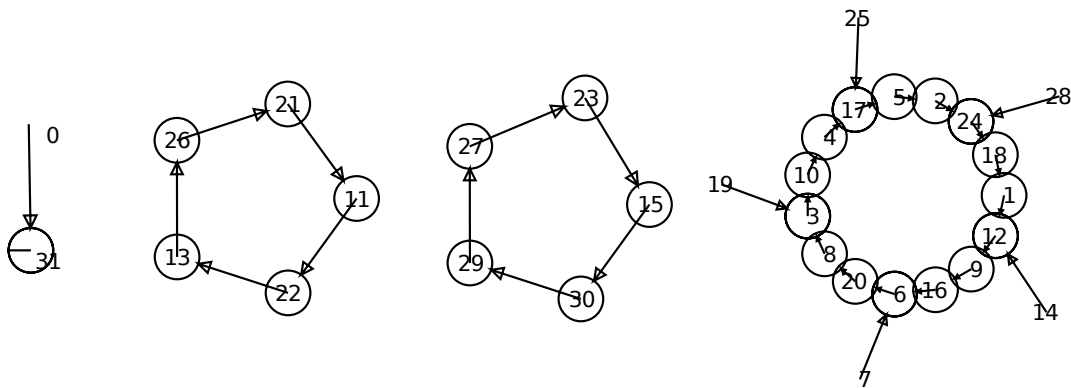


Figure 2.5: Symmetry classes for a ring of length 5.

- Configurations 19, 25, 28, 14 and 7 are eventually periodic, since they evolve into the cycle of period 15

De Bruijn diagrams were originally used to analyse sequences of symbols from an alphabet in the context of shift dynamical systems, thus they provide an excellent tool to describe the evolution of a cellular automaton (for a detailed analysis see [50]). In the one-dimensional case, a De Bruijn diagram is a directed graph with k^{2r} nodes and k^{2r+1} edges, with $r = (|N| - 1)/2$. Each node is a sequence of $2r$ symbols from the set of states Q , two nodes are connected if the last $2r - 1$ symbols from the initial node are the same that the first $2r - 1$ symbols of the final node. Each edge of the graph represents a complete neighborhood of the CA, thus edges describe the way in which neighborhoods overlap. Sometimes the edge is labeled using this neighborhood, in some other cases it is labeled using the state at which the neighborhood evolves. Figure 2.6a shows the de Bruijn diagram for rule 169. Paths in the diagram might represent configurations or classes of configurations related to the evolution of the automata. If some criteria exists to eliminate certain edges, the resulting sub-diagram consists of those neighborhoods that match the elimination criteria. If we eliminate those edges that represent neighborhoods where the transition does not change the state of a cell, the resulting diagram (see Figure 2.6b) defines sequences which are invariant to the evolution of the automaton, the so called

“still lifes”. There are two still lifes for rule 169, the first represented by strings in 1^* (the operator $*$ represents the Kleene star), and the second by strings in $00(1^*)$.

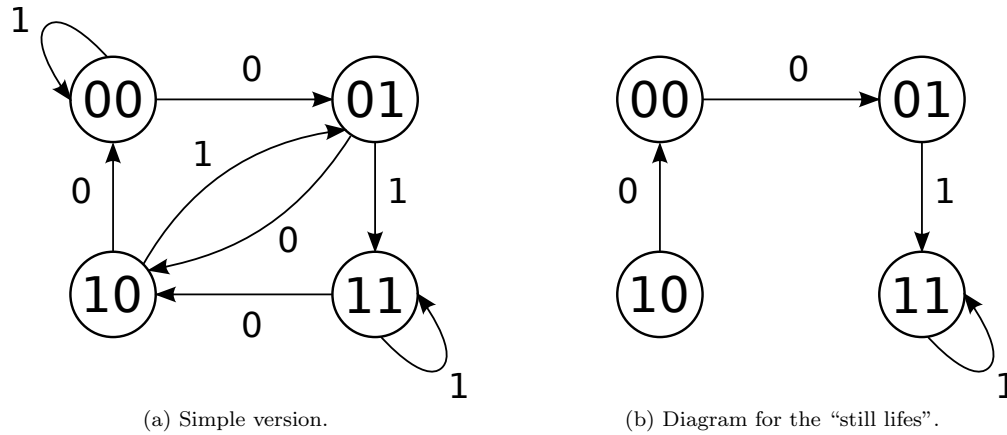


Figure 2.6: De Bruijn diagrams for rule 169.

It is possible to describe periodic configurations through a de Bruijn diagram, e.g., it is possible to describe configuration that moves faster than r each generation, such configuration are called “superluminal”. Let us consider (for rule 169) a shift of two cells to the right each generation, to determine the configurations that match this criteria follow the next procedure:

1. Start with a neighborhood of three cells denoted by abc (see Figure 2.7)
2. Let x be the cell whose state is determined by abc , since x is the result of a shift of two cells to the right, there is a cell to the left of a that also has state of x .
3. Let y be the cell whose state is determined by the neighborhood bcd , however, due to the shift, the state of this cell is that of cell a . Up to this point, the state of cell d is unknown.
4. To determine the state of cell d , it is necessary to use the transition table of rule 169, the partial neighborhood bc , and the state of cell y give enough information to calculate the state of cell d . According to Table 2.1 there is only one possible state that fulfills the conditions described thus far, though this is not necessarily true for other rules.
5. Once the state of cell d has been obtained, we can express the neighborhood $xabcd$ as the overlap of two partial neighborhoods: $xabc$ and $abcd$, each one of these represents a node in a de Bruijn diagram, since the starting neighborhood abc can be chosen in 8 different ways (since $|Q| = 2$, the resulting de Bruijn diagram will have 8 nodes.

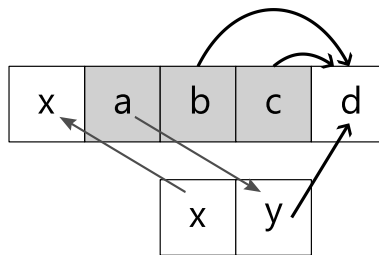


Figure 2.7: A shift of two cells to the right in one generation.

Figure 2.8a shows the de Bruijn graph for the previously described shift, in such diagram the nodes have been colored according to the state of the rightmost cell in the partial neighborhood represented by a node. A path in the graph represents a configuration with the desired shift, from the analysis of the diagram we can conclude:

- Configuration 1^* represents a trivial shift, since any group of only ones can only evolve in another group of ones.
- There is a cycle of length 3, represented by configuration $(110)^*$, the evolution of such configuration is shown in Figure 2.8b
- There is a cycle of length 4 corresponding to configuration $(1000)^*$, the evolution of this configuration is show in Figure 2.8c

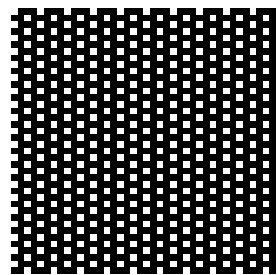
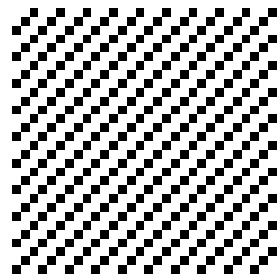
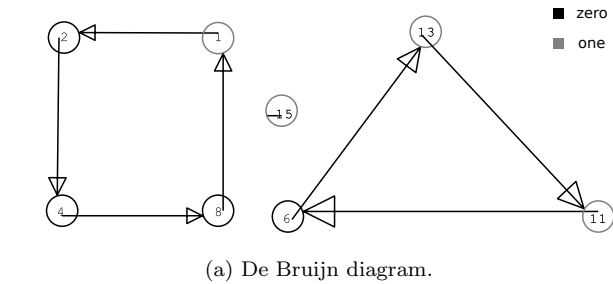


Figure 2.8: A shift of two cells to the right in one generation according to rule 169.

A similar procedure can be used to obtain longer shifts with bigger periods. Figure 2.9 shows the de Bruijn diagram for a shift of three cells in two generations, the results given by the analysis of the graph are as follows:

- There exists a cycle of length 5 represented by $(01011)^*$ (see Figure 2.9b).
- A second cycle of length 5 includes configurations of the form: $(11110)^*$, Figure 2.9c shows the evolution of this configuration.
- Configurations in $(010011100100011000001)^*$ form a cycle of length 21, the corresponding evolution is shown in Figure 2.9d

2.3. Mean field theory for elementary cellular automata

Another interesting question regarding the long term behavior of a cellular automaton concerns the evolution of the density of a certain state $q \in Q$, i.e., is it possible to predict the number of cells having state q as the evolution of the automaton proceeds?

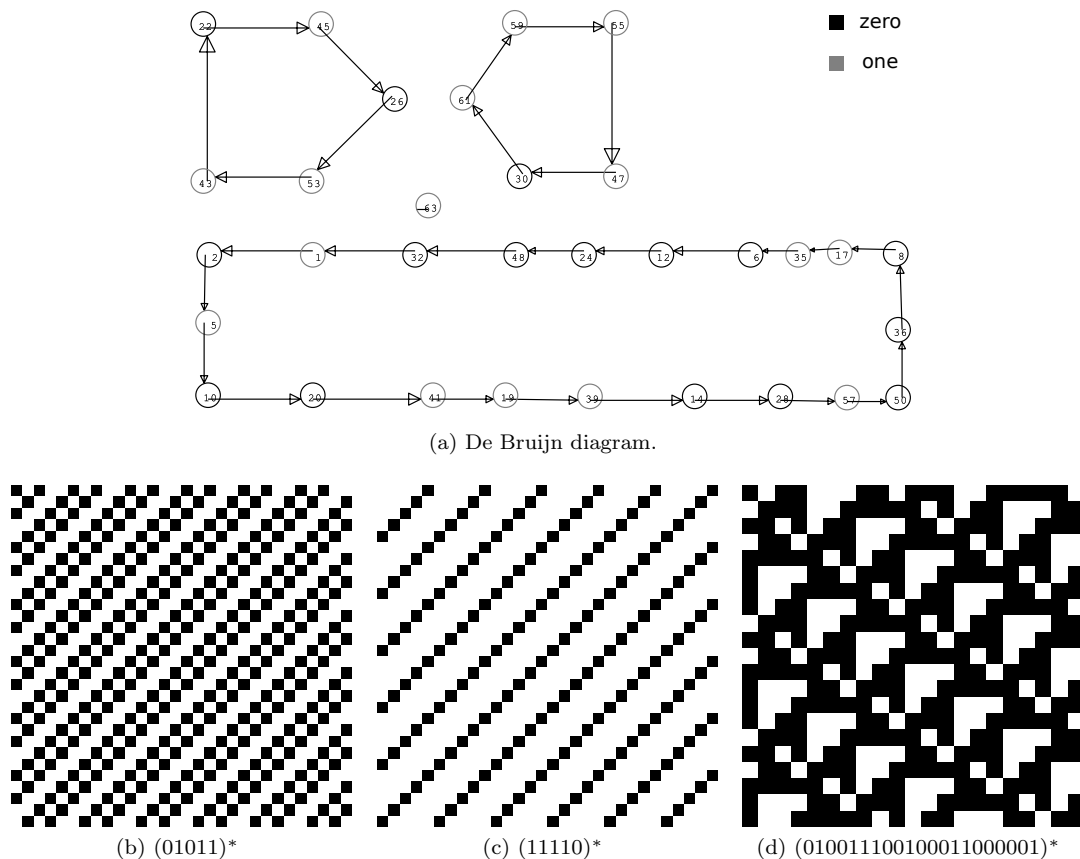


Figure 2.9: Shifts of three cells in two generations for rule 169.

A simple approach would be to count the number of configurations that evolve into q . Consider once again the transition function for rule 169 (see Table 2.1), if we wish to calculate the probability of having a cell with state one, we see that there are four neighborhoods that produce this state, since there are 8 possible configurations, the probability of having this state would be $1/2$, of course there are no reasons to make each configuration equally likely, so a more reasonable approach would be to assign different probabilities to each state in Q , and then calculate the probability of each configuration of the neighborhood.

The mean field theory arises from the assumption that the probabilities for each one of the cells in a neighborhood are independent, since the neighborhoods overlap, this assumption is of course wrong, however, it represents a good compromise between the ease of analysis and accuracy [51]. Let p denote the probability of a cell having state one, and $1 - p$ the probability of state zero, since we assume independence, we can calculate the probability of a particular configuration through the product of individual probabilities, e.g.:

$$P(010) = (1 - p)(p)(1 - p) = p(1 - p)^2$$

If $w = (c(\vec{n} + \vec{n}_1), \dots, c(\vec{n} + \vec{n}_m)) \in Q^m$ is a configuration of the neighbors of cell \vec{n} , then

$$W_q = \{w : f(w) = q\} \tag{2.13}$$

is the set of all configurations that evolve into state q . According to this we can compute the probability of a cell having state q at time $t + 1$ as follows:

$$P(c^{t+1}(\vec{n}) = q) = \sum_{W_q} P(w) \tag{2.14}$$

To clarify this, consider the probability of having a one in $t+1$ in a cellular automaton that evolves according to rule 169, such probability is given by:

$$\begin{aligned}
 P(c^{t+1}(\vec{n}) = 1) &= P(000) + P(011) + P(101) + P(111) \\
 P(c^{t+1}(\vec{n}) = 1) &= (1-p)^3 + p^2(1-p) + p^2(1-p) + p^3 \\
 P(c^{t+1}(\vec{n}) = 1) &= -2p^3 + 5p^2 - 3p + 1
 \end{aligned} \tag{2.15}$$

Just as we did with the logistic equation, we may obtain the fixed points for the density equation by solving:

$$p = -2p^3 + 5p^2 - 3p + 1 \tag{2.16}$$

The fixed points are $p_1^* = 0.5$ and $p_2^* = 1$. The derivative at p_1^* is 0.5, so this is an attracting fixed point. The derivative at p_2^* is 1.0, i.e., a neutral fixed point. To further analyze this results we may plot the orbit of Equation 2.15 by means of a cobweb diagram. Figure 2.10a shows an orbit starting from a density of 0.01, the plot shows that p_2^* repels this orbit during the first iterations to finally decay into p_1 , thus we can expect a long transient until the orbit stabilizes. A similar plot starting from a density of 0.8 is shown in Figure 2.10b, here it is possible to observe a rapid decay into p_1^* .

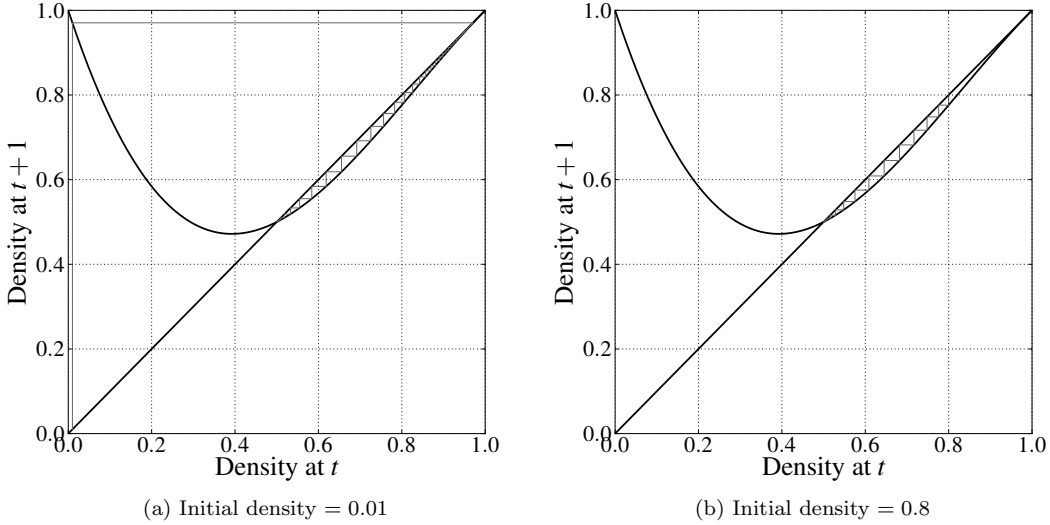
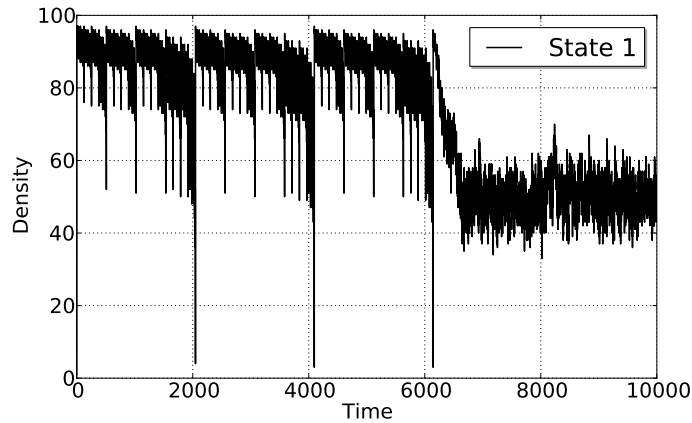
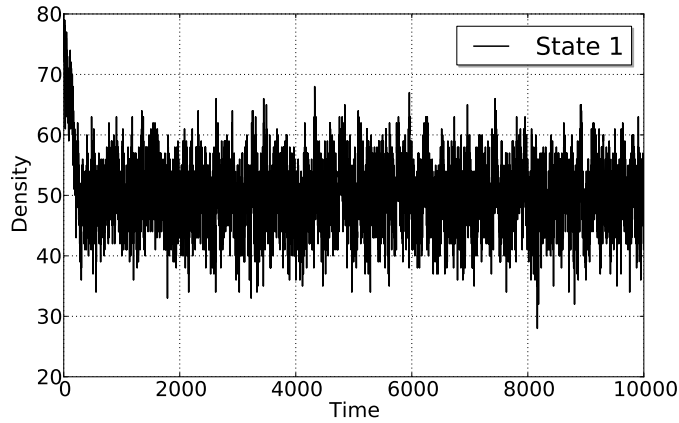


Figure 2.10: Mean field theory predictions.

A simulation of the automaton (Figure 2.11a) with an initial density of 0.01 confirms the transient predicted by figure 2.10a, however, instead of stabilizing, the number of cells with state one oscillates around the predicted density of 0.5 (the plots shown correspond to a ring of length 100). The corresponding simulation for an initial density of 0.8 is shown in Figure 2.11b the results show a similar behavior as the one predicted by figure 2.10b, i.e, a rapid decay away from p_2^* followed by an oscillation around p_1^* . There is then a deviation from the results obtained by the mean field theory from the results given by a direct simulation of the automata. The reason behind this difference comes from the initial assumption of independence, and from the fact that the mean field theory does not take into account the spatial structure of the neighborhoods of a cell, e.g., configurations 011 and 101 have the same probability: $p^2(1-p)$. An approach that explicitly consider the overlap of cells appears in [52], here, the authors consider an arrangement of cells known as block, the length of this block is chosen in such a way that no overlap among blocks exists, and probabilities can be considered truly independent.



(a) Initial density = 0.01



(b) Initial density = 0.8

Figure 2.11: Experimental results for rule 169.

2.4. Probabilistic Cellular Automata (PCA)

This kind of automata represent a generalization of those described in section 2.2, instead of being updated deterministically, the image of the local transition function for any neighborhood is given by the distribution of a discrete random variable with values in Q [53].

As an example consider the one-dimensional totalistic PCA described in [54], this automata is an extension of the Domany-Kinzel cellular automaton [9]. The local transition function of the automaton is given in Table 2.4

where s is given by:

$$s = \sum_{i=-1}^1 c^t(\vec{n} + i)$$

and the quantities p_s are the conditional probabilities that $c^{t+1}(\vec{n}) = 1$, given that the sum of states over the neighborhood is s .

A good starting point to analyse this automaton is to set $p_0 = 0$ (to prevent spontaneous generation), and $p_3 = 1$, under this conditions, there are two quiescent states, the first corresponding to the configuration $(0, \dots, 0)$, and the second corresponding to the configuration $(1, \dots, 1)$. If ρ denotes the density of cells having state one at times t , then

$c^t(\vec{n}-1)$	$c^t(\vec{n}-1)$	$c^t(\vec{n}-1)$	s	$c^{t+1}(\vec{n}) = 0$	$c^{t+1}(\vec{n}) = 1$
0	0	0	0	$1 - p_0$	p_0
0	0	1	1	$1 - p_1$	p_1
0	1	0	1	$1 - p_1$	p_1
0	1	1	2	$1 - p_2$	p_2
1	0	0	1	$1 - p_1$	p_1
1	0	1	2	$1 - p_2$	p_2
1	1	0	2	$1 - p_2$	p_2
1	1	1	3	$1 - p_3$	p_3

Table 2.4: Transition table for the probabilistic cellular automaton.

$$P(c^{t+1}(\vec{n}) = 1) = 3p_1\rho(1 - \rho)^2 + 3p_2\rho^2(1 - \rho) + \rho^3 \quad (2.17)$$

is the mean-field equation for the density of cells having state one. Equation 2.17 has three fixed points:

$$\rho_0^* = 0 \quad (2.18)$$

$$\rho_1^* = \frac{3p_1 - 1}{3p_1 - 3p_2 + 1} \quad (2.19)$$

$$\rho_2^* = 1 \quad (2.20)$$

The stability of these fixed points is as follows:

- The fixed point ρ_0^* is stable for $0 \leq p_1 < 1/3$
- If $1/3 < p_1 \leq 1$ and $0 \leq p_2 < 2/3$ then ρ_1^* is stable.
- ρ_2^* is stable if $2/3 < p_2^* \leq 1$

At the boundary $p_1 = 1/3$, $0 \leq p_2 < 2/3$ there is a transition from the quiescent state given by the configuration $(0, \dots, 0)$ to configurations where the density of cells having state one is not zero (active state). Another transition from the active state to the quiescent state given by the configuration $(1, \dots, 1)$ occurs at the boundary $1/3 < p_1 \leq 1$, $p_2 = 2/3$.

2.5. Particle Swarm Optimization

PSO is a bio-inspired algorithm based on the collective behavior of several groups of animals (flocks, fish schools, insect swarms, etc.) [55]. Its main objective is the searching of an optimum in a search space that defines the set of possible solutions to a particular problem. Each point in the search space represents an specific set of features that qualify that position, it is possible then to assign a numerical value to each candidate solution through a measure imposed on the search space, such value is called *fitness*.

To clarify these concepts, consider the problem of finding the absolute minimum of the following function:

$$f(x) = \frac{1}{2} + \frac{\sin^2(x^2) - \frac{1}{2}}{(1 + 0.001x^2)^2} \quad (2.21)$$

A plot of the function is shown in Figure 2.12, commonly a function such as $f(x)$ is called *objective function*. It is easy to observe that the minimum value of $f(x)$ occurs at the point $x = 0$, this is the solution we are looking for. However, the shape of the plot shows several points where the value of

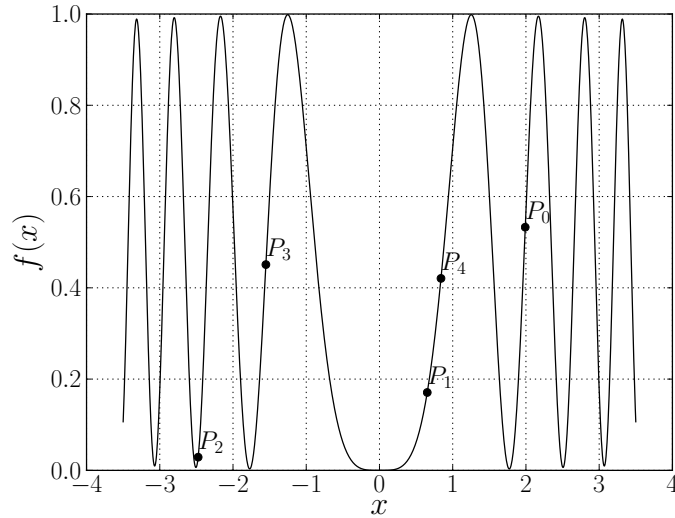


Figure 2.12: A plot of the function defined in Equation 2.21.

$f(x)$ is close to the absolute minimum. This feature of the function defined in Equation 2.21 makes it ideal to study the behavior of the PSO algorithm.

The domain of variable x , i.e., the set \mathbb{R} of real numbers, represents the search space of the minimization problem. For this problem, it is possible to use Equation 2.21 directly as a fitness function, then the solution of the problem is given by the element of the search space with the minimum fitness value.

PSO considers an initial population of particles (the swarm) randomly distributed through the search space. Figure 2.12 shows these particles as dots on the graph of $f(x)$. In order to find an optimal solution, particles move in discrete time steps, using the information they have acquired individually and the information received from the swarm. The movement of a particle is described in terms of its position and velocity. Furthermore, each particle is able to record the best position it has visited so far, for a minimization problem, if the particle moves to a position with a lower fitness value than that of its current best known position, then such position is updated.

The position X_i^t of each particle is updated in discrete time steps according to the next equations:

$$V_i^{t+1} = \omega V_i^t + k_1 q_1 (P_i^t - X_i^t) + k_2 q_2 (P_g^t - X_i^t) \quad (2.22)$$

$$X_i^{t+1} = X_i^t + V_i^{t+1} \quad (2.23)$$

where:

- V_i^t is the velocity vector at time t of particle i .
- k_1 and k_2 are the cognitive and social factor respectively.
- $q_1 \in [0, 1]$ and $q_2 \in [0, 1]$ are uniformly chosen random numbers.
- P_i^t denotes the position with the highest fitness value found by particle i until time t , i.e., the best position found by particle i .
- P_g^t denotes the position with the highest fitness value found by the swarm at time t . If a local PSO is used, P_g^t is replaced by $P_{l_i}^t$, this term denotes the position with the highest fitness value found by the neighbors of particle i at time t .
- ω is the inertia weight, this term serves as a mechanism to favor the exploration of the search space, or the exploitation of known good solutions.

Each term of Equation 2.22 plays a different role in the PSO algorithm:

- The ωV_i^t term is responsible for keeping the current direction of movement of the particle, is commonly known as the *inertia component*. The parameter ω is known as *inertia weight*, higher values of ω speed up the current direction of movement with produces long range movements of the particle, lower values “decelerate” the particle, which produces small sized movements. In order to take advantage of this behavior, the value of ω is linearly decreased as the execution of the algorithm advances. Thus, during the first iterations of the algorithm, the long range movements of the particle favour the exploration of the search space. At the final iterations, the movements of a particle are more constrained, which encourages the search in zones with a known good fitness values, this phenomenon is called *exploitation*.
- The term $k_1 q_1 (P_i^t - X_i^t)$ is known as the *cognitive component*, and serves to guide the movement of the particle towards zones where the particle has previously found good fitness values. The parameter k_1 and the coefficient q_1 determine the magnitude of the contribution of this term to the new velocity vector of the particle.
- The term $k_2 q_2 (P_g^t - X_i^t)$ is known as the *social component*, its purpose is to direct the movement of the particle towards the best zone found by the swarm. The parameter k_2 and the coefficient q_2 determine the contribution of this term to the new velocity vector of the particle.

A typical global PSO algorithm proceeds as follows:

1. Initialize the position of each particle with a uniformly distributed random vector.
2. Set the best known position of each particle to its initial position.
3. Initialize the velocity of each particle with a uniformly distributed random vector.
4. Determine the swarm’s best known position.
5. Update the velocity of each particle according to Equation 2.22.
6. Using Equation 2.23 calculate the new position of each particle.
7. If necessary, update the best known position of each particle.
8. If a particle finds a position with a better fitness value than that of the swarm’s best known position, update such position.
9. If the stop condition is met (a good enough solution has been found, a certain number of iterations has been performed, etc.), then the algorithm stops and P_g^t contains the solution found by the algorithm. Otherwise return to step 5.

Consider again the swarm depicted in Figure 2.12, Table 2.5 summarizes the status of each particle after the initialization process.

Particle	Position	Velocity	Fitness
P_0	1.9894	-2.7016	0.5304
P_1	0.6523	-2.0154	0.1706
P_2	-2.476	0.5104	0.0289
P_3	-1.551	3.0651	0.4509
P_4	0.8395	-2.2173	0.4198

Table 2.5: Status of the swarm after initialization.

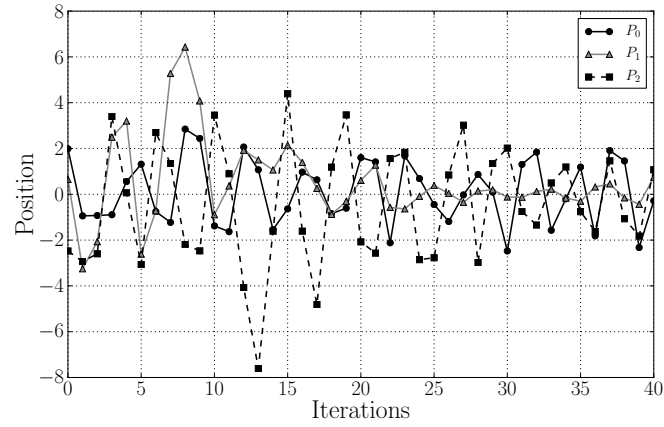
From the table it is clear that after initialization, P_g^t corresponds to the position of P_2 , i.e., the point $x = -2.476$, note that even if the fitness value of P_2 is close to zero, the position of this particle is still far from the position that corresponds to the absolute minimum of $f(x)$.

For $k_1 = k_2 = 2$, $q_1 = 0.8598$, $q_2 = 0.056$ and a $\omega = 0.9$, the velocity and position of P_0 are updated as follows:

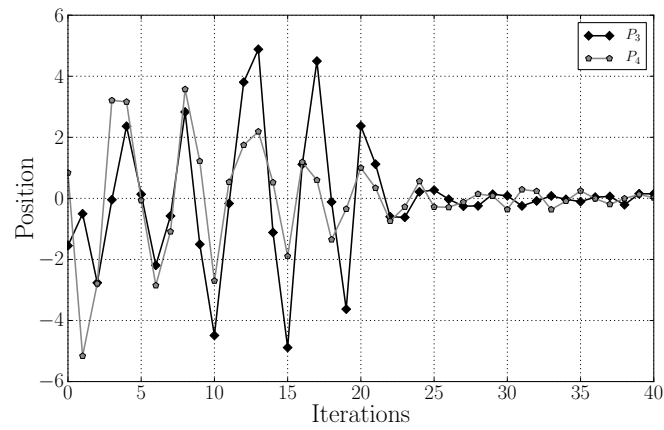
$$\begin{aligned}V_0^1 &= \omega V_0^0 + k_1 q_1 (P_0^0 - X_0^0) + k_2 q_2 (P_g^0 - X_0^0) \\V_0^1 &= (0.9)(-2.7016) + (2)(0.8598)(1.9894 - 1.9894) + \\&\quad (2)(0.056)(-2.476 - 1.9894) \\V_0^1 &= -2.9316 \\X_0^1 &= X_0^0 + V_0^1 = 1.9894 + (-2.9316) = -0.9422\end{aligned}$$

The position of the remaining particles is calculated in a similar way. Of course, the best position found by each particle and the best position found by the swarm must be updated as needed. Figures 2.13a and 2.13b shows the change in position of each particle during the first 40 iterations of the algorithm, for this example the value of ω was decreased linearly from a starting value of 0.9 to a final value of 0.4, such range was proposed by Eberhart and Shi in [56]. It is clear that particles P_1 , P_3 and P_4 quickly converge towards a good solution. on the other hand, particles P_0 and P_2 still oscillate far away from the solution, this behavior is expected given the small number of iterations reported in the figures. After 100 iterations, the best position found by the algorithm was $x = -2.48235 \times 10^{-6}$ with a corresponding fitness value of 6.21725×10^{-15} , the result is remarkable given the small number of particles used for the example.

Typically, a particle uses one of two schemes to obtain information from other individuals [57]: in the first all particles are connected to each other, and every particle is under the influence of the particle in the position with the best fitness value among all particles of the swarm, this is the global PSO. In the second scheme called, a neighborhood comprising a particle of the swarm and its m nearest neighbors is created; each particle is then influenced by the performance of these local neighbors, this approach defines the local PSO.



(a) P_0 , P_1 and P_2



(b) P_3 and P_4

Figure 2.13: Change in position of the particles depicted in Figure 2.12.

Chapter 3

State of the art

Lattice models based on cellular automata, are abundant in ecological modelling due to their capacity to describe with great detail the local interactions among the organisms that compose an ecosystem. The analysis of such interactions has provided new insights on the underlying processes that determine the global behavior of such systems: e.g., the self-organized criticality in an hierarchical food chain [58], the long term maintenance of species diversity [22], or the effects of the interspecific competence at local scale on the coexistence and diversity of multiple competing species [24]. The purpose of this chapter is to describe the tools that have been used and developed to analyse these models, specifically those that deal with the study of the long term dynamics of a probabilistic cellular automaton.

3.1. Mean field theory approaches

In section 2.3 we used the mean field theory to obtain a density equation for the evolution of an elementary cellular automaton, the equation obtained ignores space and assumes independence. This approach allowed us to apply the methods of the dynamical systems theory to analyse the temporal dynamics of the automaton. The purpose of this section is to show the use of this approach to characterize the long term behavior when applied to ecological models.

3.1.1. A prey-predator system with pursuit and evasion

Consider the prey-predator system described in [31], the model considers a two-dimensional lattice of width L , where periodic boundaries have been implemented, the set of states Q is defined as follows:

$$Q = \{0, 1, 2\} \tag{3.1}$$

where 0 denotes an empty cell, 1 represents a cell occupied by a prey, and 2 a cell inhabited by a predator. Depending on the current state of the cell, two different neighborhoods are considered: a von Neumann “predation neighborhood”, and a M_2^2 “pursuit and evasion” neighborhood, this neighborhood is divided into four quarters along its diagonals (see Figure 3.1), and prey and predator densities are evaluated at each quarter. The evolution of the system is governed by the next set of rules:

1. A prey has probability d_h of being eaten by a predator in its predation neighborhood.
2. If there is no predator in its predation neighborhood, a prey has probability b_h of giving birth to a prey at an empty cell of this neighborhood.
3. After having eaten a prey, a predator has probability b_p of giving birth to a predator at the cell previously occupied by the prey.
4. A predator has probability d_p of dying.

5. In order to catch prey, predators move to a cell of their predation neighborhood following the direction of highest local prey density in the pursuit and evasion neighborhood. In case of equal highest density in two or four directions, one of them is chosen randomly. If three directions correspond to the same highest density, predators select the middle one. Preys move to a neighboring cell in the opposite direction of highest local predator density. If the four directions are equivalent, one is selected at random. If three directions correspond to the same maximum density, preys choose the remaining one. If two directions correspond to the same maximum density, preys choose at random one of the other two. If H and P denote, respectively, the prey and predator densities, then mHL^2 preys and mPL^2 predators are sequentially selected at random to perform a move. This sequential process allows some individuals to move more than others. The parameter m , which is a positive number, represents the average of the number of tentative moves per individual during a unit of time.

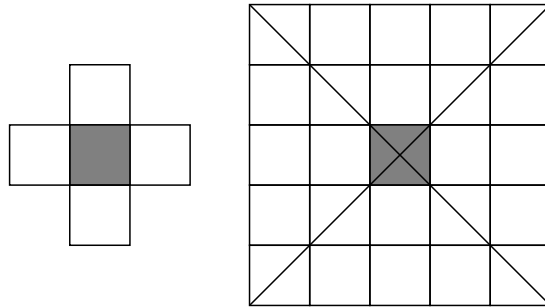


Figure 3.1: Von Neumann “predation neighborhood” and M_2^* “pursuit and evasion neighborhood” ($r = 2$).

Rules 1, 2, 3, and 4 are applied simultaneously, rule 5 is applied sequentially. Predation, birth, and death processes are modeled by a three-state two-dimensional cellular automaton.

If H_t and P_t denote the densities at time t of preys and predators respectively, and assuming that the probability that either a prey or a predator occupies a cell is proportional to the density of the corresponding population, then it is possible to establish the next mean-field equations:

$$P_{t+1} = P_t - d_p P_t + b_p H_t f(1, d_h P_t) \quad (3.2)$$

$$H_{t+1} = H_t - H_t f(1, d_h P_t) + (1 - H_t - P_t) f(1 - P_t, b_h H_t) \quad (3.3)$$

where the function f is defined as:

$$f(p_1, p_2) = p_1^4 - (p_1 - p_2)^4$$

This expression can be derived as follows: if $p_2 = d_h P(t)$, then p_2 represents the probability that, at time t , a prey is eaten by a predator located at a specific cell of the predation neighborhood. Then $1 - (1 - p_2)^4 = f(1, p_2)$ is the probability that, at time t , a prey is eaten by a predator located at any of the four cells of the predation neighborhood. If $p_1 = 1 - P(t)$ and $p_2 = b_h H(t)$, then p_1 represents the probability that, at time t , a specific cell is not occupied by a predator and p_2 the probability that, at time t , a prey gives birth to a prey at a specific cell. Then $p_1^4 - (p_1 - p_2)^4 = f(p_1, p_2)$ is the probability that a prey gives birth to a prey at any of the four cells of the predation neighborhood if there are no predators in this neighborhood.

The fixed points of the mean-field equations can be obtained by solving:

$$d_p P_t - b_p H_t f(1, d_h P_t) = 0 \quad (3.4)$$

$$H f(1, d_h P) - (1 - H - P) f(1 - P, b_h H) = 0 \quad (3.5)$$

$P = 0$ is a solution to Equation 3.4 since $f(1,0) = 0$, under this conditions, equation 3.5 has two solutions: either $H = 0$ or $H = 1$. The solution $P = 0, H = 0$ is always unstable if $b_h \neq 0$. Solution $P = 0, H = 1$ is stable if $d_p - 4b_p d_h > 0$. If $P \neq 0$ another solution to equations 3.4 and 3.5 may be found, this solution may create a limit cycle through a Hopf bifurcation. Figure 3.2a shows a fixed point in the prey-predator phase space obtained using the mean-field equations. Computer simulations of the model shows that for these parameters, a fixed point in agreement with the mean field approximation exists when m increases to 500 as shown by Figure 3.2c. For $b_p = 0.6, d_p = 0.2, b_h = 0.2,$ and $d_h = 0.9$. The mean-field equations predict a stable limit cycle (see Figure 3.2b), however, such cycle is not observed for “large” lattices, however a quasi-cyclic behavior is observed when the lattice has a size of the order of the mean displacements of the individuals (see Figure 3.2d). Other works that study the oscillatory behavior of prey-predators lattice models report similar results, i.e., limit cycles are observed for “small” lattices [59].

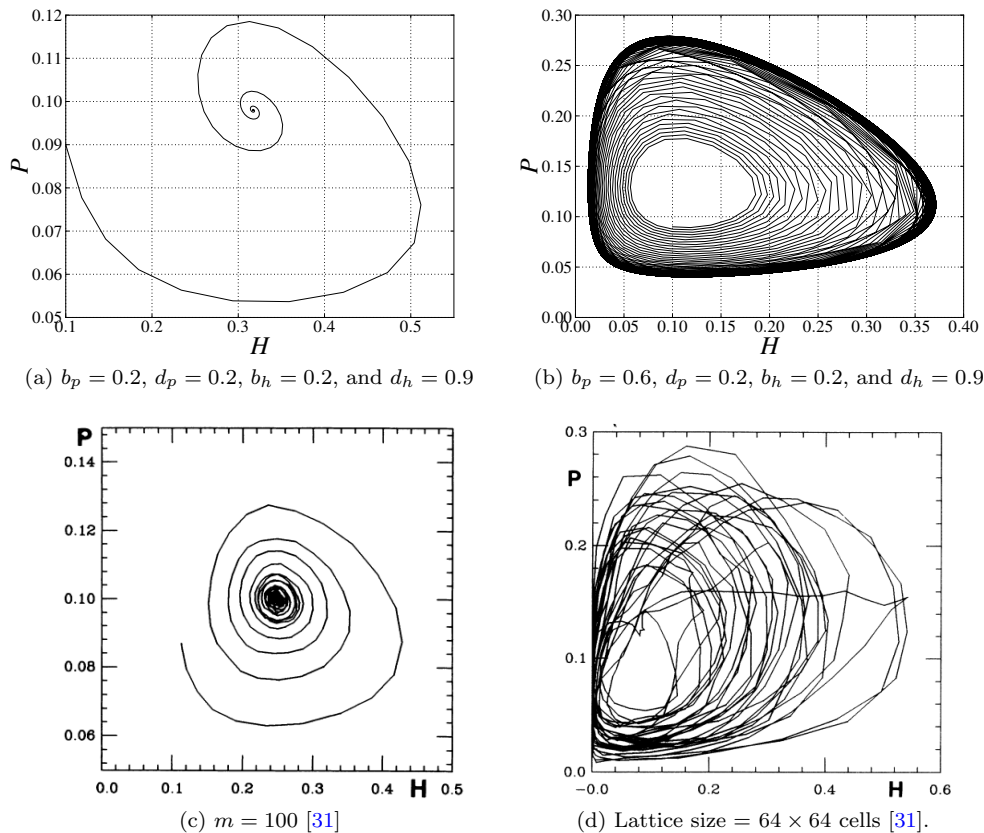


Figure 3.2: Fixed points and limit cycles of the pursuit and evasion model.

Monetti, Rozenfeld and Albano [32] analyzed a variant of this model, however, they focused on the study of the system’s dependence on the predator’s death and reproduction probabilities. They found that the systems enters an oscillatory regime when a “percolating cluster” of preys that spans the whole lattice, and such cluster is populated by small colonies of predators.

3.2. Time series analysis

One of the most natural approaches to study the behavior of a lattice model is to analyse the results of computer simulations. Often, the data collected represent the change in time of the number of individuals belonging to a certain species. If each species is identified with a state of the automaton,

then the time series contains important information about the evolution of the density of states. Since there is nothing special about the time series produced by a lattice model, it is possible to apply any technique that would be used to analyse a data set belonging to a discrete dynamical system, e.g., frequency domain analysis, statistical methods, autocorrelation analysis, etc.

3.2.1. Spectral density

A tool particularly useful to study the temporal dynamics of a lattice models is the spectral density analysis. For a time series $f(t)$ the spectral density analysis describes how the variance of the time series is distributed over the frequency components into which it may be decomposed. For a discrete time series $f(t)$ such as the one obtained from a lattice model, spectral densities may be obtained calculating the Fourier transform of each point in the series (see [60]) according to:

$$S(\omega_j) = \frac{1}{N} \left\langle \left| \sum_{n=1}^N f(t) e^{i\omega_j n} \right|^2 \right\rangle \quad (3.6)$$

where:

$$\omega_j = \frac{\pi(j-1)}{N}, \quad j = 1, \dots, N \quad (3.7)$$

It is a common procedure to subtract from each point in $f(t)$ the mean value of the series to avoid divergence in $S(\omega)$, when $\omega = 0$. The resulting spectrum may be then used to detect the presence of oscillatory behavior in the model; if such is the case, the main frequency components of the series appear as “peaks” at the corresponding frequency (see, e.g., [32] [34] [44]); if not, the spectrum is broadly distributed. In [61] Lipowski uses a lattice model to study the oscillatory behavior of a prey-predator system, the evolution of the system is controlled by a parameter r that determines the probability of birth and death of preys and predators. Computer simulations of the model in one, two and three dimensions were performed; the results of the spectral density analysis for each corresponding time series may be summarized as follows:

- For the one-dimensional version of the model a very broad spectrum was found, this agrees with the “random” fluctuations observed in the density plot of the simulation.
- In two dimensions, the densities also evolve irregularly, however, for a certain range of the parameter r , it is possible to observe a pronounced peak in the spectrum at a certain frequency.
- The density plot for the three-dimensional version of the model shows very regular oscillations, the corresponding spectrum has a very high and sharp peak. This oscillatory behavior can only be observed for a certain range of r , if the value of this parameter is set too low, or too high, the oscillations disappear.

Lipowski also observed evidence of high order harmonics in the frequency spectrum of the population data. The author states that this behavior together with the random fluctuations inherent to the model are responsible for the cyclic behavior of the model through stochastic resonance.

Another example can be found in [62], the authors study a prey-predator lattice model that evolves according to the following rules:

1. If a cell is empty, then the probability that it becomes occupied by a prey is $p_a n_a / \zeta$, or remains empty with probability $1 - p_a n_a / \zeta$.
2. If a cell is occupied by a prey, then the prey is replaced by a predator with probability $p_b n_b / \zeta$, or remains a prey with probability $1 - p_b n_b / \zeta$.
3. If the cell is populated by a predator, it dies with probability p_c or survives with probability $1 - p_c$.

where:

- n_a (n_b) is the number of neighbors occupied by preys (predators).
- ζ is the total number of neighbors.
- p_a , p_b , and p_c are parameters of the model associated with the birth of prey, the death of prey and birth of predators, and the death of predators respectively.

Simulations of the model reveal a prey-absorbing state represented by a lattice full of preys, a non-trivial fixed point where preys and predators coexist, the trivial absorbing-state where the lattice is empty, and finally an oscillatory regime where preys and predators coexist. Besides obtaining the period of oscillations through spectral density analysis, the authors use the features of the spectrum to define a phase transition of the model, in particular the authors define a phase transition at the point where the low modes of the spectral density have the same value as $S(\omega_{max})$.

3.2.2. Power-law scalings and patchiness

An study concerned with the problem of determining whether population and community patterns are intrinsic to an ecosystem, or if such patterns merely reflect environmental fluctuations or some other random event appears in [63]. The authors argue that there exists properties of spatial patterns that are robust to the details and parameters of local interactions, e.g. the size and perimeter of patches of individuals belonging to the same population,

The authors studied two different lattice models: the first considers single occupancy of a cell, i.e., a cell might contain exactly one prey, one predator or be empty. The model uses a von Neumann neighborhood and considers the next rules:

- Prey growth. A prey chooses a neighbouring cell at random and gives birth at rate β_1 onto it only if this cell is empty.
- Predators hunt for preys by inspecting their neighborhood for the presence of preys at rate 1. If prey are present, the predator selects one at random and eats it, moving to this neighboring cell.
- If a predator found a prey during the previous stages, it reproduces with probability β_2 , the offspring is placed at the original cell of the predator.
- Predators that do not find a prey are susceptible to starvation and die with a probability δ .
- Random movements of predators occurs through mixing: neighbouring cells exchange state at a constant rate v .

The rates specified in the rules identify an event that occurs according to a Poisson distribution with the corresponding rate. In order to characterize the spatial dynamics a cluster is defined as a group of cells containing a prey connected through their neighborhood. Simulations of the model show that prey clusters change continuously as a consequence of the growth and predation process.

When the number of clusters $n(s)$ within a given area s (the size of this area is given by the number of cells that it contains) was measured as a function of time, it was observed that the distribution of $n(s)$ exhibits a power law decay over two orders of magnitude according to:

$$n(s) \propto s^{-\alpha} \tag{3.8}$$

where $\alpha = 1.99$, this value was related to the Korcak exponent (a quantity originally used to describe the distribution of Aegean islands). Simulations of the model show that the cluster size distribution is independent of the values of β_2 and δ in the coexistence regime and only weakly dependent on the other parameters. The value of α obtained corresponds to high level of patchiness, i.e., patterns with many small clusters. Another property worth investigating is the perimeter of clusters, which is defined as the set of cells containing a prey, that belong to the cluster with at least one non prey neighbour cell (a non prey cell is either occupied by a predator or empty). The mean perimeter $\tau(s)$ is then given by averaging over the size of individual perimeters for all clusters of the same area s . When plotted against s (the area of a cluster) it was found that the perimeter scale according to:

$$\tau = bs^\gamma \tag{3.9}$$

both the exponent γ and the scaling coefficient b are close to one, as a result the perimeter grows as a power law of the area and does so almost at the fastest possible rate.

The second model, motivated by prey-predator interactions in a plankton community, considers multiple occupancy of a cell, i.e., a cell might contain several individuals. The rules that govern the transition of the model are as follows:

- A prey takes up nutrients within the same cell with probability β_1 . Nourishment of a prey leads to the production of one offspring at the same cell.
- A predator finds and eats prey with probability β_2 , if its hunt is successful, it produces one offspring at the same cell.
- If a predator fails to find a prey, it starves and dies with probability δ .
- Once the state of all cells has been updated, a random mixing of individuals and nutrients occurs across the lattice. Each predator and prey moves with probability v to one of its four nearest neighbors.

As before, simulation of the model shows that preys aggregate into clusters. The resulting size distribution is similar to the model of single occupancy: it is given by a power law with exponent $\alpha = 1.75$, and is only weakly dependent on the other parameters. A power-law scaling also holds for the perimeter of clusters as a function of the area of a cluster. Once again, the value of the exponent ω is close to one (0.92). Thus, the two models exhibit similar power-law scalings for the prey clusters, in spite of significant differences in the details of the processes and implementation of the transition functions.

3.3. Finite size effects

One of the obvious limitations of lattice models is that they must be simulated using a finite number of cells, thus an immediate question is: what effects has the size of the lattice on the long-term dynamics of these models? A reasonable approach to deal with this question is to compare prey-predator lattice models with other approaches that omit the spatial component, e.g., models based on difference and differential equations; in particular, comparisons against the corresponding mean field models have provided interesting results.

In [64] the authors analyse the dynamics of a prey-predator lattice model where individuals of the predator species move according to two different schemes:

- Homogeneous movement. All predators are redistributed randomly over the entire lattice.
- Diffusive movement. Predators move randomly to one of their nearest neighbors; if the destination cell is already occupied by another predators, no movement occurs.

The dynamics of the model is compared against the corresponding set of mean field differential equations; the results show that when predators move homogeneously, the observed dynamics of the lattice model and the dynamics of the equations are very close (both qualitative and quantitative); specifically, both models exhibit large amplitude oscillations for a low death rate of predators. Such phenomenon agrees with the results of Durrett regarding the behavior of the contact process [38], i.e., predictions made by the mean field equations become exact when the dispersal of individuals is large. The authors also note that when predators move according to the diffusion rules, there is no significant change in the average densities of preys and predators when compared to the results obtained through homogeneous movement (independence of the average densities from the lattice size has also been confirmed by Sutherland and Jacobs [65]); moreover, even though a slight decrease in the number of preys eaten by a predators was observed, the functional response of the predators remains

the same. The biggest difference is that when the diffusion rule is used no oscillations are observed, and the density of preys and predators remains more or less constant, i.e., local interactions have an stabilizing effect on the populations. To further analyse the behavior of the model the population dynamics at different spatial scales was studied; for each different scale, the coefficient of variation cvs was determined as follows:

$$cvs = \sigma / \text{mean value} \quad (3.10)$$

where σ is the standard deviation of the corresponding time series, this value offers a measure of the variability in the prey and predators densities. At small spatial scales the cvs for homogeneous and diffusive movement are similar; as the size of the lattice is increased, the two values deviate more and more, with the cvs corresponding to diffusive movement decreasing proportionally to the square root of the area of the lattice. The point at which the cvs corresponding to the diffusion rule deviates from the cvs of the homogeneous movement rule is known as the “natural scale” of the system, and can be regarded as a transition point, below which the dynamics of the diffusion rule are reminiscent of the behavior observed when individuals move homogeneously. For larger scales however, the diffusive movement of predators results in weak couplings between different sections of the lattice; sections that are far away are out of phase are, which counteracts any oscillatory behavior.

Similar scalings were found by Lipowski [61] when analysing the oscillatory behavior of a prey-predator lattice model. In order to determine the behavior of the amplitude of the observed oscillations as $L \rightarrow \infty$ (where L is the width of the lattice of the model), the standard deviation σ of the population data was calculated from simulations in one, two, and three dimensions, σ can be interpreted as a rough measure of the amplitude of the oscillations. As σ is plotted against the values of r it was possible to determine that the amplitude of the oscillations should scale according to $1/L^2$, thus $\sigma \rightarrow 0$ as $L \rightarrow \infty$. For $d = 1, 2$ the previous argument holds, however, the data obtained from runs of 5×10^4 Monte Carlo steps for systems of linear size up to $L = 150$ shows that for the three-dimensional case it is likely that σ remains finite in the thermodynamic limit.

Antal and Droz ([66]) investigated how the finite nature of a lattice model influences some key properties of the oscillations of a prey-predators system. The model studied by the authors is actually a spatial continuous-time Markov process where each cell can be in one of the following states: 0 (empty cell), 1 (prey), or 2 (prey and predator simultaneously). The model has the following transition rules:

- $0 \rightarrow 1$ at rate $\lambda_a (n_{i,1} + n_{1,2}) / 4$
- $1 \rightarrow 2$ at rate $\lambda_b (n_{i,2}) / 4$
- $2 \rightarrow 0$ at rate 1

where $n_{i,\sigma}$ denotes the neighbors of cell i having state σ . Spreading of preys and predators are controlled by the first two rules, the third rules represents in-cell extinction due to predation. The mean-field model that results from the common assumption that individuals are randomly distributed on the lattice, predicts an absorbing state where the lattice is fully covered by preys; there is also a co-existence state in phase space where certain regions are characterized by oscillations in the populations of preys and predators. The phase diagram of the lattice model, obtained through Monte-Carlo simulations, shows a similar behavior: there is a pure prey state, and a coexistence state with and without oscillatory behavior. The authors show that oscillation are present for large systems, though their amplitude scales according to $1/L^2$ with L being the width of the lattice; such scaling implies that any oscillatory behavior should banish in the thermodynamic limit. The authors state that the presence of isolated predators “islands” located in sparse prey areas, which causes growing prey populations; in time this phenomenon allows predators to disperse and feed again.

In [67] Pascual and Levin study the behavior at different spatial scales of a continuous time version of the WATOR model, in particular, events occur according to a Poisson process with rate α according to the following rules:

- A fish gives birth at rate β_1 , the new individuals is placed at a neighbouring empty cell.

- A shark searches q neighbours for preys, if present, the shark chooses one cell at random, eats the fish and moves there. The shark then gives birth with probability β_2 . If there is no fishes, the shark does not move and dies with probability δ .
- Stirring (movement of sharks). Each pair of neighbors exchange states at rate v .

Instead of using different lattice sizes, the densities of preys and predators are measured within an observational window inside a lattice of 700×700 cells. For a small window (8×8 cells) random oscillations of high amplitude are observed; at an intermediate scale (64×64 cells) there is a decrease in the amplitude of the oscillations, but they appear to be more “smooth” with a well defined period; finally, for a window that spans the whole lattice weak oscillations around a fixed point are observed. These results were compared against two different mean-field models: the first is obtained by considering that individuals are randomly distributed over the lattice, thus they interact according to average densities; the second results from adding noise to the mean field equations, and then use such equations to evolve an array of cells through Monte-Carlo simulations. For the first model, the dynamics converge to a limit cycle; however, the period of the oscillations, their modulation, as well as their variance do not correspond to the results of the lattice model. The second model has two absorbing states: complete extinction of preys followed by the extinction of predators, and extinction of predators followed by all cells populated by preys. Before reaching any of these states an oscillatory transient can be observed; however, these oscillations are fuzzy (due to the noise added to the mean-field equations) and differs in period, variance, and modulation from the oscillatory behavior observed in the lattice model. It is worth noting that despite these differences, the behavior of the lattice model and its corresponding mean-field equations agree with the classification given by Durrett and Levin (see Section 1.3).

Continuing with the analysis of the continuous-time WATOR model, Durrett and Levin [68] prove that when the mean-field equations that correspond to lattice model have an attracting limit cycle solution, then sharks and fishes coexist in a reaction-diffusion equation that considers the stirring rate; moreover, this result implies the existence of a stationary distribution for the lattice model whenever the stirring rate is large enough. By now such behavior is unsurprising, as with other models, when the dispersion of individuals is large, there is a better agreement between the lattice models and the equations that attempt to describe their behavior.

For prey-predator lattice models where oscillatory behavior is observed, it is common that such oscillations persist only when the model is simulated using small lattices, or when both species are aggregate at small scales; as the size of the lattice is increased oscillations die out and only small random fluctuations around a fixed point are observed [31] [40] [61] [64] [67] [68] [66] [69] [70].

Chapter 4

Proposed model

Ecological models often need to be simple enough to be tractable and to help to determine the underlying processes that drive the dynamics of an ecosystem, also they need to be complex enough to reflect a realistic behavior. Indeed, lattice models were first considered because they offered a simple, yet realistic enough approach to model the interactions among the organisms that comprise an ecosystem. However, often only the negative effects of such interactions are considered, e.g., competition or crowding, and beneficial effects appear only as a greater chance of reproduction. This is particularly evident when the behavior of a predator is considered, most rules proposed to model predation neglect any kind of interaction between predators: see e.g. [71]. However, cooperation is common among animal communities: birds flocks, swarms, herds, and fish schools are good examples of the phenomenon. A member of any of these animal groups is able to react based on the information it has acquired on an individual basis or by communicating with the other members of the community, e.g., to flee from a predator or to keep a flight pattern. The observation and study of the social behavior of animal communities led to the development of the “Swarm Intelligence” algorithms, a critical event towards the development of Particle Swarm Optimization (PSO), was to recognize the fact that the social behavior among organisms represents an advantage that may outweigh the negative effects of competition [72], through cooperation an individual may benefit from the experience of other members of the community. Surprisingly enough, even when since its inception PSO has been successfully applied to problems such as: numerical optimization [73], the deployment of wireless sensor networks [74] or image processing [75], its application to ecological modelling is to the best of our knowledge non existent.

The purpose of this section is to present a lattice model where the movement of predators is modelled through a PSO algorithm, in order to accomplish this goal, a fitness function that measures the local density of preys at each cell is used.

4.1. Description

Consider a theoretical ecosystem comprised by a sessile prey and a its predator. In order to ensure their survival, predators hunt for preys, moving from zones low on resources to zones where preys are abundant. The movement of predators occurs within a migration stage inspired by the behavior of insects described in [76], and the related lattice model presented in [77]. A PSO algorithm is used to model the movement of predators, i.e., each particle of the swarm represents an individual of the predators species. We have developed two version of the proposed PSO algorithm:

- **Global.** When using this implementation, predators move by taking into account their best known position and the best position found by the whole swarm.
- **Local.** In this version of the proposed PSO algorithm, particles obtain the fitness of the cells populated by other particles in a finite neighborhood, using this information they move from zones where food is scarce to zones populated by preys.

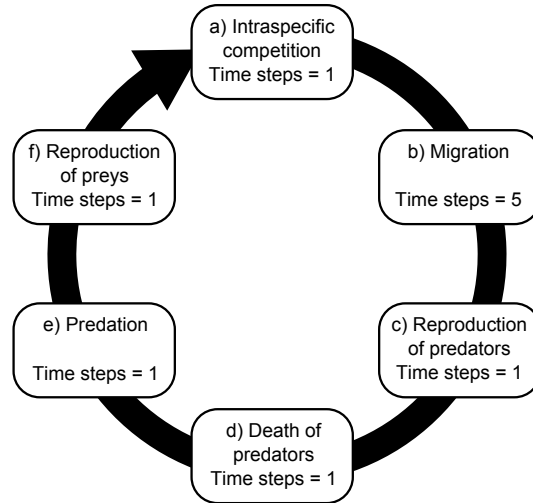


Figure 4.1: A season of the model.

The space in which species live and interact is represented by the lattice $L \subset \mathbb{Z}^2$, periodic boundaries have been implemented, i.e. the cellular space takes the form of a torus. The set of allowed states for each cell is:

$$Q = \{0, 1, 2, 3\} \quad (4.1)$$

where:

- 0 is an empty cell.
- 1 denotes a cell inhabited by a prey.
- 2 represents a cell containing a predator.
- 3 denotes a cell containing a prey and a predator at the same time.

Both preys and predators obey a life cycle that describes their dynamics at each time step. The stages occur sequentially, forming a cycle that defines a “season” (see Figure 4.1). With the exception of the migration rule, which lasts for five time steps, all stages take one time step. At each stage the rule applied to the cells changes accordingly. It must be noted that from now on when referencing some parameter that depends on time, e.g., P_i^t , such usage of t will always mean “time steps”, and the term “season” will be stated explicitly.

1. **Intraspecific competence.** Preys die with a probability proportional to the number of individuals of the prey species within an M_c neighborhood (the competition neighborhood). If $c^t(\vec{n}) = 1$, then the probability of death ($c^{t+1}(\vec{n}) = 0$) is given by:

$$\rho(\text{death}) = \frac{\alpha h}{m} \quad (4.2)$$

where:

- $\alpha \in [0, 1]$ is the intraspecific competence factor, which determines the intensity of competence exercised by preys in the neighborhood of cell \vec{n} .
- h is the number of preys in the neighborhood of cell \vec{n} .
- $m = |M_{r_c}^2|$, is the cardinality of the neighborhood.

2. **Migration.** During this stage, predators move within the cellular space according to their own experience and the information received from other members of their species. Our experiments have shown that applying this rule during 5 consecutive time steps is enough to ensure a good exploration of the solution space.
3. **Reproduction of predators.** During the reproduction stage, each predator chooses randomly a cell in the reproduction neighborhood M_z . If the cell is not already populated by a predator, then a new predator is created at the target cell, otherwise, no reproduction takes place. This process is repeated as many times as the reproductive capacity of the species.
4. **Death of predators.** Those predators that are not in a cell containing a prey, die by starvation.
5. **Predation.** If a predator shares a cell with a prey, then the prey is eaten by the predator.
6. **Reproduction of preys.** Like predators, preys spawn new individuals at random in an M_y neighborhood. Reproduction is successful only if the target cells do not contain already a prey.

4.2. PSO as a migration algorithm

There are important differences in the use of PSO in traditional problems such as numerical optimization [55], and its role as a migration algorithm in the proposed model:

- **Fitness.** In numerical optimization, it is common to use the function to be optimized as a mean to obtain a measure of a solution's fitness. In the proposed model, the search space is given by the lattice of the CA, so each cell represents a candidate solution to the migration problem. Since the landscape of the ecosystem changes continuously, it is impossible to speak of an absolute best cell, instead each predator moves to the known "good enough" zones and exploits them. Once depleted, predators migrate to search for new zones for feeding and procreation, so instead of aiming for a global optimum, particles exploit known local optima.
- **Search space.** As stated before, the lattice takes the form of a torus and represents the search space in which each particle of the swarm moves. Thus the movement of a particle might go from one edge of the lattice to the other, this encourages exploration.
- **Variable swarm size.** In the classical version of the PSO algorithm the size of the swarm remain fixed for all time steps. In our model, each particle is a predator, consequently, they can die, and they can reproduce, this changes the size of the swarm each season.

The movement of a predator changes the state of the cell from which the movement starts according to the following state transitions:

$$\begin{aligned} c^t(\vec{n}) = 2 &\rightarrow c^{t+1}(\vec{n}) = 0 \\ c^t(\vec{n}) = 3 &\rightarrow c^{t+1}(\vec{n}) = 1 \end{aligned}$$

So a cell that contains only a predator (state 2) will be empty (state 0) after the movement, and a cell that contains a prey and a predator (state 3) will contain only a prey (state 1). Similarly, the cell at which the predator ends its migration could experience the next state transitions:

$$\begin{aligned} c^t(\vec{n}) = 0 &\rightarrow c^{t+1}(\vec{n}) = 2 \\ c^t(\vec{n}) = 1 &\rightarrow c^{t+1}(\vec{n}) = 3 \end{aligned}$$

Multiple occupancy of a cell by predators is forbidden, a predator can't move to a cell that is already populated by a predator. If during any of the five time steps of the migration stage, a predator tries to move to a cell that is already populated by a predator, then no movement takes place, and the predator remains at its original location.

Our fitness function $g : \mathbb{Z}^2 \rightarrow \mathbb{Z}$ quantifies the density of preys in the neighborhood M_c of each cell. Clearly the maximum fitness values is $|M_c|$, and the minimum value is zero.

4.3. Global implementation

During migration a particle moves according to the information it has acquired on an individual basis, and the information it has received from the swarm (the best position found thus far). Figure 4.2 shows the movement patterns of a group of particles as they approach a “good” zone in a simplified lattice. Black disks represent the starting position (P_i^t) of the particles, white disks denote their positions at the next time step (P_i^{t+1}), and a gray disk denotes the best position known by the swarm at time t (P_g^t). A solid arrow denotes the velocity (V_i^t) of the particle i at time t . In Figure 4.2a the four particles explore the neighborhood of P_g^t , at the next time step P_4 has found a position with a better fitness value, hence P_g^{t+1} will be on that location (see Figure 4.2b), and now all individuals will move there to explore the neighborhood of that zone.

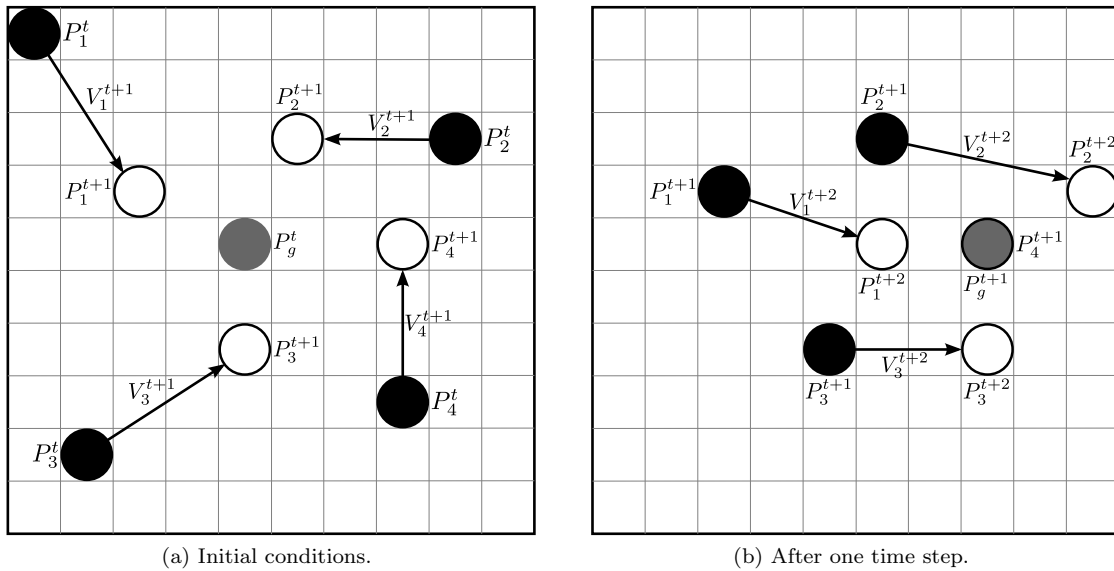


Figure 4.2: Movement of predators in the global implementation. (a) Individuals move to the direction of the swarm’s best known position. (b) The swarm moves to the recently discovered “good” zone.

Even if the behavior shown by the global implementation seems reasonable enough, there are some issues with its design: first, from a biological perspective, it is unreal that all members of the swarm share information among them, even if they are far away from each other. Moreover, under this method if an individual is located near to a zone with a moderate level of resources, and then is informed by the swarm about an abundant zone that is however far away from its current location, such individual will try to move to that location. Since the predator only has a finite amount of time to complete its migration, there is a high chance that it will die as a consequence of this effort.

4.4. Local Implementation

The local version of our PSO algorithm aims to model the social interactions among the members of the swarm. As two or more individuals come together, they exchange information about the current status of the ecosystem. Predators then use this information to guide their movements to zones with a greater level of resources. In order to model this behavior we assign to each particle i a neighborhood M_i , inside of which a predator is able to obtain the fitness value of the cells occupied by other predators, according to this, migration proceeds as follows:

1. The best position (P_i^t) among the neighbors located within the M_i neighborhood of particle i is determined, such position corresponds to the cell with highest fitness value currently inhabited by a particle in M_i .

2. Once $P_{l_i}^t$ has been obtained, particle i updates its velocity according to equation 2.22
3. A particle moves to its new position by adding V_i^{t+1} to its current position X_i^t .
4. If necessary the best position known by the particle P_i^t is updated.

As a particle moves, its neighborhood overlaps with those of other individuals, and as a consequence a particle is able to adapt its movement as new information becomes available. Figure 4.3a shows five predators (depicted as black circles), and the neighborhoods (dashed lines) inside of which they obtain the fitness of other predators (white circles). Figure 4.3b shows the updating process in detail: a black circle depicts the current position of particle i , the best position found in the $M_{r_l}^2$ neighborhood is represented as a gray circle, a black dot marks the best position known by the particle i , finally a gray dot shows the new position of the particle.

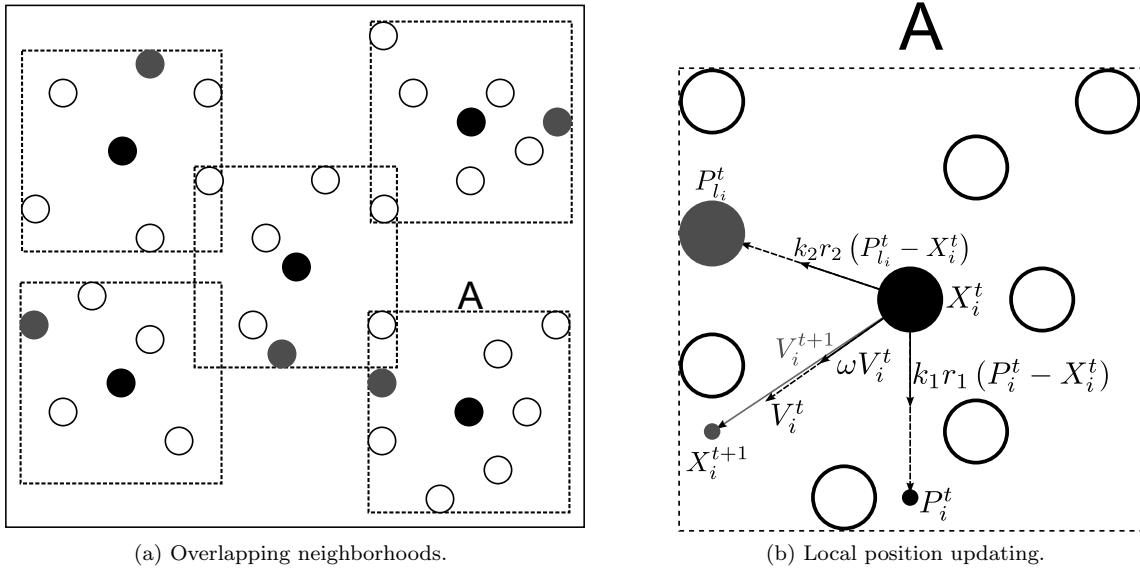


Figure 4.3: Local implementation of the migration algorithm.

As a final point in the description of our model, it is convenient to summarize the parameters involved in our experiments, such information is presented in Table 4.1.

Parameters for preys	Notation
Initial number of preys	Y_0
Prey's reproduction neighborhood radius	y
Per capita reproductive capacity of preys	ϵ_Y
Radius of the competition neighborhood	c
Competition factor	α
Parameters for predators	
Initial number of predators	Z_0
Predators' reproduction neighborhood radius	z
Per capita reproductive capacity of predators	ϵ_Z
Radius of the social neighborhood	l
Cognitive factor	k_1
Social factor	k_2
Inertia weight	ω
Maximum speed of a particle	$\ V\ _{max}$

Table 4.1: A summary of the parameters of the model

Chapter 5

Spatial and population dynamics

In this section we explore the temporal and spatial dynamics of the proposed model. In all figures that follow, the next color code is used to identify the state of a cell:

- **Black.** Denotes an empty cell (state 0).
- **Green.** Represents a cell inhabited only by a prey (state 1).
- **Red.** A cell that contains only a predator (state 2).
- **Yellow.** A cell inhabited by a prey and a predator (state 3).

5.1. Analysis of the global implementation

5.1.1. Dynamics in the absence of movements

By setting k_1 and k_2 to zero in equation 2.22, the velocity vector of each particle is the zero vector for all time steps. Since there is no movement of predators, only reproduction remains as a mean of the species dispersal, which is controlled by four parameters: r_Y and r_Z , the radius of the neighborhood inside of which preys and predators reproduce respectively, and the per capita reproductive capacity of each population. Under these conditions, r_Y and r_Z determine the speed of dispersal of each population. In Figure 5.1, the temporal dynamics of the model with a fixed r_Y , and an increasing r_Z are shown. As r_Z grows, the speed at which the population of predators attains the carrying capacity of the ecosystem also increases.

When the speed of dispersal and the per capita reproductive capacity of both populations are approximately equal, the lattice is dominated by target patterns and spirals. Figure 5.2b shows the results of a simulation with the parameters specified by Table 5.1.

Patterns such as these have been reported previously in works dealing with prey-predator spatial models [44, 27], and all of them are examples of self-organization starting from highly heterogeneous initial conditions. In the proposed model, the conditions that lead to these patterns are as follows: a single cluster of predators feeds on prey leaving a group of empty patches in those locations, when predators reproduce they expand the original cluster. Since there is no movement, those individuals in the center of the cluster will die due to starvation, the result is a thick circle of predators. Now prey reproduction will diminish the width of this circle, and at the same time, there is a chance that some of the new individuals will invade the formerly empty space, and thus starting the formation of a new pattern.

5.1.2. Social interactions, cognitive knowledge and density dependence

In this section we describe the behavior of model when the global PSO algorithm is used to model the movement of predators. In order to accomplish this we have selected the parameters presented in Table 5.2, we focus on the effects that the PSO parameters have on the global dynamics of the model.

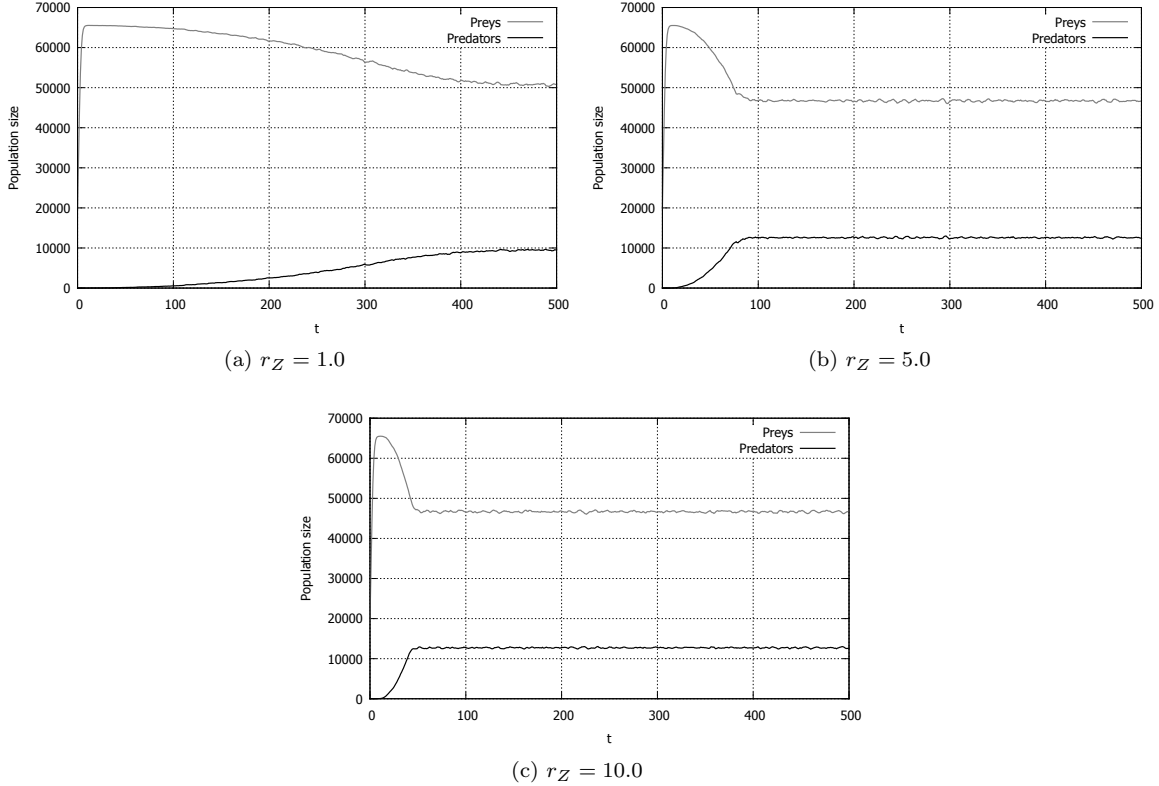


Figure 5.1: Temporal dynamics under an increasing predator reproduction radius.

When $k_2 > 0$, the velocity vectors of all particles will point (to some degree) to P_g^t , a consequence of this behavior, and in a typical PSO fashion [57], is that particles oscillate around this position. The magnitude of such oscillations depend on the values taken by ω , k_1 , k_2 and $|V|_{max}$, and determine the size of a cluster formed as predators move. Figure 5.3 shows the increase in size of such cluster as $|V|_{max}$ grows, in a simulation where $k_1 = 0.0$ and $k_2 = 2.0$. In Figures 5.3a and 5.3b the cluster's size is greatly limited by a small $|V|_{max}$, is worth noting that under this conditions the size of the population of predators do not depends on the amount of resources available, moreover the impact they have on the population of preys is negligible. As $|V|_{max}$ increases (Figures 5.3c to 5.3f), more preys are eaten each season and density dependence becomes relevant, i.e., the size of the swarm depends heavily on the amount of resources available.

When only $k_1 > 0$, a particle moves taking into consideration only its best known position. Figure 5.4 shows the spatial patterns that results from a simulation where $k_1 = 2.0$ and $k_2 = 0.0$. From Figure 5.4a we can observe that most of the predators remain close to the borders between patches of preys and empty zones. As a particle moves towards one of these borders, the fitness value of the positions it encounters keeps improving; but eventually only two things can happen:

- The fitness value of a new position is worse than that of a previous cell, so at the next time step the particle will move to a previously visited zone.
- The particle finds a zone with the highest fitness value, thus $P_i^{t+1} = P_i^t$ and the particle oscillates around this zone until it no longer moves (due to the effects of ω).

When a particle stops moving, either because it cannot find a better position or because migration has ended, it reproduces; after predation most of the new individuals lie near of a recently created border, where the cycle will be repeated. Due to this process the effects of $|V|_{max}$ on the spatial dynamics of the ecosystem are limited: in Figures 5.4b and 5.4c we can observe a reduction in size of the prey patches; however, the differences with the patches shown in Figure 5.4a are minimal.

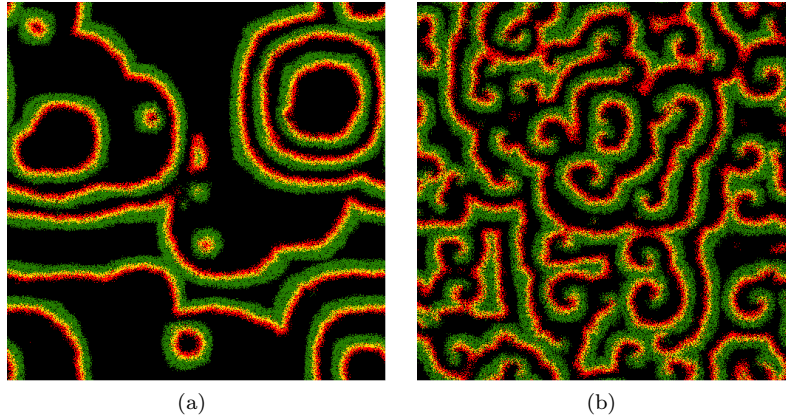


Figure 5.2: Target patterns and spirals form when the rate of dispersal of both species is approximately equal (Lattice size = 512×512 cells).

Parameter	Value
Migration steps	5
$ V_{max} $	Not important
α	0.15
Y_0	50% of cells
ϵ_Y	10
r_Y	5
Z_0	1
ϵ_Z	10
r_Z	5
r_c	1
k_1	0.0
k_2	0.0
ω	0.0

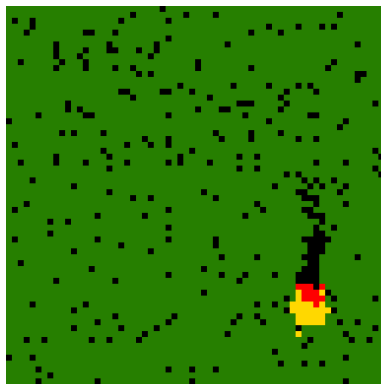
Table 5.1: Parameters used to produce target and spiral patterns.

Another important consequence of the pure cognitive behavior of the predators is that even if there is no social interaction among them, the prey - predator interactions become local. When $k_2 > 0$ “locality” is superseded by the global behavior of the swarm. We have seen that even if $|V|_{max}$ is small enough to prevent long jumps across the lattice, this has the undesired effect of a limited growth of the population of predators due to the coordinated movement, even if resources are abundant. Does this mean that this kind of movement is wrong or unreal? It becomes unreal if prey - predator interactions are a local process, but it is not unreasonable to think in animal populations that can travel long distances in a relatively short time.

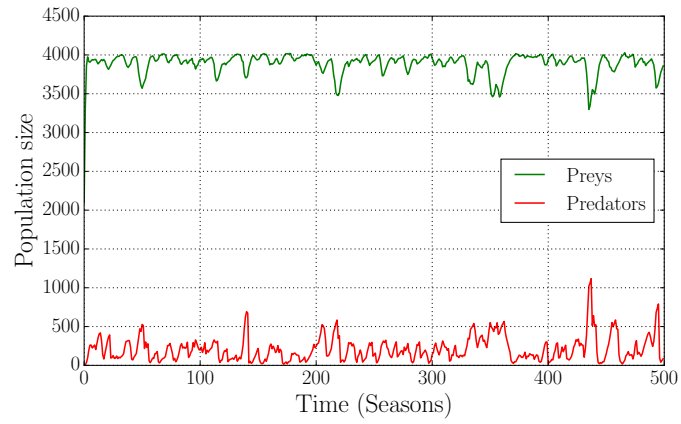
The population dynamics under these conditions (see Figure 5.5) reveal a strong density dependence between both populations, this is in agreement with several works where a predator moves to zones where the density of preys is high [44, 31, 71].

Finally if both $k_1 > 0$ and $k_2 > 0$ then the value taken by k_2 becomes critical. Figure 5.6a shows the results of a simulation where $k_1 = 1.0$ and $k_2 = 0.05$, most of the swarm is dispersed, however, since most of the particles carry a component pointing towards P_g^t (which in the figure has been marked with a \times) in their velocity vector, there is still a coordinated movement (albeit very slow) towards that position. Figure 5.6b shows the population dynamics corresponding to these conditions, most of the oscillations that were evidence of density dependence have almost disappeared.

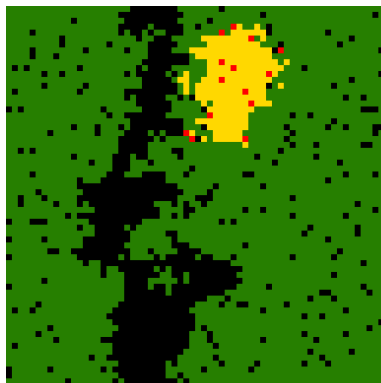
As the value of k_2 continues to grow the swarm becomes more compact and the behavior degenerates



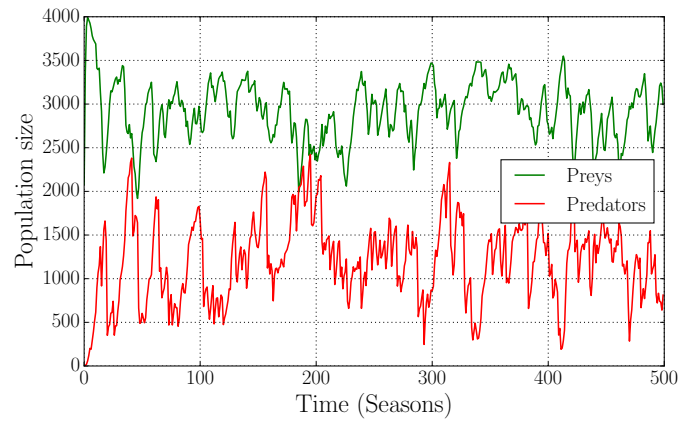
(a) $|V|_{max} = 5$



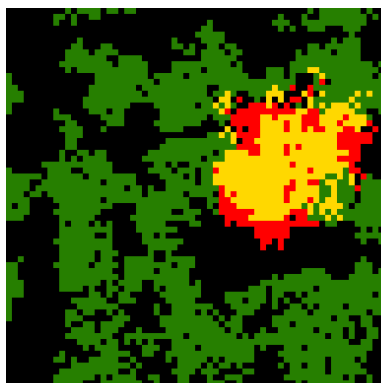
(b)



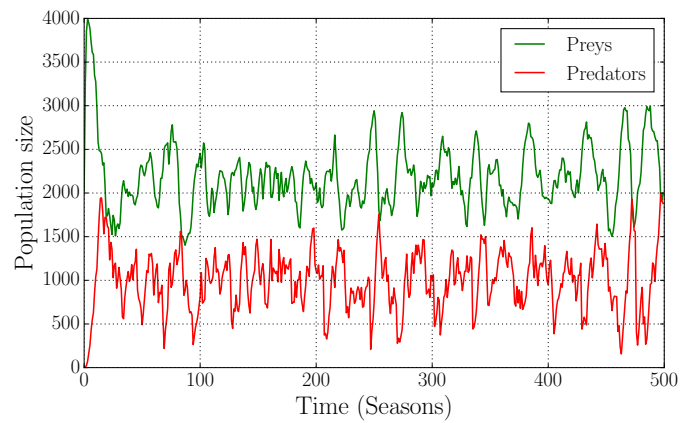
(c) $|V|_{max} = 15$



(d)



(e) $|V|_{max} = 20$



(f)

Figure 5.3: As $|V|_{max}$ grows the size of the cluster increases, and density dependence becomes more evident (Lattice size = 64×64 cells.)

Parameter	Value
Migration steps	5
α	0.05
Y_0	50% of cells
ϵ_Y	2
r_Y	1
Z_0	1
ϵ_Z	5
r_Z	2
r_c	5
ω	0.9 - 0.2

Table 5.2: Parameters used to investigate the behavior of the model under the effects of the PSO algorithm.

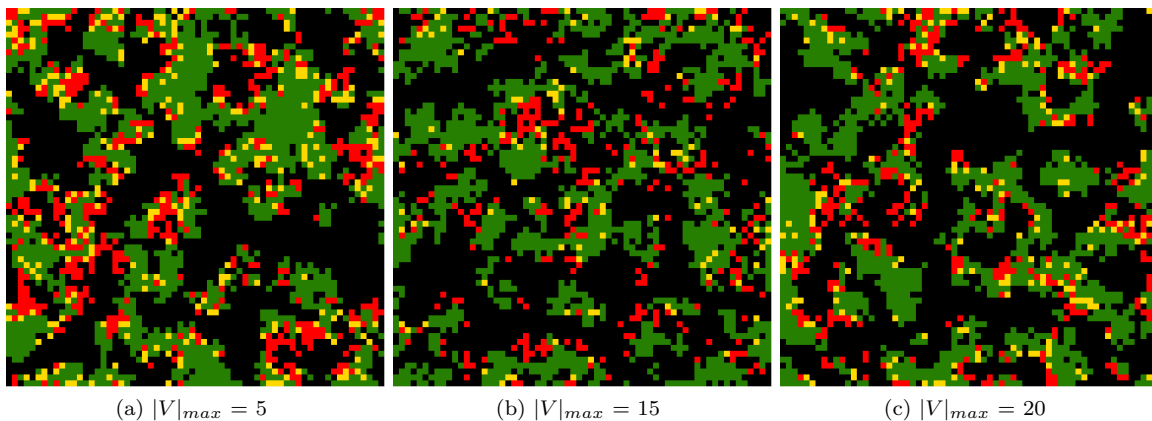
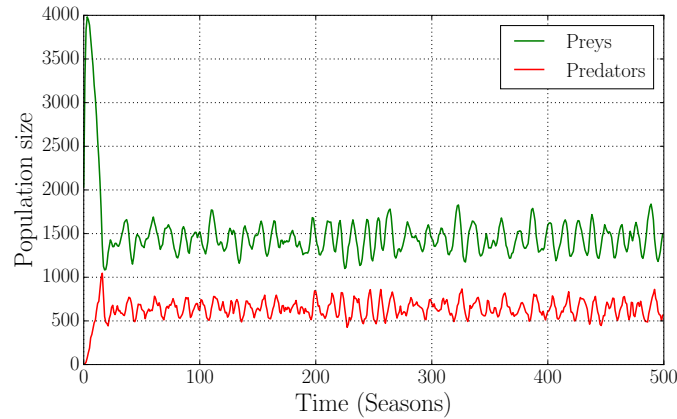


Figure 5.4: Dispersion of predators in a simulation where $k_1 = 2.0$ and $k_2 = 0.0$ (Lattice size = 64×64 cells.)

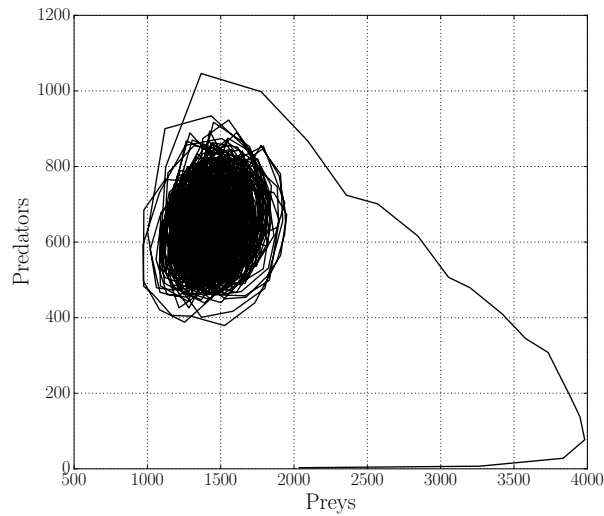
into the one observed when only k_2 had a small value greater than zero (see Figures 5.7a and 5.7b).

Even if the dynamics shown by the global implementation seems reasonable enough, there are some issues with its design: first from a biological perspective, it is unreal that some sort of “collective consciousness” inform individuals about the findings of other members of the swarm in some remote location of the lattice. Moreover under this method, if an individual is located near of a zone with a moderate level of resources, and then it is informed by the swarm about an abundant zone that is however, far away from its current location, it will try to move to that location. Since the predator only has a finite amount of time to complete its migration, there is high chance that it will die as a consequence of this effort, this is particularly evident when k_2 dominates the dynamics of the model.

Clearly most issues arise from the “global” nature of the algorithm, by adapting a local PSO to the communication of predators it is expected that model reflects spatial dynamics that agree more with the spatial patterns observed in nature, specially when switching to a pure cognitive movement already results in oscillations where density dependence is present. An interesting application of a local PSO in a CA context appears in [78], where an hybrid approach to numerical optimization is presented, here the authors emphasise the need to strengthen the communication structures among the particles of the swarm.



(a) Population dynamics.



(b) Dynamics in the Prey - Predator phase space.

Figure 5.5: Population dynamics under a pure cognitive movement.

5.2. Analysis of the local implementation

5.2.1. Social dynamics

In order to explore the social behavior of the predators, the effects of the parameters k_1 and ω are eliminated by setting them to zero, then equations 2.22 and 2.23 become:

$$V_i^{t+1} = k_2 r_2 (P_{l_i}^t - X_i^t) \quad (5.1)$$

$$X_i^{t+1} = X_i^t + V_i^t \quad (5.2)$$

To explore the spatial and population dynamics of the local PSO algorithm we have selected the parameters presented in Table 5.3. Such parameters depict an ecosystem where preys have a smaller reproductive capacity than that of predators, which makes possible to observe the movement of predators in detail. Also note that the reproduction radius of preys is bigger than the reproduction radius of predators, which reflects the higher dispersal capacity of preys due to factors like the wind

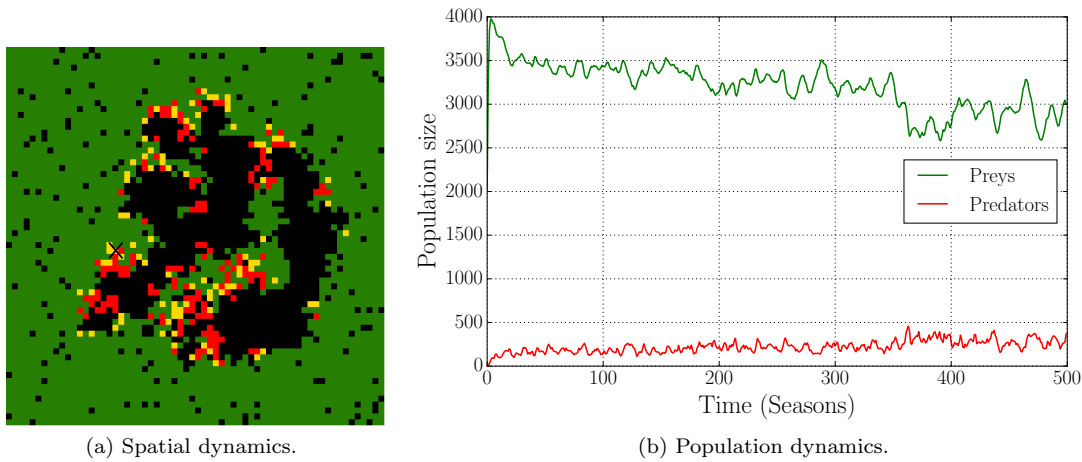


Figure 5.6: As a result of a weak social factor ($k_2 = 0.05$) and a strong cognitive factor ($k_1 = 1.0$), the swarm disperses, but keeps moving towards P_g^t .

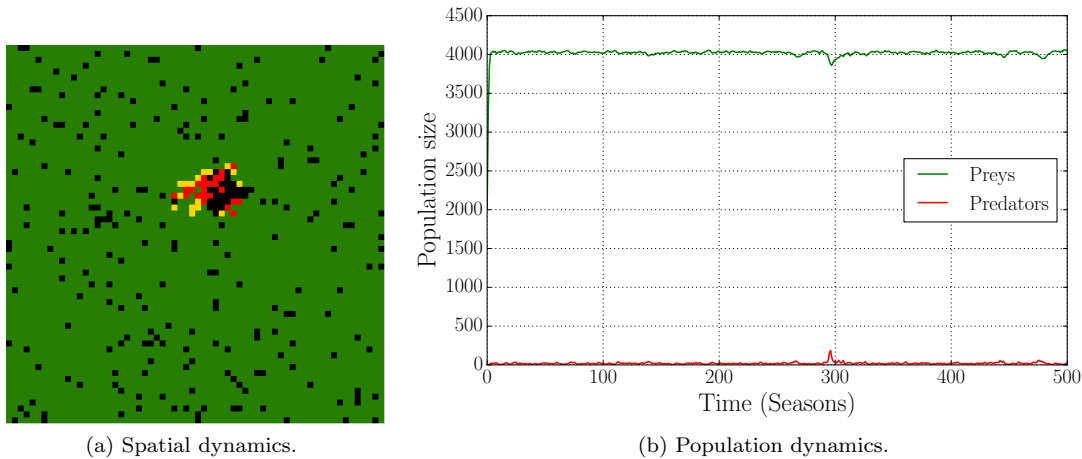


Figure 5.7: Density dependence is non-existent as a consequence of the increase of the social factor ($k_1 = 1.0$ and $k_2 = 0.35$).

or animal vectors. Finally, since we are interested in the social interactions of the predators, we use a rather big neighborhood (radius 7) in order to observe such interaction with detail.

When $k_2 > 0$, V_i^{t+1} points only towards $P_{l_i}^t$. If a particle i is located at a good position, then all particles that are neighbors of i will be attracted to it, forming a cluster whose size depends on the radius of the social neighborhood M_l and the magnitude of the oscillations around $P_{l_i}^t$. However due to the exploration of the search space and the reproduction of predators, a particle is able to separate from the cluster, allowing the formation of a new pattern. Figure 5.8a shows a single cluster formed after 10 seasons in a simulation where $k_2 = 1.0$. Figure 5.8b shows that after 620 seasons the cluster has separated in three new patterns. Figure 5.8c shows the ecosystem after 1000 seasons, it is possible to distinguish regions populated by isolated clusters, and zones where two or more clusters have merged together, due to a greater number of predators, those zones are subjected to a more intense predation. However, the effects of these “super” clusters on the ecosystem are short lived due to the fragmentation in smaller clusters, and the local extinctions resulting from a higher consumption of resources. As the

Parameters for preys	Value
Y_0	90% of cells
y	3
ϵ_Y	1
c	3
α	0.05
Parameters for predators	
Z_0	1
z	1
ϵ_Z	3
l	7

Table 5.3: Parameters used to analyze the behavior of the proposed model under the effects of the local PSO algorithm.

value of k_2 grows, the magnitude of the oscillations around $P_{i_i}^t$ increases; consequently, there is an increase in the size of the clusters, as shown in Figures 5.8d - 5.8f.

The effects of a $k_2 > 0$ on the spatial dynamics of the model are specially evident when k_1 and ω are restored to values that are also greater than zero. The purpose of the ωV_i^t term is to enhance the exploration of the search space at the beginning of the algorithm, and to favor the exploitation of “good” known solutions at the final iterations of the algorithm, this is achieved through a decreasing scaling of the velocity vector at time t by the factor ω . Figure 5.9a shows a section of the ecosystem where two large clusters are visible at the middle, the first two migration steps are characterized by a long range movement of predators into the zones populated by preys as shown in Figure 5.9b, these movements result in the fragmentation of the clusters. Figure 5.9c shows that subsequent movements will group the particles as they converge towards a common solution.

When the cognitive term is restored ($k_1 > 0$), the velocity vector of a particle contains a component pointing to P_i^t , ideally, this would cause a fragmentation of clusters as each particle moves according to its own experience. However, the component of V_i^{t+1} that points to $P_{i_i}^t$ ensures a “coordinated” movement towards this position even for large values of k_1 . So even if the clusters look more dispersed they still retain some degree of cohesion.

So far only the effects on the spatial dynamics of the model as result of the behavior of the predators have been discussed. The next sections will focus on the population dynamics of the ecosystem, we will pay special emphasis to the oscillatory behavior that results from an enhanced predator mobility.

5.2.2. Predator mobility and density dependence

Section 5.2.1 showed that any increase to k_2 causes an increase in the size of the clusters, in Figure 5.8c most of the ecosystem is populated by small sized clusters, as a consequence, the carrying capacity of the population of predators is much less than that of the population of preys. The temporal dynamics (see Figure 5.10a) reveals irregular oscillations where it is possible to observe some patterns typical of density dependence, such irregularity is easily explained once we note that the peaks of the plot correspond to the predation levels that arise as the consequence of the merging of two or more clusters. Since the number of these events during a migration stage is essentially random, and since the size of the resulting clusters is different from season to season, the corresponding population cycle is very irregular. It is reasonable to expect that as the value of k_2 increases, the carrying capacity of the population of preys decreases as a consequence of the pressure exercised by the predators. Figure 5.10b shows the results of a simulation where $\omega = 0$, $k_1 = 0$ and $k_2 = 1.5$, besides showing the expected decrease in the population of preys, it is possible to observe that both populations oscillate with the typical “out of phase” behavior of prey-predator systems. The enhanced predator mobility caused by the increase of k_2 , provokes a faster movement away from zones with a low fitness and increases the rate at which the clusters merge. As a result more gaps are created each season, which translates in a

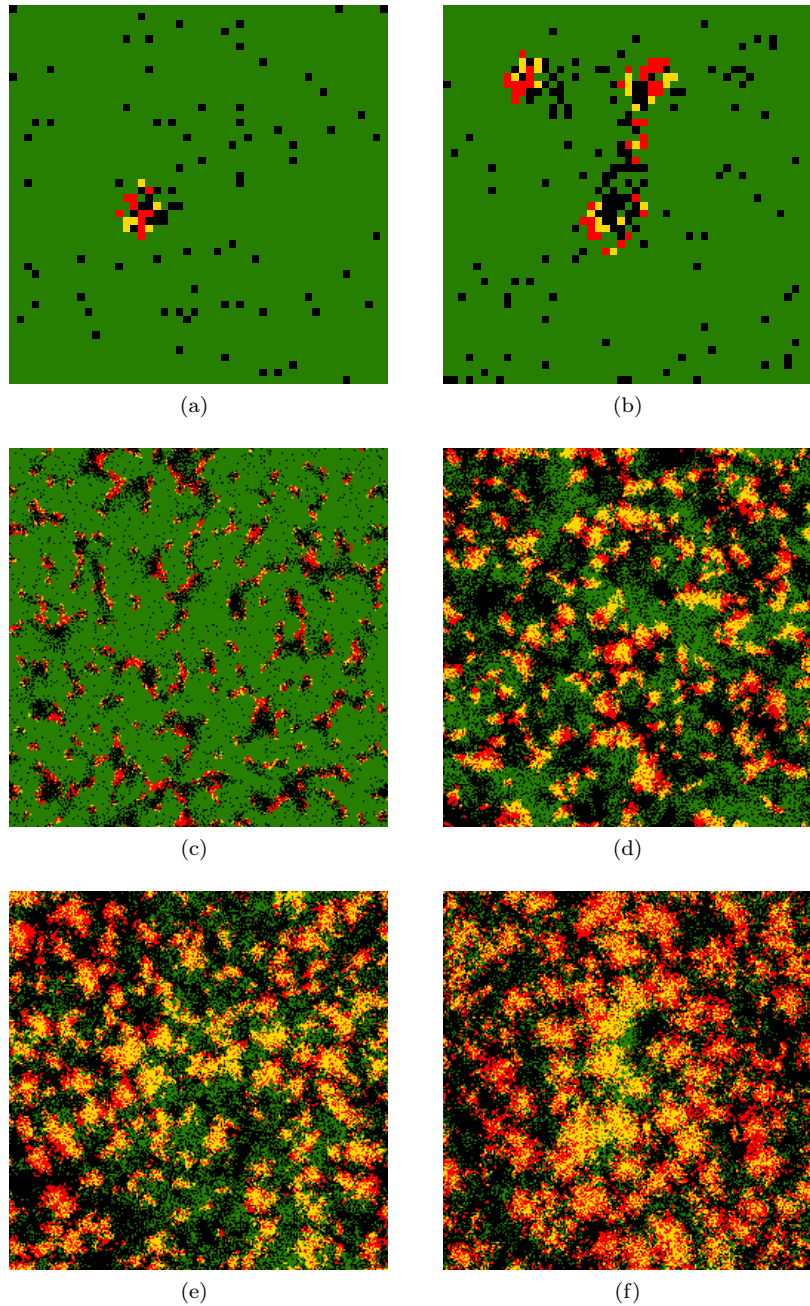


Figure 5.8: Spatial dynamics due to the social interactions among predators. (a) Predators grouped together. (b) A cluster divides as a consequence of a finite $M_{r_1}^2$. The size of the clusters increases as a result of a fast movement to cells with a high fitness: (c) $k_2 = 1.0$, (d) $k_2 = 1.5$, (e) $k_2 = 2.0$, (f) $k_2 = 2.5$

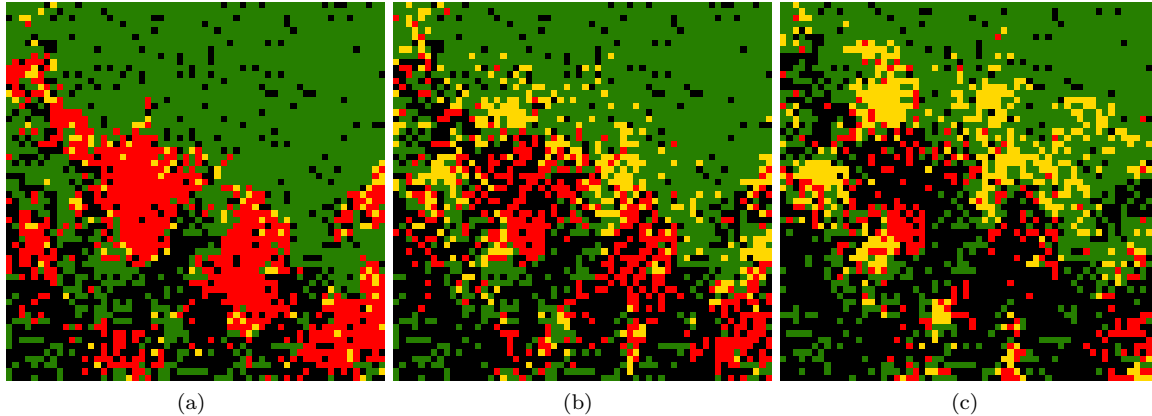


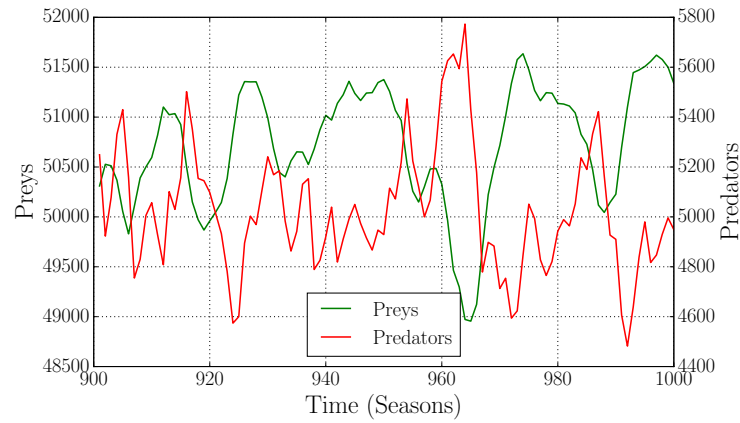
Figure 5.9: Effects of an $\omega > 0$ on the movement patterns of predators: (a) Distribution before migration. (b) During the first stages of migration, a predator executes long range movements that will likely produce the fragmentation of a cluster. (c) The final stages of migration are characterized by small steps that favor exploitation and form new clusters.

greater prey mortality. Figure 5.10c shows a new decrease in the number of preys obtained for $\omega = 0$, $k_1 = 0$ and $k_2 = 2$.

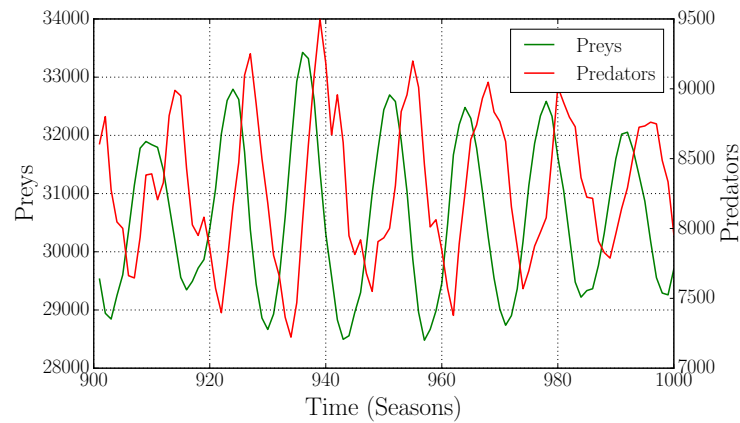
Besides illustrating density dependence, Figures 5.10a to 5.10c show that as the value of k_2 increases, the ecosystem enters into an oscillatory regime. Figure 5.11a shows a phase plot corresponding to the time series of Figure 5.10a, it is possible to observe that “random” oscillations remain in the long term time limit (after a thousand seasons). However, the phase plot for $k_2 = 2$ that appears in Figure 5.11c shows a limit cycle at the same time lapse. This suggests that under such conditions, the time lag between the creation of gaps, and the time until these zones are qualified again as “good” by the predators becomes regular. It is possible to investigate further this cyclic behavior by means of the Fourier spectra: Figure 5.11b shows the spectra corresponding to $k_2 = 1.0$, the spectra obtained presents a single peak at the zero frequency, which corresponds to the random patterns observed in the time series. The spectra obtained for $k_2 = 2$, see Figure 5.11d, shows a sharp peak at a frequency value of 0.08 (12.5 seasons), this peak identifies the frequency component responsible for the cyclic behavior in the time series for a value of $k_2 = 2$. A second peak is observed at a frequency value of 0.172, i.e., twice the frequency of the first peak.

In order to further investigate the nature of the oscillations in our model, we performed additional simulations using the parameters presented in Table 5.4, such parameters correspond to an initial configuration close the prey-only absorbent distribution with a single individual of the predators species.

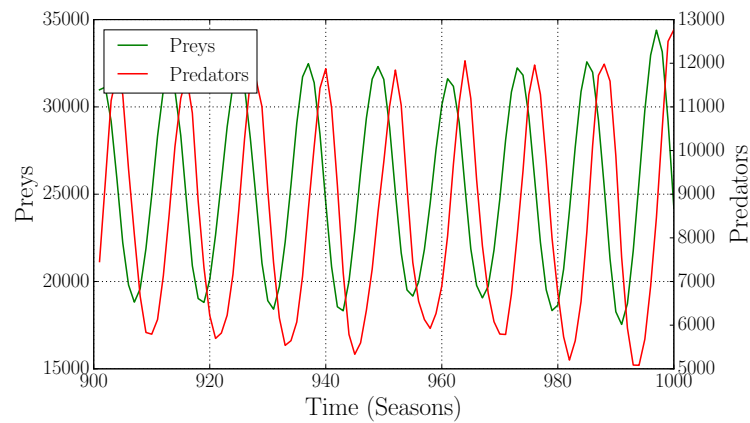
Figure 5.12 shows the invasion of the prey domain by predators. In Figure 5.12a several swarms of predators grouped at the source of the invasion can be observed, due to the high density of preys, the formation of these patterns occurs quickly after the start of the simulation. As predation takes place, swarms move outwards following the direction of highest prey density; however, the movement of swarms located near the source of the invasion is limited by swarms located far from the source of the invasion: if an “inner” swarm tries to expand, it is possible for its destination to be already occupied by an “outer” swarm, or it may also be the case that zones predated by “outer” swarms make an expansion a futile effort. Such process results in an expanding wavefront of “outer” swarms moving at the same speed, while “inner” swarms remain behind (see Figure 5.12b). It must be noted that the wavefront is not homogeneous; i.e., swarms do not cover the whole perimeter of the wave (see Figure 5.12c), which in turn allows some preys to survive the invasion. Zones with a low density of preys behind the wavefront are repopulated by the survivors, thus creating new clusters of preys (see Figure 5.12d), which become the target of the “inner” swarms of predators. There is then a division between a prey-only state ahead of the invasion front, and a coexistence state behind, where swarms continuously migrate from zones with a low density of preys to zones highly populated by them. Similar divisions have been analysed previously: for a two-dimensional coupled map lattice and



(a) $\omega = 0, k_1 = 0, k_2 = 1.0$



(b) $\omega = 0, k_1 = 0, k_2 = 1.5$



(c) $\omega = 0, k_1 = 0, k_2 = 2.0$

Figure 5.10: Population dynamics of the local implementation under an increasing k_2

two-dimensional reaction diffusion equations, Sherrat et al. [28] observed periodic travelling waves that persist or decay into irregular spatio-temporal oscillations due to being intrinsically unstable. Arashiro et al. [29] obtained a similar division for a probabilistic cellular automaton; behind the initial

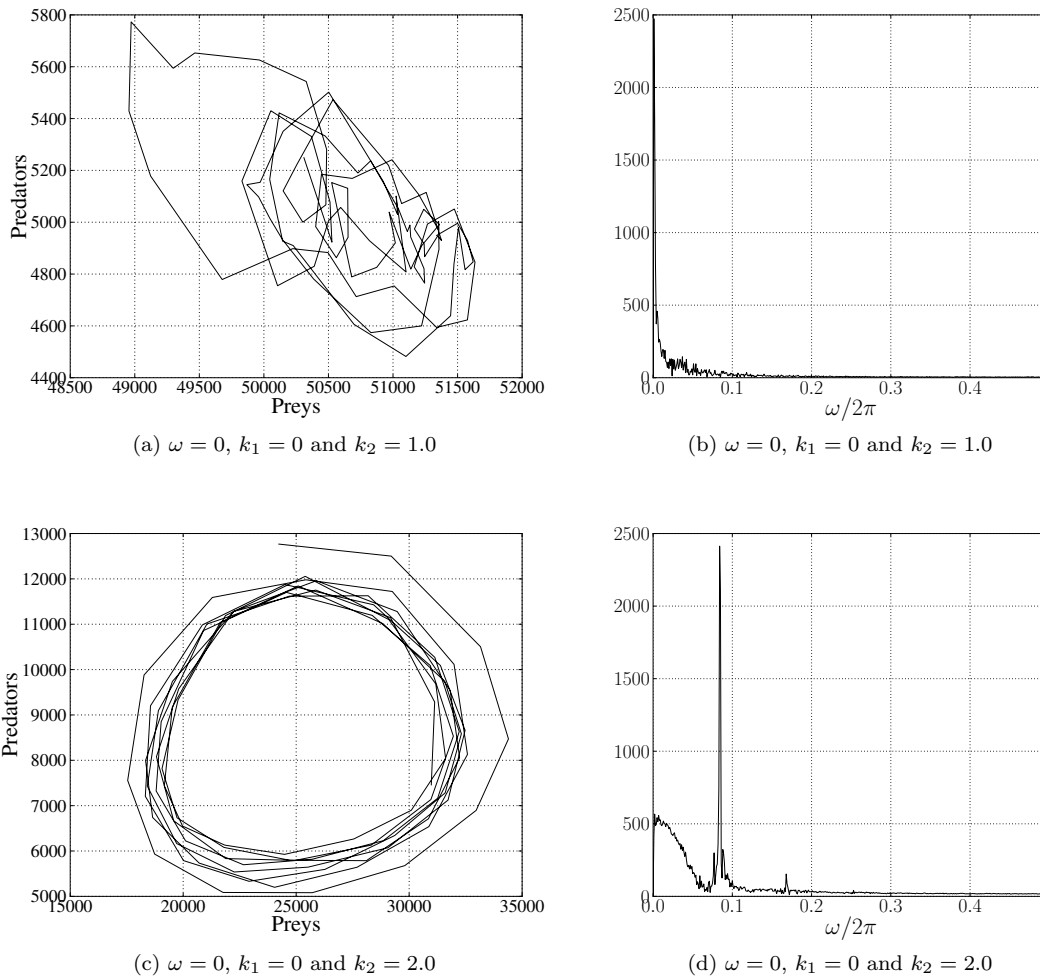


Figure 5.11: Transition to the oscillatory regime.

wave front they observed a coexistence characterized by local time coupled oscillations where small clusters of predators invade large clusters of preys. A second coexistence state where both populations are grouped into small clusters isolated from each other was observed for a low death probability of predators which is compensated by higher birth probabilities.

The population dynamics for the proposed model under the parameters specified by Table 4.1 is shown in Figure 5.13. The expansion of the initial wavefront produces a monotonic approach to a non-trivial fixed point during the transient period of the system; once such approach ends, it is possible to observe weak oscillations around the fixed point, which corresponds to subsequent travelling waves that are produced when surviving preys repopulate the space behind the wavefront, only to be consumed by the “inner” swarms. Such process is short lived, and waves will eventually disappear; after the transient, both populations oscillate with a very regular period and the typical “out of phase” behavior of prey-predator systems (see the right inset of Figure 5.13).

From an ecological point of view, the nature of the cyclic behavior of an ecosystem is diverse: time lags in the reproductive cycles of preys and predators, migration, seasonal hunting, weather conditions, behavioral patterns such as aggressiveness, among others [19].

Parameter	Value
Ψ_0	1
ϵ_Y	1
y	3
α	0.05
c	3
Φ_0	1 predator = 3.8147×10^{-6}
ϵ_Z	2
z	1
Migration parameter	Value
k_1	1
k_2	2
l	7
ω	linear decrease from 0.9 to 0.2

Table 5.4: Parameters used in computer simulations.

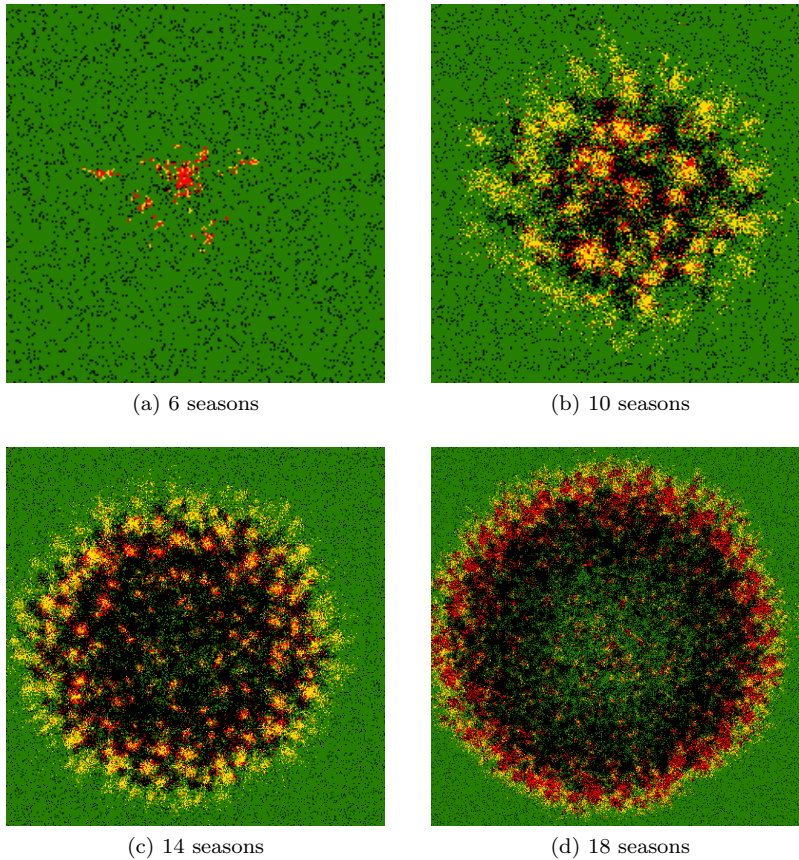


Figure 5.12: Invasion of preys by predators.

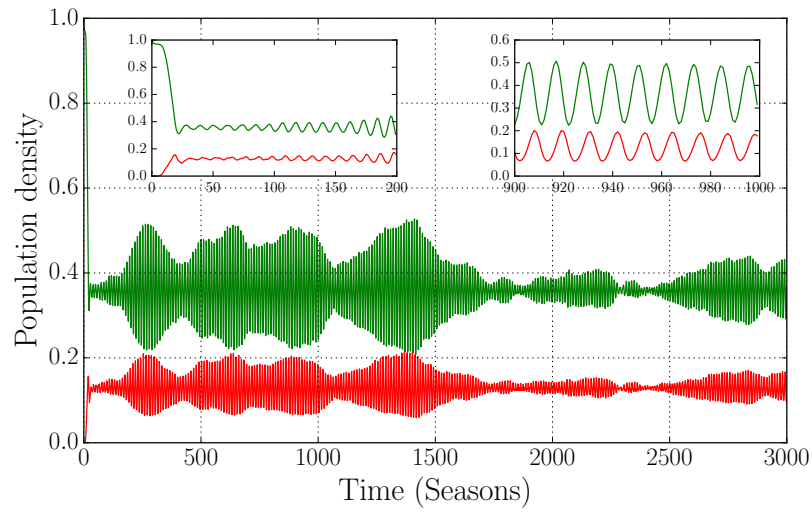


Figure 5.13: Population dynamics of the proposed model under the parameters of Table 4.1. The left inset shows a monotonic approach to a fixed point during the transient phase of the simulations, which corresponds to traveling wavefronts that appear during the invasion process. The right inset shows that oscillations have a very regular period and are out of phase.

Chapter 6

Mean field analysis

6.1. Mean field terms for the proposed model

In this section we obtain the mean field terms for each rule that comprises the proposed model, later a complete mean field model that describes the changes in density for both populations that occur during a season will be built using these terms. Before analysing each rule, let us introduce some notation:

- $\Psi_t \in [0, 1]$ is the density of preys at time t .
- Y_t is the number of preys at time t .
- $\Phi_t \in [0, 1]$ is the density of predators at time t .
- Z_t is the number of predators at time t .

6.1.1. Intraspecific competition

During this stage preys die with a probability proportional to the number of individuals of the prey species within a M_c neighborhood, i.e.

$$P[c^{t+1}(\vec{n}) = 0 \mid c^t(\vec{n}) = 1] = P[c^{t+1}(\vec{n}) = 1 \mid c^t(\vec{n}) = 2] = \frac{\alpha y}{|M_c| - 1} \quad (6.1)$$

where:

- $\alpha \in [0, 1]$ is the intraspecific competition coefficient, which determines the intensity of the competition exercised by other preys in the neighborhood of cell \vec{n} .
- y is the number of preys within the neighborhood M_c of cell \vec{n}
- $|M_c|$ is the cardinality of the neighborhood M_c .

For example, if during the intraspecific competition stage, a cell is inhabited by a prey ($c^t(\vec{n}) = 1$), the neighborhood M_1 ($c = 1$) contains five preys and $\alpha = 0.5$, then the prey in cell \vec{n} dies with probability:

$$P[c^{t+1}(\vec{n}) = 0 \mid c^t(\vec{n}) = 1] = \frac{\alpha y}{|M_1| - 1} = \frac{(0.5)(5)}{8} = 0.3125 \quad (6.2)$$

In order to derive a mean field equation that describes the intraspecific competition stage, let us ask the following: What is the expected number of deaths in a season due to the intraspecific competition? As it was shown previously, the death of a prey depends on the number of individuals of the prey species contained in the neighborhood M_c , it is reasonable then to expect that the mean number of

deaths each season depends on the mean number of individuals in the neighborhood of each cell, let \bar{y}_t represent this number.

To calculate \bar{y}_t we proceed as follows: it is clear that if $\Psi_t = 0$, then the mean number of preys in each neighborhood M_c is also zero, similarly if $\Psi_t = 1$, then the mean number of preys within each neighborhood M_c (excluding the prey at cell \vec{n}) is $|M_c| - 1$, an interpolation between the points $(0, 0)$ and $(1, |M_c| - 1)$ (see Figure 6.1) gives the equation:

$$\bar{y}_t = (|M_c| - 1) (\Psi_t) \tag{6.3}$$

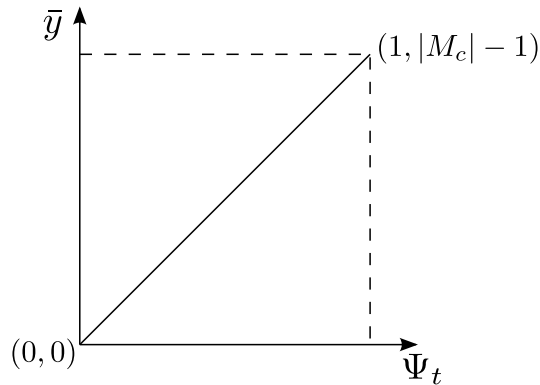


Figure 6.1: This interpolation assumes proportionality between Ψ_t and the number of preys in the neighborhood M_c .

Then, the probability that a prey dies as a consequence of the intraspecific competition is:

$$\frac{\bar{y}_t}{|M_c| - 1} = \frac{(|M_c| - 1) (\Psi_t)}{|M_c| - 1} = \Psi_t \tag{6.4}$$

The death of the all preys in the lattice is a sequence of events that can be described through a random variable with binomial distribution X . If Y_t denotes the number of preys in the lattice at time t , then the expected number of prey deaths is given by:

$$EX = \Psi_t Y_t \tag{6.5}$$

where E is the expected value operator, and Y_t is given by:

$$Y_t = \Psi_t |L| \tag{6.6}$$

thus:

$$EX = \Psi_t^2 |L| \tag{6.7}$$

To incorporate this quantity in the mean field equation, it must be converted into a density, this is done by dividing EX by $|L|$, and scaling the result by the coefficient α , obtaining that the density of preys that is eliminated each season is $\alpha \Psi_t^2$. Finally the mean field equation that describes the intraspecific competition is:

$$\Psi_{t+1} = \Psi_t - \alpha \Psi_t^2 = \Psi_t (1 - \alpha \Psi_t) \tag{6.8}$$

6.1.2. Prey reproduction

During this stage, each prey produces new individuals at random within a neighborhood M_y , the number ϵ_Y of new individuals that each prey produces is known as the per capita reproductive capacity.

Consider a cell with no prey, let us call such cell u . During the reproduction stage, all neighbors of u containing a prey might change its state, the number of neighbors being equal to $|M_y| - 1$. Since

each neighbor chooses the location for new preys at random, the probability that a cell chooses cell u during reproduction is:

$$P_u = \frac{1}{|M_y| - 1} \quad (6.9)$$

The mean number of preys in the neighborhood of u is given by \bar{y}_t , thus the total number of reproduction “attempts” is:

$$\epsilon_Y \bar{y}_t \quad (6.10)$$

where:

- ϵ_Y is the reproductive capacity of preys.
- $\bar{y}_t = (|M_y| - 1)(\Psi_t)$ is the mean number of preys in the neighborhood of cell u (see Section 6.1.1).

Let X denote the random variable that counts the number of times cell u is chosen for reproduction, it is clear that X is a binomial random variable with parameters $(P_u, \epsilon_Y \bar{y}_t)$. Now $(1 - P_u)^{\epsilon_Y \bar{y}_t}$ is the probability that none of the preys in the neighborhood of u chooses it for reproduction, then $1 - (1 - P_u)^{\epsilon_Y \bar{y}_t}$ is the probability that cell u is chosen at least once during the reproduction stage. The mean density of cells with no preys that are chosen for reproduction during the corresponding stage is:

$$(1 - \Psi_t)(1 - (1 - P_u)^{\epsilon_Y \bar{y}_t}) \quad (6.11)$$

6.1.3. Death of Predators

Each season, if a predator is not located at a cell containing a prey, it dies with probability 1. The number of predators that die each season is proportional to the number of cells not containing a prey, the probability of finding a cell with such a property is given by:

$$\frac{|L| - Y_t}{|L|} = 1 - \frac{Y_t}{|L|} = 1 - \Psi_t \quad (6.12)$$

Then the expected number of deaths that occur each season is given by:

$$(1 - \Psi_t) Z_t$$

Finally the expected decrease in density is:

$$(1 - \Psi_t) \Phi_t \quad (6.13)$$

6.1.4. Reproduction of predators

This process behaves just like the reproduction of preys, the mean density of of cells not inhabited by a predator that are chosen for reproduction during the corresponding stage is:

$$(1 - \Phi_t)(1 - (1 - P_u)^{\epsilon_Z \bar{z}_t}) \quad (6.14)$$

where:

- Φ_t is the density of predators at time t .
- $P_u = 1/(|M_z| - 1)$ is the probability that cell u becomes a target for reproduction after being selected by a predator in the neighborhood $|M_z|$.
- ϵ_z is the reproductive capacity of the predator species.
- \bar{z}_t is the mean number of predators in the neighborhood of cell u at time t .

6.1.5. Predation

Each season if a prey is located at a cell containing a predator, it dies with probability 1. The probability of finding a cell with a predator is:

$$\frac{Z_t}{|L|} = \Phi_t \quad (6.15)$$

The expected number of preys dying each season is:

$$\Phi_t Y_t \quad (6.16)$$

And the expected decrease in density is given by:

$$\Phi_t \Psi_t \quad (6.17)$$

To end this section, it must be noted that since no density changes occur during the migration stage, there is no mean field term associated to such rule, the resulting effects of migration will be accounted in another way.

6.2. Mean field models for the long term dynamics

Tough it is entirely possible to construct a pair of mean field equations that describe the change in density of preys and predators from the individual terms derived in the previous section, here, we will take the simpler approach of considering the changes in density that occur through each stage of the model, and then formulate a set of mean field equations that account for such changes.

6.2.1. Predator dynamics

As an example, consider a model where preys and predators obey the next life cycle:

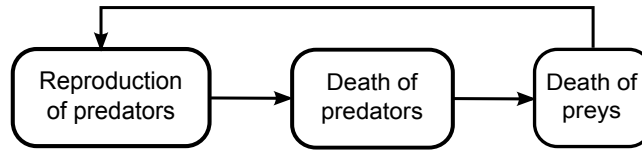


Figure 6.2: A simple life cycle for preys and predators

This model does not take into account intraspecific competition or the reproduction of preys, the corresponding set of mean field equations is:

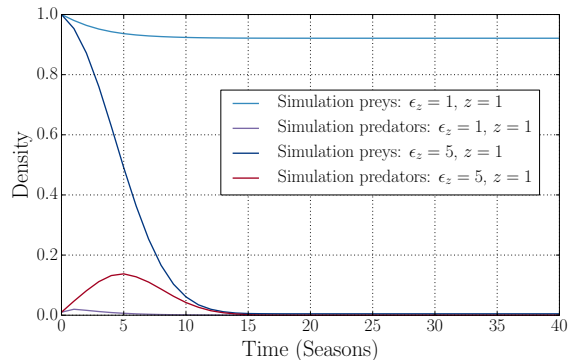
$$\Phi_R = \Phi_t + (1 - \Phi_t)(1 - (1 - P_u)^{\epsilon_Z \bar{z}_t}) \quad (6.18)$$

$$\Phi_{t+1} = \Phi_R - (1 - \Psi_t)\Phi_R \quad (6.19)$$

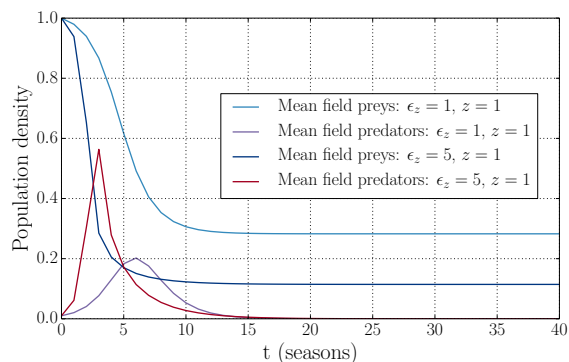
$$\Psi_{t+1} = \Psi_t - \Phi_{t+1}\Psi_t \quad (6.20)$$

where:

- Φ_R is the density of the predator species after the reproduction stage.
- $P_u = 1/(|M_z| - 1)$ is the probability that cell u becomes a target for reproduction after being selected by a predator in the neighborhood $|M_z|$.
- \bar{z}_t is the mean number of predators in the neighborhood of cell u at time t .



(a) Computer simulation.



(b) Mean field model.

Figure 6.3: Population dynamics of the reproduction of predators: mean field model and computer simulations.

Figure 6.3 shows the population dynamics of the reproduction of predators of both the mean field model (Equations 6.18 to 6.20) and the computer simulation. It is easy to observe that the population of predators belonging to the mean field model grows faster than the population depicted in the computer simulation.

To explain these differences, let's look again at the current life cycle of preys and predators: the last stage before the cycle starts again is the “death of preys”, during this stage all preys that share a cell with a predator die due to predation. After this process, all remaining predators (whose density is Φ_t) are located at a cell devoid of an individual of the prey species; during the “death of predators” stage of the next season (that is at the $t + 1$ iteration of the model) all predators of the previous season will die due to a lack of movement of the species (we are not considering migration), thus the only remaining individuals are those that were spawned as a consequence of the reproduction of predators, such quantity is $\Phi_R - \Phi_t$. The remaining predators will die according to $(1 - \Psi_t)(\Phi_R - \Phi_t)$. Now during the new “death of preys” stage, all remaining predators are located at a cell that contains a prey, so the number of preys that die represents a density equal to Φ_{t+1} . Taking into account all of this, we can adjust our mean field model as follows:

$$\Phi_R = \Phi_t + (1 - \Phi_t)(1 - (1 - P_u)^{\epsilon_z \bar{z}_t}) \quad (6.21)$$

$$\Phi_{t+1} = \Phi_R - \Phi_t - (1 - \Psi_t)(\Phi_R - \Phi_t) \quad (6.22)$$

$$\Psi_{t+1} = \Psi_t - \Phi_{t+1} \quad (6.23)$$

Figure 6.4 shows a comparison of the results obtained through this model and the corresponding computer simulations. It is easy to observe that the adjustments made to the mean field model have

produced better results. The remaining differences come from the fact that the mean field model does not consider space, e.g., the mean field term for the reproduction of predators “describes” a system where individuals are uniformly distributed, thus avoiding the saturation of space that is present in the computer simulation of the ecosystem.

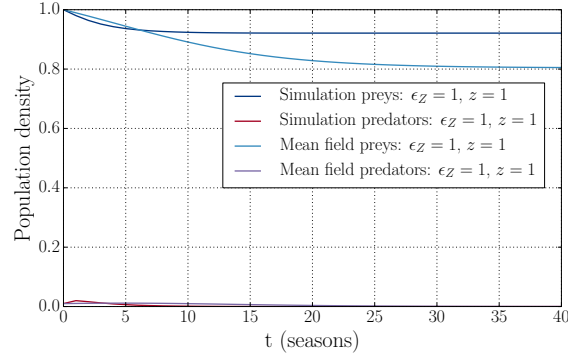
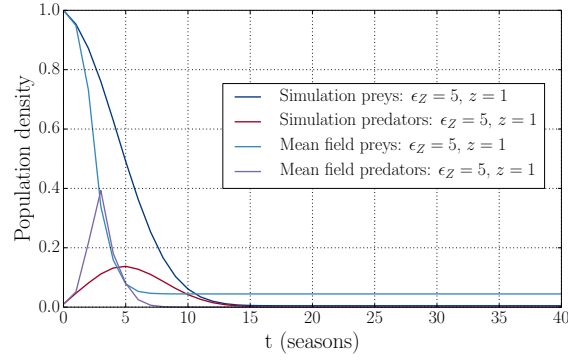

 (a) $\epsilon_Z = 1$

 (b) $\epsilon_Z = 5$

Figure 6.4: Comparison of the population dynamics of the reproduction of predators: adjusted mean field model vs computer simulations.

It is possible to test this hypothesis by increasing the value of z (the radius of reproduction) in the computer simulation. Such action should decrease the saturation of space during the reproduction stage in the CA model, thus allowing a faster growth of the population of predators. Figure 6.5 shows a comparison for $z = 10$, the resulting dynamics of the predator species for the CA model shows a growth rate that matches that of the mean field equations.

6.2.2. A model without migration

Let us now analyse a model where the only absent stage is the migration rule, the life cycle for preys and predators that define such model is depicted in Figure 6.6.

The corresponding mean field model is given by the following set of equations:

$$\Psi_I = \Psi_t - \alpha \Psi_t^2 \quad (6.24)$$

$$\Phi_R = \Phi_t + (1 - \Phi_t)(1 - (1 - P_Z)^{\epsilon_Z \bar{z}_t}) \quad (6.25)$$

$$\Phi_{t+1} = \Phi_R - (1 - \Psi_I)\Phi_R \quad (6.26)$$

$$\Psi_D = \Psi_I - \Phi_{t+1} \quad (6.27)$$

$$\Psi_{t+1} = \Psi_D + (1 - \Psi_D)(1 - (1 - P_Y)^{\epsilon_Y \bar{y}_t}) \quad (6.28)$$

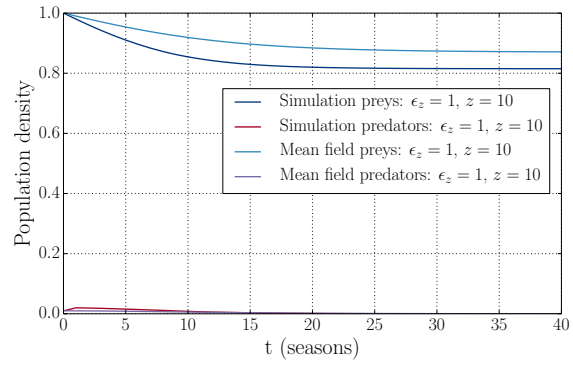
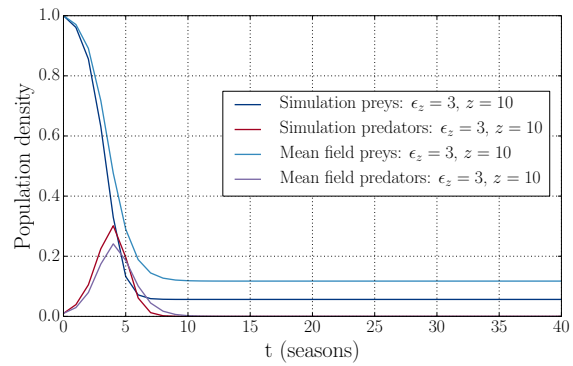
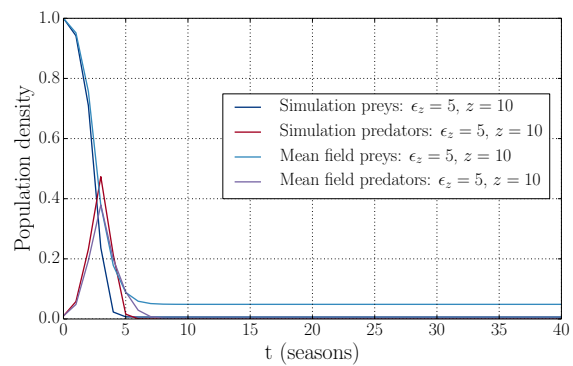
(a) $\epsilon_Z = 1$ (b) $\epsilon_Z = 3$ (c) $\epsilon_Z = 5$

Figure 6.5: Increasing the value of z produces a good agreement of results between the mean field equations and the CA model.

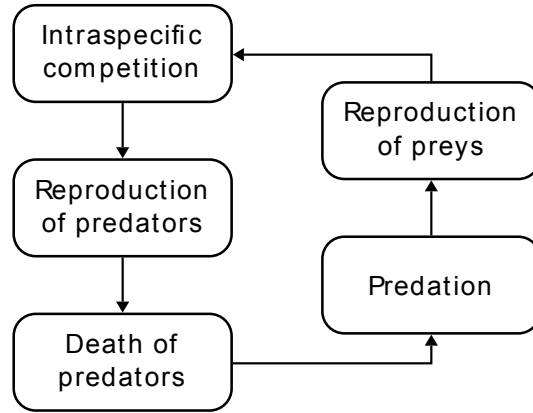


Figure 6.6: The life cycle of a model where there is no migration stage.

where:

- Ψ_I denotes the density of preys after the intraspecific competition stage.
- Φ_R is the density of the predator species after the reproduction stage.
- Ψ_D denotes the density of the prey species after the predation stage.
- $P_Y = 1/|M_y|$ is the probability that a cell devoid of a prey be selected for reproduction by one of its neighboring preys.
- $P_Z = 1/|M_z|$ is the probability that a cell devoid of a predator be selected for reproduction by a neighboring predator.

Note that the mean field term for the "death of predators" stage appears in the form given in Section 6.1.3, since our current model includes the "reproduction of preys" stage, the previous assumption about the number of predators that survive their death is no longer valid, thus, we must assume that the process is purely random.

Unless otherwise stated, the experiments of this section assume $\Psi_0 = 1.0$, $\Phi_0 = 0.001$ and $\alpha = 0.1$

In agreement with computer simulations of the proposed model, the mean field equations have two trivial fixed points: the first corresponds to an ecosystem where both populations go extinct; the second is obtained when all the individuals of the predator species die, leaving behind an ecosystem only populated by preys. Figure 6.7 shows the plots of the population dynamics of the mean field model and the corresponding computer simulation for $\epsilon_Y = 1$, $y = 1$, $\epsilon_Z = 1$, $z = 1$ and $c = 1$. Populations in the mean field model quickly converge towards a fixed point; whereas in the computer simulation, there is a short oscillatory transient before equilibrium is reached. Note that the long-term densities predicted by the mean field model are lower than those observed in the computer simulation. Both of these outcomes are to be expected, it is well known (see, e.g., [67]) that mean field models such as the one given by Equations 6.24 to 6.28 provide only a rough description of the dynamics of a lattice model, since they do not take space into account and assume a "well mixed" environment where individuals are randomly distributed on the lattice.

As with previous experiments, it is possible to obtain a better agreement of the results observed in computer simulations and the results from the mean field model for higher values of y , z and c , as shown in Figure 6.8. Due to the lack of a spatial component, the mean field model represents the behavior of the CA-based model when the neighborhoods generated by y , z and c span the whole lattice, i.e., the limit $M_y = M_z = M_c = L$. Under such conditions, preys compete globally with all other members of their species; when reproducing individuals are able to choose any cell of the lattice as a target for reproduction.

Figure 6.9 shows the phase plots of the mean field vs computer simulations for an increasing value of ϵ_Z and "large" values of y , z and c . In all cases, both long-term dynamics show the presence of

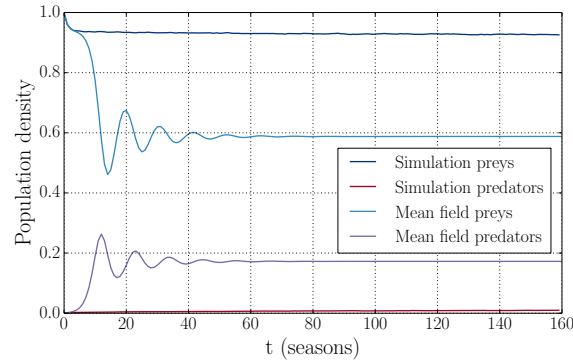


Figure 6.7: A comparison of the mean field model and a computer simulation for $\epsilon_Y = 1$, $y = 1$, $\epsilon_Z = 1$, $z = 1$ and $c = 1$

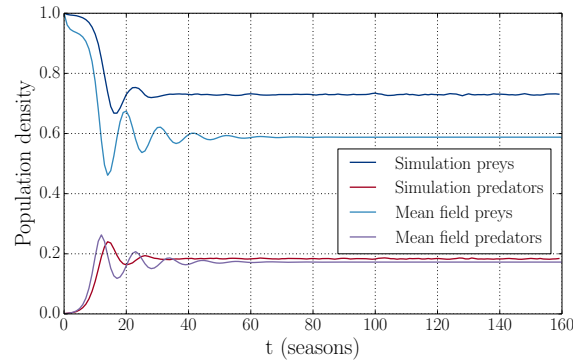


Figure 6.8: Mean field model vs computer simulation: $\epsilon_Y = 1$, $y = 20$, $\epsilon_Z = 1$, $z = 20$ and $c = 20$

a limit cycle. It is interesting to note that as the value of ϵ_Z increases, so does the amplitude of the oscillations.

Figure 6.10 shows the corresponding results for an increasing ϵ_Y , here it is possible to observe an evolution towards a fixed point. This outcome suggests that as the reproductive capacity of preys increases, predators have little influence on the dynamics of the prey species, the carrying capacity of the preys barely moves from a density equal to 0.75

The mean field model developed so far has a reasonable accuracy predicting the dynamics of the proposed CA model for large values of y , z and c , this behavior is expected since when the values taken by these parameters are large enough, space becomes unimportant. The following section describes a method to adjust the current mean field model in order to predict the dynamics of the CA model, when smaller neighborhoods are used.

6.2.3. A mean field model for small neighborhoods

In order to obtain a mean field model for small neighborhoods, we will follow a methodology first developed in [69] to determine the long term dynamics at different spatial scales of an stochastic lattice model where time is continuous. The methodology parts from the very impressive result that certain quantities, e.g., the growth rates of preys and predators, preserve their functional form at different sizes of a sampling window, where the densities of preys and predators are measured. By first obtaining the predation and prey growth rates directly from the simulation, it is possible to obtain the parameters of the relevant function by means of statistical regression methods.

We will not make use of the “sampling window”, instead we’ll part from the assumption that the functional forms of the rate of predation, the death rate of predators and growth rates are preserved

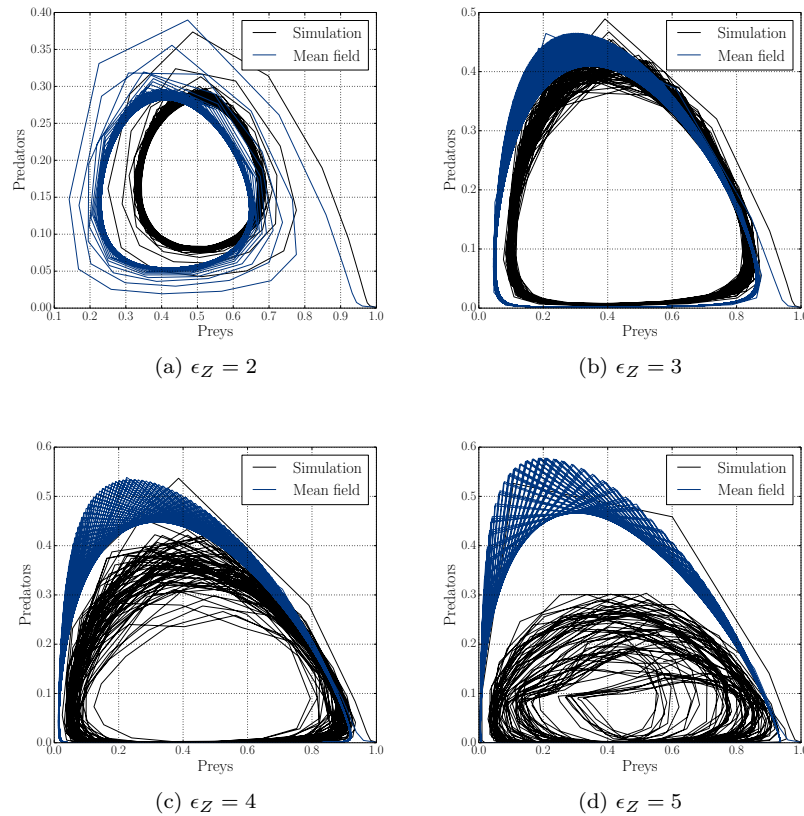


Figure 6.9: Phase plots of the mean field model vs computer simulations: $\epsilon_Y = 1$, $y = 20$, $z = 20$ and $c = 10$

for different sizes of the corresponding neighborhoods. As an example, consider the plot for the growth rate of preys shown in Figure 6.11, here the rate was measured from a simulation where the only enabled rule is the reproduction of preys; such conditions allows us to observe the whole curve that corresponds to the functional form for the growth rate. By comparing this curve with a plot of the mean field term for the reproduction of preys (see Equation 6.11) it is easy to see that both have the same functional form, of course, the scale is different, which suggests that the parameters that control the curve depend on the size of the reproduction neighborhood. Since the reproduction of predators is analogous to the reproduction of preys, we can assume that its functional form is similar. Each mean field term obtained in Section 6.1 defines the functional form of the corresponding stage, using this information we can choose an appropriate regression method and obtain the value of the parameters, e.g. ϵ_Y or ϵ_Z , for a particular neighborhood size.

To analyze the methodology in detail, let's consider again the model described in Section 6.2.2, as can be seen in Figure 6.7 the mean field model given by equations 6.24 to 6.28 fails to predict the behavior observed in the lattice model. This outcome is expected, since for small neighborhoods, the growth rate of a population is limited because of the fast decay in the number of cells available for reproduction, which differs from the unrestricted growth rates described by the corresponding mean field terms.

We start by measuring the growth rate for both populations, for such purposes, we use a simulation where $\Psi_0 = 1$, $\Phi_0 = 0.001$, $\alpha = 0.1$, $\epsilon_Y = 1$, $y = 1$, $\epsilon_Z = 1$, $z = 1$ and $c = 1$, the simulation was performed using a lattice of 512×256 cells; 10000 seasons were simulated, but only the last 9000 seasons were used in experiments, this is necessary in order to eliminate transients. To obtain a fitted curve for the measured data, a non linear least-squares algorithm, using Equations 6.11 and 6.14 as

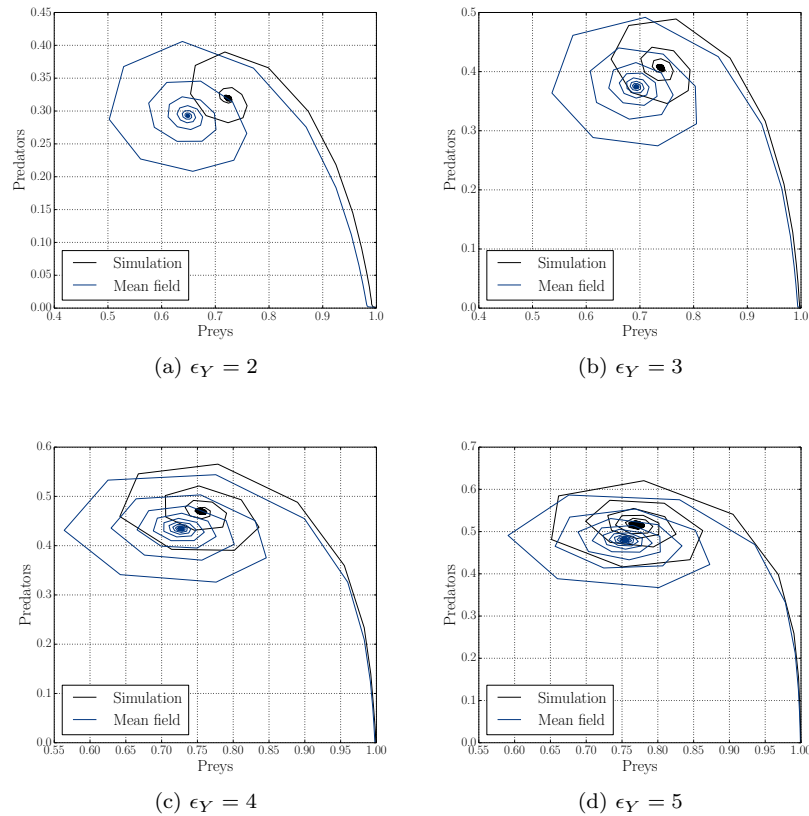


Figure 6.10: Phase plots of the mean field model vs computer simulations: $y = 20$, $\epsilon_Z = 1$, $z = 20$ and $c = 10$

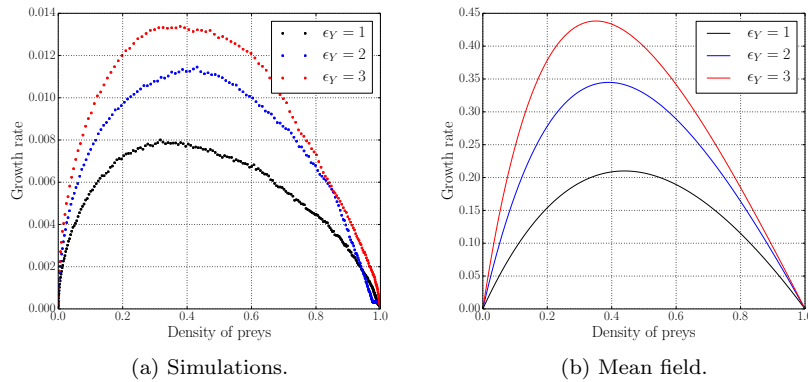


Figure 6.11: Functional form for the growth rate of preys. In (a) $\epsilon_Y = 1, 2, 3$, $y = 1$, and $\Psi_0 = 0.0001$; in (b) Equation 6.11 was plotted for $\epsilon_Y = 1, 2, 3$ using 100 values of Ψ_t linearly distributed in $[0, 1]$

inputs was used. The results obtained from the regression show that the growth rate of preys behaves as if in average $\epsilon_Y = 0.9404$, and the regression for the growth rate of predators shows that in average $\epsilon_Z = 0.8543$, it is interesting to note that both parameters are lower than the values used in the simulation, which account for the lower growth rate due to the saturation of space.

The mean field terms for the predation rate and the death rate of predators given by Equations

6.17 and 6.13 need to be analyzed in a different way. These terms depend on both Ψ_t and Φ_t , so at first sight, in order to obtain a fitted curve for the data, it would be necessary to use a multiple regression method. However, we can take advantage of the fact that the first factor in both terms represents the death probability of an individual due to predation, or to a lack of preys, while the second factor is just the number of events that occur during the corresponding stage divided by the size of the lattice in order to obtain a density. The functional form of the first term is that of a first order polynomial, so it makes sense to use a polynomial regression method to obtain a fitted line for the death probability of both populations. The only parameters that define the behavior of the predation probability and the death probability of predators, are the coefficients of the first order polynomial for each line. For easy reference, let us call such coefficients a , b , d , and e , thus the mean field term for the death probability of predators can be written as follows:

$$b + a\Psi_t \tag{6.29}$$

with $a = -1$ and $b = 1$, meanwhile the equation for the predation probability can be expressed as:

$$e + d\Phi_t \tag{6.30}$$

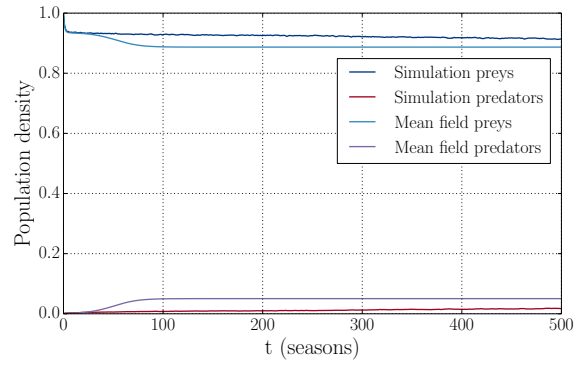
with $e = 0$ and $d = 1$. The regression for the death probability of predators gives the coefficients $a = -0.5513$, $b = 0.9040$, meanwhile the results for the predation probability give the values $d = 1.2617$ and $e = -0.0011$. Table 6.1 summarizes the results obtained so far, and presents some additional results for different sets of parameters used in computer simulations. Note that in all cases, the obtained values of ϵ_Y or ϵ_Z are less than the corresponding values used in the simulations, also note that as we increase the value of y or z the values obtained in the statistical regression approach the values of the simulation. As expected, a plot of the population dynamics of the simulation, and the mean field model with the adjusted parameters, as seen in Figure 6.12, shows a good agreement of the results.

CA parameters	Statistical regression					
	ϵ_Y	ϵ_Z	a	b	d	e
$\epsilon_Y = 1, y = 1, \epsilon_Z = 1, z = 1, \alpha = 0.1, c = 1$	0.9404	0.8543	-0.5513	0.9040	1.2617	-0.0011
$\epsilon_Y = 1, y = 1, \epsilon_Z = 2, z = 5, \alpha = 0.1, c = 1$	0.9365	1.9563	-0.8537	0.9854	1.5994	-0.0840
$\epsilon_Y = 3, y = 1, \epsilon_Z = 1, z = 1, \alpha = 0.1, c = 1$	2.3234	0.9484	-0.8947	0.9845	1.1752	0.0815
$\epsilon_Y = 3, y = 5, \epsilon_Z = 1, z = 1, \alpha = 0.1, c = 1$	2.9429	0.9746	-1.0280	1.0757	1.0245	0.1374

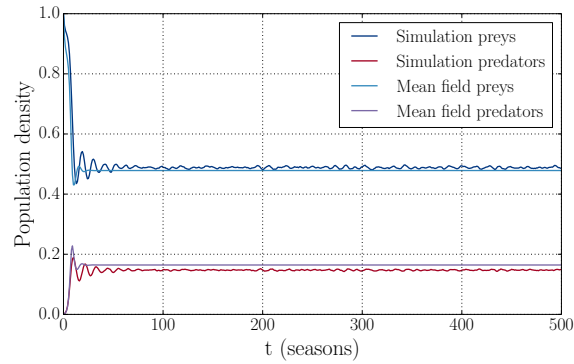
Table 6.1: Adjusted parameters for the mean field model via statistical regression.

6.2.4. The migration stage

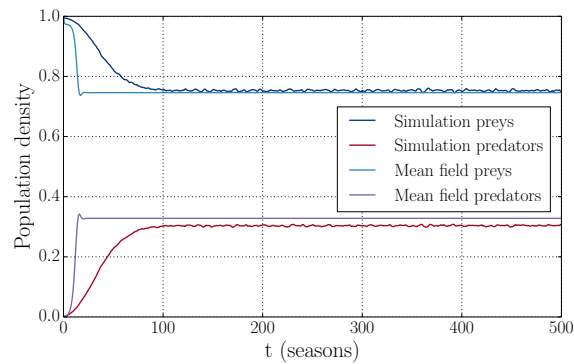
To finish the analysis of the proposed model, let's turn now our attention to the migration stage, here, predators move to catch preys according to a local PSO algorithm. No change in density occurs during this stage, predators merely move from zones where the local density of preys is low, to zones more abundantly populated by preys, as stated before, predation and the death of predators occur at later stages. The migration stage was inspired by the behavior of insects described in [76], and the related lattice model presented in [77]. It has been shown previously (see [79]) that as a consequence



(a) $\epsilon_Y = 1$, $y = 1$, $\epsilon_Z = 1$, $z = 1$ $\alpha = 0.1$, $c = 1$



(b) $\epsilon_Y = 1$, $y = 1$, $\epsilon_Z = 2$, $z = 5$ $\alpha = 0.1$, $c = 1$



(c) $\epsilon_Y = 3$, $y = 1$, $\epsilon_Z = 1$, $z = 1$ $\alpha = 0.1$, $c = 1$

Figure 6.12: Comparison of the results obtained from the computer simulations and the results of the mean field model with adjusted parameters.

of the movement of predators during the migration stage, the individuals of this population group into clusters that propagate through the lattice. The size of the clusters depends on the size of the social neighborhood, and on the values of the parameters k_1 and k_2 , the cognitive and social factor respectively. Furthermore, it was found that as the value of k_2 increases, the population dynamics of the model enter an oscillatory regime. Due to the movement of predators during the migration stage, we can expect a change in the death probability of a predator when comparing against the results obtained in a simulation where no migration occurs. Ideally, migration should provide better conditions for the survival of a predator, or the survival of its progeny; however, the effects of such change on a global scale are not easily predicted. To test our hypothesis, we have selected the parameter sets shown in Table 6.2, set *A* disables the movement of predators, so parameters like k_1 and k_2 are set to zero.

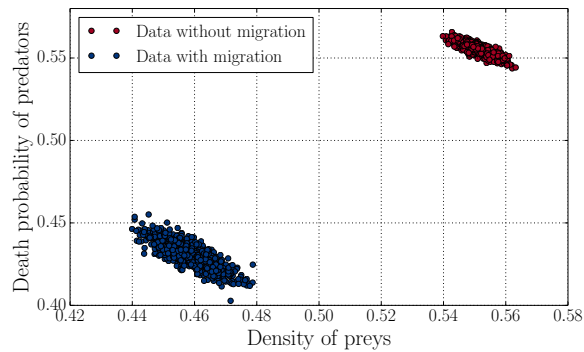
Parameter	Set <i>A</i>	Set <i>B</i>
Ψ_0	0.9	0.9
ϵ_Y	1	1
y	3	3
α	0.05	0.05
c	3	3
Φ_0	0.001	0.001
ϵ_Z	2	2
z	1	1
Migration parameter	Set <i>A</i>	Set <i>B</i>
k_1	0	1
k_2	0	1
l	1	7
ω	0	linear decrease from 0.9 to 0.2

Table 6.2: Parameters used to analyse the migration stage.

For both simulations, we have measured the following quantities: (a) the density of preys at the start of the death of predators stage Ψ_I ; (b) the death probability of predators. Figure 6.13 shows these measurements, it is easy to see that when set *A* is used, our data concentrates in an small area, which corresponds to an orbit towards a fixed point obtained when no migration occurs. Due to the oscillatory behavior resulting from the movement of predators, the data obtained for set *B* follows a pattern akin to a limit cycle, thus spanning a wider area. The results show a lower density of preys for set *B*, nevertheless, the corresponding death probability of predators is lower than the death probability observed in set *A*. These results suggest that predators hunt with a greater efficiency, i.e., they survive under more adverse conditions when the migration stage is active. Note also that the functional form for the death probability of predators remains unchanged by the migration stage.

We may use then the procedure described in Section 6.2.3 to generate a mean field model that takes into account the effects of migration. Table 6.3 shows the parameters obtained through statistical regression for both simulations. Note that the value of ϵ_Z obtained for set *B* is lower than the value obtained for set *A*, such result is to be expected, since when migrating, predators form clusters, which reduces the space available for reproduction.

Figure 6.14a shows a comparison between a simulation that uses set *B*, and a mean field model that uses the corresponding parameters from Table 6.3, a non-trivial fixed point where both populations coexist can be observed; as expected, the mean field model using adjusted parameters provides an accurate prediction of the long term density of both populations after a very short transient. However, the dynamics of the lattice model shows small oscillations around the predicted density. Increasing the value of k_2 in set *B*, drives the dynamics of the lattice model towards oscillatory behavior. Figure 6.14b shows such phenomenon for $k_2 = 2$, it is easy to see, that the densities predicted by the adjusted mean field model correspond to the points around which the densities of preys and predators oscillate when the migration stage is enabled; once again, a mean field model that includes adjusted parameters

Figure 6.13: Measurements of the death probability of predators for parameters sets A and B .

Parameter set	Statistical regression					
	ϵ_Y	ϵ_Z	a	b	d	e
A	0.9053	1.7098	-0.6808	0.9302	1.5220	0.0478
B	0.8520	0.9485	-0.8542	0.8225	1.5076	0.0990

Table 6.3: Parameters obtained through statistical regression for simulations using parameters sets A and B .

is only able to predict the mean long term density of both species, failing to predict the oscillations observed in the lattice model. We may summarize the effects of the movement of predators on the carrying capacity of the populations as follows: when moving towards zones where the density of preys is high, a predator increases their chance of survival; also, it increases the probability that its progeny survives the “death of predators” stage. With a greater number of predators surviving, there is an increase in the predation probability, which increases the death rate of preys. It is interesting to note that by increasing their odds of survival, the population of predators create harsher conditions for their species, despite the fact that predators are able to survive under such conditions, the carrying capacity of both preys and predators is lower than the densities observed under a “well mixed” environment.

Besides changing the mean density of the populations, the movement of predators also causes a transition to the oscillatory behavior. The oscillations have a very regular period, however, their amplitude, while bounded, is very difficult to predict (see Figure 5.13). Previous works have shown that such oscillations in a prey-predator system should banish in the thermodynamic limit (see [66] [61] [31] [40] [70] [80]), i.e., their amplitude diminishes as the size of the lattice is increased. To investigate such phenomenon, we performed additional computer simulations for lattices of size 2^{6+i} for $i = 0, 1, 2, 3, 4, 5$, i.e., from a lattice of size 64×64 cells to a lattice of size 2048×2048 cells; 10000 seasons were simulated using the parameters of Table 4.1. To obtain a measure of the amplitude of the oscillations, we calculated the standard deviation of the time series of the density of preys, since the predators species has a similar behavior, we do not report those data. Figure 6.15 shows the results of our simulations, as expected, the amplitude of the oscillations decays as the size of the lattice increases: for small lattices, an evolution towards a noisy limit cycle can be observed; as the size increases, the limit cycle destabilizes and the pattern of Figure 5.13 appears. Additional increments to the size of the lattice further diminish the amplitude; however, in stark contrast to the results reported in [31] where noisy oscillations of low amplitude are observed for large lattices, we have found that the qualitative behavior of the density of preys remains unchanged: the amplitude of the oscillations is still bounded, but difficult to predict, and their period is preserved. Such behavior raises the need to emphasize the differences between our model and previous work where scaling effects are studied. First it must be noted that our predators have a higher mobility than the one commonly found in other lattice models, where dispersal (whether by movement, reproductive processes, or both) is restricted to first

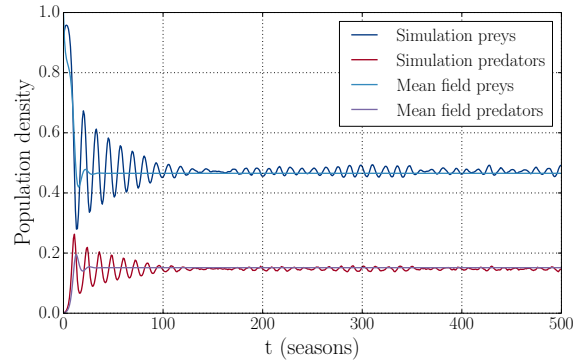
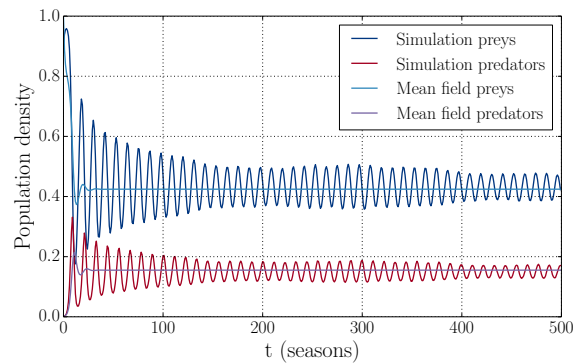
(a) $k_2 = 1$ (b) $k_2 = 2$

Figure 6.14: Simulations using set B compared to a mean field model that uses adjusted parameters via statistical regression.

neighbors. It is well known that large dispersal ranges bring the distribution of individuals on the lattice close to the “well mixed” case [40] [81], so oscillations might arise as a consequence of long range movement. Second, the spatial dynamics of oscillating prey-predator systems are commonly characterized by patterns akin to the initial invasion process, i.e., there are fronts of predators that invade prey rich areas leaving behind a few cells populated by preys, these survivors quickly repopulate predated areas and the process starts again, Rozenfeld and Albano refers to these phenomena as “alternating percolation events” [34]. As noted in section 5.2.2, in the proposed model such events are only observable during the transient phase; afterwards, we observe predators grouped together as swarms moving through the whole lattice while searching for zones with a “good” density of preys (a curious enough reader might wish to compare the spatial patterns found in [66] [31] [70] and [34] with Figure 5.8), the oscillatory behavior observed when migration is enabled suggest that the time lapse between the predation of a particular zone by a swarm and the moment until such zone is qualified again as “good” by a swarm is regular.

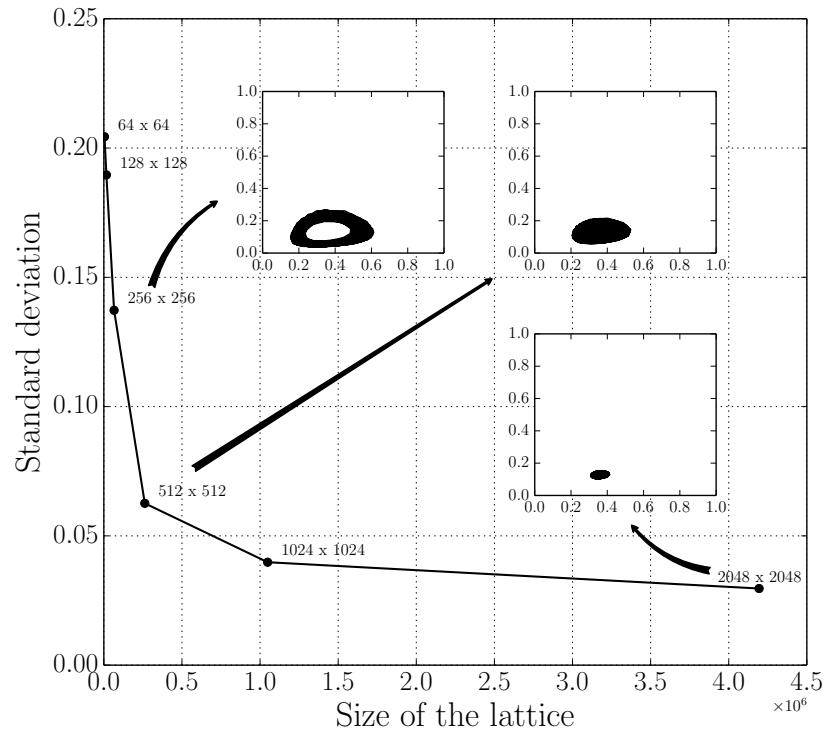


Figure 6.15: Scaling behavior of the proposing model. Small lattices produce orbits to a noisy limit cycle; as the size of the lattice increases, the amplitude of the oscillations diminishes and the limit cycle destabilizes. For large lattices a new decrease of the amplitude is observed; however, the oscillations still have a regular period and their amplitude remains bounded, yet difficult to predict.

Chapter 7

Conclusions

We presented a qualitative analysis of the spatial and population dynamics of a prey-predator system, where the movement of predators is modelled through a PSO algorithm. So when moving a predator not only takes into account the information it has acquired by itself, but it also evaluates the information that comes from other individuals in a finite neighborhood.

It is worth noting that the implementation of the PSO algorithm presented here is one of many possible designs that would be adequate to model the social interactions among organisms in lattice models. A first step would be the design of other fitness functions that qualify each cell of the lattice according to other environmental factors besides density, e.g., temperature, pollution, soil nutrients, etc. Another possibility comes from the fact that the neighbors who influence the decision of a particle, does not necessarily have to be those nearer in a geometrical sense, but may be those closer according to some hierarchy existing in the population, according to Kennedy and Eberhart [57]: “Who influences you is defined by your connections in the social network, not by positions in a belief space”.

Our results show that in the absence of movement, the spatial patterns observed correspond to those of a diffusion process. When working with the global version of our PSO algorithm, a pure cognitive movement of predators produce a high density dependence between both populations. Under this conditions the movement of predators is restricted to the borders between empty space and the zones populated by preys. Social interactions result in a coordinated movement of the whole population, thus the spatial dynamics shows a single cluster moving through the lattice, this limits the growth of the predators even if resources are abundant.

The analysis of the local implementation of the model shows that by increasing the mobility of predators towards zones with a high fitness, the time lag between the creation of gaps, and the moment when these zones are repopulated and thus qualified again as “good zones” becomes regular as illustrated by the time series belonging to both populations. Such behavior is consistent with previous works dealing with the cyclic behavior of prey-predator systems. We have also shown that our local PSO algorithm increases the proficiency of predators, which produces a decrease in their death probability with respect to a simulation where no migration occurs. A higher density of predators results in an increase in the predation probability with a corresponding decrease in the density of preys.

Our results show that quantities such as the growth rates, and the probabilities of predation and death of predators, preserve their functional form for different sizes of the corresponding neighborhoods. This outcome makes possible to generate a mean field model that predicts accurately the mean densities that characterize the long-term dynamics of the proposed model. For large sized neighborhoods, the dynamics of the lattice model match those of a mean field model whose parameters describe a well mixed environment, here limit cycles are common. For small neighborhoods, adjusting the parameters of the mean field model through statistical regression methods, produces orbits to fixed points that are also observed in the lattice model. Finally, for mid sized neighborhoods, the proposed methodology is only able to predict the mean densities of the populations, failing to reproduce the oscillatory behavior observed in the lattice model, here we found evidence of sensitivity to initial conditions.

When the movement of predators is included in the simulations, a change in the death probability

of predators occurs due to such movement; nevertheless, the functional form of the death probability of predators remains unchanged. Thus, the effects of the migration stage can be taken into account by the proposed methodology. However, when an increase to k_2 (the social factor) drives the lattice model into oscillatory behavior, the methodology is once again unable to reproduce such behavior, predicting orbits to a fixed points that represents the mean density of preys and predators.

Bibliography

- [1] Stephen Wolfram. Cellular automata. *Los Alamos Science*, 9:2–21, 1983.
- [2] Stephen Wolfram. Statistical mechanics of cellular automata. *Rev. Mod. Phys.*, 55:601–644, 1983.
- [3] M. A. Shereshevski. Lyapunov exponents for one-dimensional cellular automata. *Journal of Nonlinear Science*, 2:1–8, 1992.
- [4] Jesús Urías, Raúl Rechtman, and Enciso Agustín. Sensitive dependence on initial conditions for cellular automata. *Chaos*, 7:688–693, 1997.
- [5] Jin Weifeng and Chen Fangyue. Global attractors and chaos of complex bernoulli-shift rules. In *2010 International Workshop on Chaos-Fractal Theory and its Applications*, 2010.
- [6] Y. Pomeau. Periodic behavior of cellular automata. *Journal of Statistical Physics*, 70:1379–1382, 1993.
- [7] José Manuel Gómez Soto. *Comportamiento Colectivo no-Trivial en Autómatas Celulares*. PhD thesis, Centro de Investigación y de Estudios Avanzados del IPN, 2007.
- [8] Leon O. Chua. A nonlinear dynamics perspective of wolfram’s new kind of science part i: Threshold of complexity. *International Journal of Bifurcation and Chaos*, 12:2655–2766, 2002.
- [9] Eytan Domany and Wolfgang Kinzel. Equivalence of cellular automata to ising models and directed percolation. *Physical Review Letters*, 53(4):311–314, 1984.
- [10] Joel L. Lebowitz, Christian Maes, and Eugene R. Speer. Statistical mechanics of probabilistic cellular automata. *Journal of Statistical Physics* 1990, 59:117–170, 1990.
- [11] G. A. Kohring and M. Schreckenberg. The domany-kinzel cellular automaton revisited. *Journal of Physique I*, 2:2033–2037, 1992.
- [12] Tânia Tomé. Spreading of damage in the domany-kinzel cellular automaton a mean-field approach. *Physica A*, 212:99–109, 1994.
- [13] Niels K. Petersen and Preben Alstrom. Phase transitions in an elementary probabilistic cellular automaton. *Physica A*, 235:473–485, 1997.
- [14] P. Balister, B. Bollobás, and R. Kozma. Large deviations for mean field models of probabilistic cellular automata. *Random Struct. Algorithms*, 29(3):399–415, 2006.
- [15] Ana Busic, Jean Mairesse, and Irene Marcovici. Probabilistic cellular automata, invariant measures, and perfect sampling . In *28th International Symposium on Theoretical Aspects of Computer Science (STACS 2011)*, volume 9 of *Leibniz International Proceedings in Informatics (LIPIcs)*, pages 296–307, Dagstuhl, Germany, 2011. Schloss Dagstuhl–Leibniz-Zentrum fuer Informatik.
- [16] Philippe Chassaing and Jean Mairesse. A non-ergodic probabilistic cellular automaton with a unique invariant measure. *Stochastic processes and their applications*, 121:2474–2487, 2011.

- [17] Roberto da Silva and Nelson Alvez Jr. Dynamics exponents of a probabilistic three-state cellular automaton. *Physica A*, 350:263–276, 2005.
- [18] A. K. Dewdney. Sharks and fish wage an ecological war on the toroidal planet wa-tor. *Scientific American*, 251:14–22, 1984.
- [19] Michael Begon, Colin R. Townsend, and John L. Harper. *Ecology: From Individuals to Ecosystems*. Blackwell Publishing, 4th edition, 2006.
- [20] Jonathan Silvertown, Senino Holtier, Jeff Johnson, and Pam Dale. Cellular automaton models of interspecific competition - the effect of pattern on process. *Journal of Ecology*, 80:527–534, 1992.
- [21] Timothy H. Keitt. Stability and complexity on a lattice: coexistence of species in an individual-based food model. *Ecological Modelling*, 102:243–258, 1997.
- [22] Jane Molofsky and James Bever D. A novel theory to explain species diversity in landscapes: positive frequency dependence and habitat suitability. *Proceedings of the Royal Society B: Biological Sciences*, 269:2389–2393, 2002.
- [23] Yiannis G. Matsinos and Andreas Y. Troumbis. Modeling competition, dispersal and effects of disturbance in the dynamics of a grassland community using cellular automaton model. *Ecological Modelling*, 149:71–83, 2002.
- [24] John Vandermeer and Senay Yitbarek. Self-organized spatial pattern determines biodiversity in spatial competition. *Journal of Theoretical Biology*, 300:48–56, 2012.
- [25] Parvizeh R. Hosseini. Pattern formation and individual-based models: The importance of understanding individual-based movement. *Ecological Modelling*, 194:357–371, 2006.
- [26] Elise Filotas, Martin Grant, Lael Parrot, and Per Arne Rikvold. Community-driven dispersal in an individual-based predator-prey model. *Ecological Complexity*, 5:238–251, 2008.
- [27] H. N. Comins, M. P. Hassel, and R. M. May. The spatial dynamics of host-parasitoid systems. *The Journal of Animal Ecology*, 61(3):735–748, 1992.
- [28] Jonathan A. Sherratt, Barry T. Eagan, and Mark Lewis A. Oscillations and chaos behind predator-prey invasion: mathematical artifact or ecological reality? *Phil. Trans. R. Soc. B*, 352:21–38, 1997.
- [29] Everaldo Arashiro and Tânia Tomé. The threshold of coexistence and critical behavior of a predator-prey cellular automaton. *Journal of Physics A*, 40:887–900, 2007.
- [30] Feng Fu, Martin A. Nowak, and Hauert Christoph. Invasion and expansion of cooperators in lattice populations: Prisoner’s dilemma vs snowdrift games. *Journal of Theoretical Biology*, 266:358–366, 2010.
- [31] N. Boccara, O. Roblin, and M. Roger. Automata network predator-prey model with pursuit and evasion. *Physical Review E*, 50:4531–4541, 1994.
- [32] Roberto Monetti, Alejandro Rozenfeld, and Ezequiel Albano. Study of interacting particle systems: the transition to the oscillatory behavior of a prey-predator model. *Physica A: Statistical Mechanics and its Applications*, 283:52–58, 2000.
- [33] Alejandro Rozenfeld and Ezequiel Albano. Study of a lattice-gas model for a prey-predator system. *Physica A: Statistical Mechanics and its applications*, 266:322–329, 1999.
- [34] Alejandro F. Rozenfeld and Ezequiel V. Albano. Critical and oscillatory behavior of smart preys and predators. *Physical Review E*, 63:061907, 2001.
- [35] Zi-zhen Li, Meng Gao, Cang Hui, Xiao-zhuo Han, and Honghua Shi. Impact of predator pursuit on prey evasion on synchrony and spatial patterns in metapopulation. *Ecological Modelling*, 185:245–254, 2005.

- [36] Xueting Wang, He Mingfeng, and Yibin Kang. A computational predator-prey model, pursuit-evasion behavior based on different range of vision. *Physica A*, 391:664–672, 2012.
- [37] Richard Durrett. The contact process, 1974-1989. *Lectures in Applied Mathematics*, 27:1–18, 1991.
- [38] Richard Durrett and Simon A. Levin. Stochastic spatial models: A user’s guide to ecological applications. *Phil. Trans. R. Soc. B*, 343:329–350, 1994.
- [39] Carol Bezuidenhout and Geoffrey Grimmet. The critical contact process dies out. *The annals of probability*, 18:1462–1482, 1990.
- [40] Richard Durrett and Simon A. Levin. The importance of being discrete (and spatial). *Theoretical Population Biology*, 46:363–394, 1994.
- [41] Richard Durrett. Are there bushes in a forest? *Stochastic Processes and their Applications*, 37:19–31, 1991.
- [42] Ilkka Hanski and Esa Ranta. Coexistence in a patchy environment: Three species of daphnia in rock. *Journal of Animal Ecology*, 52:263–279, 1983.
- [43] Richard Durrett and Claudia Neuhasser. Coexistence results for some competition models. *The Annals of Applied Probability*, 7:10–45, 1997.
- [44] Jordi Bascompte, Ricard V. Solé, and Norbert Martínez. Population cycles and spatial patterns in snowshoe hares: and individual-oriented simulation. *Journal of Theoretical Biology*, 187:213–222, 1997.
- [45] Bernd Blasius, Amit Huppert, and Lewi Stone. Complex dynamics and phase synchronization in spatially extended ecological systems. *Nature*, 399:354–359, 1999.
- [46] Robert M. May. Simple mathematical models with very complicated dynamics. *Nature*, 261:459–467, 1976.
- [47] Robert L. Devaney. *A first course in chaotic dynamical systems: theory and experiment*. Perseus Book Publishing, 1992.
- [48] Jarkko Kari. Theory of cellular automata: a survey. *Theoretical Computer Science*, 334:3–33, 2005.
- [49] Stephen Wolfram. *A New Kind of Science*. Wolfram Media, 1 edition, 2002.
- [50] Harold V. McIntosh. *One Dimensional Cellular Automata*. Lunivier Press, 1 edition, 2009.
- [51] Harold V. McIntosh. Wolfram’s class iv automata and a good life. *Physica D: Nonlinear Phenomena*, 45:105–121, 1990.
- [52] H. A. Gutowitz, J. D. Victor, and B. W. Knight. Local structure theory for cellular automata. *Physica D*, 28:18–48, 1987.
- [53] Nino Boccara. *Modeling Complex Systems*. Springer-Verlag, 2004.
- [54] Franco Bagnoli, Nino Boccara, and Raúl Rechtman. Nature of phase transitions in a probabilistic cellular automaton with two absorbing states. *Physical Review E*, 63:046–116, 2001.
- [55] Russell Eberhart and James Kennedy. A new optimizer using particle swarm theory. In *Proceedings of the Sixth International Symposium on Micro Machine and Human Science*, pages 39–43, 1995.
- [56] R.C. Eberhart and Y. Shi. Comparing inertia weights and constriction factors in particle swarm optimization. In *Evolutionary Computation, 2000. Proceedings of the 2000 Congress on*, volume 1, pages 84–88, 2000.

- [57] James Kennedy and Russel Eberhart. *Swarm Intelligence*. Morgan Kauffman Publishers, 1 edition, 2001.
- [58] Yang Xin-She. Characterization of multispecies living ecosystems with cellular automata. In *ICAL 2003 Proceedings of the eighth international conference on Artificial Life*, pages 138–141, 2003.
- [59] Andrzej Pekalski. A short guide to predator-prey lattice models. *Computing in Science and Engineering*, 6:62–66, 2004.
- [60] N. G. van Kampen. *Stochastic Processes in Physics and Chemistry*. North Holland, 2 edition, 1992.
- [61] Adam Lipowski. Oscillatory behavior in a lattice prey-predator system. *Physical Review E*, 60:5179–5184, 1999.
- [62] Javier E. Satulovsky and Tânia Tomé. Stochastic lattice gas model for a predator-prey system. *Physical Review E*, 49:5073–5080, 1994.
- [63] Mercedes Pascual, Roy Manojit, Frédéric Guichard, and Glenn Flierl. Cluster size distributions: signatures of self-organization in spatial ecologies. *Philos. Trans. R. Soc. Lond. Ser. B-Biol. Sci*, 357(1421):657–666, 2002.
- [64] André M. de Roos, Edward McCauley, and William G. Wilson. Mobility versus density-limited predator-prey dynamics on different spatial scales. *Proceedings of the Royal Society B: Biological Sciences*, 246:117–122, 1991.
- [65] B. R. Sutherland and Jacobs A. E. Self-organization and scaling in a lattice predator-prey model. *Complex Systems*, 8:385–405, 1994.
- [66] Tibor Antal and Droz Michel. Phase transitions and oscillations in a lattice prey-predator model. *Physical Review E*, 63:056119, 2001.
- [67] Mercedes Pascual and Simon A. Levin. From individuals to population densities: Searching for the intermediate scale of nontrivial determinism. *Ecology*, 80:2225–2236, 1999.
- [68] Richard Durrett and Simon A. Levin. Lessons on pattern formation from planet water. *Journal of Theoretical Biology*, 205:201–214, 2000.
- [69] Mercedes Pascual, Pierr Mazzega, and Simon A. Levin. Oscillatory dynamics and spatial scale: The role of noise and unresolved pattern. *Ecology*, 82:2357–2369, 2001.
- [70] Mauro Mobilia, Ivan T. Georgiev, and Uwe C. Täuber. Phase transitions and spatio-temporal fluctuations in stochastic lattice lotka-volterra models. *Journal of Statistical Physics*, 128:447–483, 2007.
- [71] Gianpiero Cattaneo, Alberto Dennunzio, and Fabio Farina. A full cellular automaton to simulate predator-prey systems. In *Proceedings of the 7th international conference on Cellular Automata for Research and Industry, ACRI'06*, pages 446–451, Berlin, Heidelberg, 2006. Springer-Verlag.
- [72] James Kennedy and Russel Eberhart. Particle swarm optimization. In *Neural Networks, 1995., IEEE International Conference on*, volume 4, pages 1942–1948, 1995.
- [73] Park Jong-Bae, Lee Ki-Song, Shin Joong-Rhin, and Y. Lee Kwang. A particle swarm optimization for economic dispatch with nonsmooth cost functions. *Power Systems, IEEE Transactions on*, 20(1):34–42, 2005.
- [74] R. V. Kulkarni and G. K. Venayagmoorthy. Particle swarm optimization in wireless-sensor networks: A brief survey. *Systems, Man, and Cybernetics, Part C: Applications and Review, IEEE Transactions on*, 41:262–267, 2011.

- [75] A. Gorai and A. Ghosh. Gray-level image enhancement by particle swarm optimization. In *Nature Biologically Inspired Computing, 2009. NaBIC 2009. World Congress on*, pages 72–77, 2009.
- [76] Douglas J. Futuyma and Steven S. Wasserman. Resource concentration and herbivory in oak forests. *Science*, 21:920–922, 1980.
- [77] Jan D. Van Der Laan, Ladislav Lhotka, and Hogeweg Pauline. Sequential predation: a multi-model study. *Journal of Theoretical Biology*, 174:149–167, 1995.
- [78] Shi Yang, Liu Hongcheng, Gao Liang, and Guohui Zhang. Cellular particle swarm optimization. *Information Sciences*, 181:4460–4493, 2011.
- [79] Mario Martínez Molina, Marco A. Moreno Armendáriz, and Juan Carlos Seck Tuoh Mora. On the spatial dynamics and oscillatory behavior of prey-predator model based on cellular automata and particle swarm optimization. *Journal Of Theoretical Biology*, 336:173–184, 2013.
- [80] Sergei Petrovskii, Bai-Lian Li, and Horst Malchow. Transition to spatiotemporal chaos can resolve the paradox of enrichment. *Ecological Complexity*, 1:37–47, 2004.
- [81] A. Brännström and D. J. T. Sumpter. Coupled map lattice approximations for spatially explicit individual-based models of ecology. *Bulletin of Mathematical Ecology*, 67:663–682, 2005.